MODELING GROUNDWATER INUNDATION UNDER SEA-LEVEL RISE SCENARIOS IN THE SURFICIAL AQUIFER OF BOGUE BANKS, NORTH CAROLINA

By:

James E. Owers

November 2017

Director of Thesis: Alex Manda

Major Department: Geological Sciences

Bogue Banks in North Carolina is expected to be impacted by sea-level rise, but the impact on the subsurface groundwater system is not well understood. A three-dimensional Visual MODFLOW steady-state model and ArcGIS 10.3 were used to quantify the extent of marine and groundwater inundation by the year 2100. Visual MODFLOW was used to simulate the water table on Bogue Banks, first at current sea-level then at different sea-level rise scenarios. The results from Visual MODFLOW were then imported into ArcGIS to calculate the area inundated by marine and groundwater inundation. Sea-level rise between 0.2 and 1.4 m above present conditions may occur at Bogue Banks and seven scenarios were envisioned as appropriate intervals to forecast. A total of 29 monitoring wells were installed in the surficial aquifer of Bogue Banks and equipped with water level loggers to collect groundwater data. Aquifer properties were constrained by studying sediment cores collected during well construction. Marine and groundwater inundation combine to impair 33% to 79% of the island by the year 2100, with 43% to 51% of the island being inundated in the most likely scenarios of 0.4 to 0.6 m of sea-level rise above current conditions. Marine inundation estimates range from 5% to 31% with 11% to 17% inundation in the most likely scenarios. Groundwater inundation estimates ranged from a minimum of 28% to 48% of the area not impaired by marine inundation, with the most likely range indicating 33% to 40% inundation. The results indicate that as sea-level rise

increases in severity, groundwater inundation covers a much larger area of the island than marine impairment. The results of the study therefore suggest that as sea-level rises, residents of Bogue Banks may need to account for marine and groundwater inundation as the environment changes and sea-level rises. A greater understanding of the combined impacts of groundwater and marine inundation on barrier islands may be useful for coastal residents in mitigating or adapting to changes due to sea-level rise not just in North Carolina, but globally.

MODELING GROUNDWATER INUNDATION UNDER SEA-LEVEL RISE SCENARIOS IN THE SURFICIAL AQUIFER OF BOGUE BANKS, NORTH

A Thesis

Presented to the Faculty of the Department of Geological Sciences

East Carolina University

In Partial Fulfillment of the Requirements for the Degree

Master of Science in Geology

By: James E. Owers

November 2017

MODELING GROUNDWATER INUNDATION UNDER SEA-LEVEL RISE SCENARIOS IN THE SURFICIAL AQUIFER OF BOGUE BANKS, NORTH CAROLINA

By:

James E. Owers

APPROVED BY:

DIRECTOR OF THESIS:____

Alex K. Manda, PhD

COMMITTEE MEMBER:____

Richard K. Spruill, PhD

COMMITTEE MEMBER:____

Michael O'Driscoll, PhD

COMMITTEE MEMBER:____

Eban Bean, PhD

CHAIR OF THE DEPARTMENT

OF GEOLOGICAL SCIENCES:____

Stephen J. Culver, PhD

DEAN OF THE GRADUATE SCHOOL:____

Paul J. Gemperline, PhD

DEDICATION

This thesis is dedicated to my family.

ACKNOWLEDGEMENTS

First, I would like to thank my family for their support. To my mother Alison, my father James Sr., and sisters Katie and Torie: I can never thank you enough for everything you've done.

I would like to thank my advisor, Alex Manda. I am honored by the opportunity to learn from your knowledge and experience and grateful for the opportunity you gave me to come to ECU.

I would also like to thank the other members of my committee. Dr. Richard Spruill, Dr. Michael O'Driscoll, and Dr. Eban Bean. Thank you all for imparting your knowledge onto me and for your assistance during the journey.

Thank you to all of my friends and fellow graduate students. I will treasure your friendship and our time together. I would especially like to thank all of those who helped with fieldwork, who are too many to name here, but I would especially like to thank Mr. James Pitt for your willingness to show me the ropes. Your experience has saved me a great deal of frustration throughout my postgraduate career.

Thank you to Jim Watson and John Woods for your endless assistance in this project. Without your knowledge and expertise, this project and this department wouldn't be everything that it is.

Lastly, I would like to thank several Bogue Banks residents for their assistance: Frank Rush, Brian Kramer, Sarah Williams, Sonny Cunningham, Trace Cooper, Meghan Dinneen, Lauren Kolodij, Stephanie Mitchell, and Robin Hunt. Thank you all so much for allowing me to conduct this project on your island. I hope these findings will be beneficial to all of you.

TABLE OF CONTENTS

LIST OF TABLES

LIST OF FIGURES

INTRODUCTION

Sea-level rise resulting from climate change is expected to impact groundwater resources of coastal regions. Sea-level is expected to rise globally between 0.2 and 1.5 m (Jevrejeva et al.; 2011, Rotzoll and Fletcher, 2013; Horton et al., 2014) by the year 2100. In that same time, sea-level is expected to rise between 0.3 and 1.3 m in North Carolina (Kopp et al., 2014, Overton et al., 2015). Sea-level rise of about 3 mm/year has been observed in Beaufort, North Carolina (https://tidesandcurrents.noaa.gov, Overton et al., 2015). This rising sea level causes increased marine inundation (where land is impaired by encroaching saltwater), but an equally important repercussion of sea-level rise is an increase in groundwater (freshwater) inundation, where the water table rises above the land surface resulting in permanent flooding (Masterson et al., 2013-a; Rotzoll and Fletcher, 2013; Manda et al., 2014).

Increased groundwater inundation has several potentially negative impacts on barrier island settings including land degradation, infrastructure destruction, and changes in vegetation assemblages (Masterson et al., 2013-a, Manda et al., 2014). On-site wastewater treatment systems (OWTS) on barrier islands may be compromised due to the rising water table (Manda et al., 2014), while sea-level rise has the potential to cause significant urban flooding (Rotzoll and Fletcher, 2012) which is already observed as nuisance flooding in the southeastern United States (Sweet et al., 2014). Barrier island ecosystems may be altered by the thinning of the vadose zone- the unsaturated portion of the aquifer system- before inundation even occurs, disrupting vegetation assemblages and altering the island landscape (Masterson et al., 2013-a). These problems may not be confined to one geographic location, as there are more than 2100 barrier islands across the globe that constitute about 10% (20,783 km) of coastline (Stutz and Pilkey, 2011) and house about 10% of the world’s population (Nicholls and Cazenave, 2010). Some of these areas may see the effects of groundwater inundation equal to or greater than marine inundation (Rotzoll and Fletcher, 2012, Manda et al., 2014).

Shallow coastal aquifers are expected to experience an increase in water levels as a direct result of sea-level rise (Masterson and Garabedian, 2007, Oude Essink et al., 2010 Masterson et al., 2013-a, Manda et al., 2014). Prior work on rising water tables has examined the impacts of sea-level rise on drinking water supplies (Ferguson and Gleeson, 2012, Guha and Panday, 2012, Langevin and Zygnerski, 2013) and OWTS (Flood and Calhoun, 2011, Manda et al., 2014). However, while research has been performed to study the consequences of thinning vadose zones on barrier islands (Masterson et al., 2013-a, Masterson et al., 2013-b), much less attention has been paid to groundwater inundation resulting from sea-level rise.

This study focuses on Bogue Banks, a developed barrier island on the coast of North Carolina (Figure 1). Bogue Banks is characterized by high elevation dunes and low-lying swales ranging from sea-level to approximately 17 m elevation, which are representative of many barrier island systems. It is an almost east-west trending barrier island on the east coast of North Carolina. The island shows morphologic variability, with the western sections being regressive while the eastern section of the island is transgressive (Timmons et al., 2010). The number of permanent residents is only about 6,600 (http://www.census.gov), but seasonal populations swell during tourist season. Emerald Isle, on the western section of Bogue Banks, swells from approximately 3,700 residents to about 40,000 residents during peak tourist times (http://www.emeraldisle-nc.org/pdfs/2004LUPw2008Amendments.pdf). Town managers on Bogue Banks are already concerned about flooding after storm events, which is costly and time consuming for the town to remediate (Kramer, personal communication, February 2015).

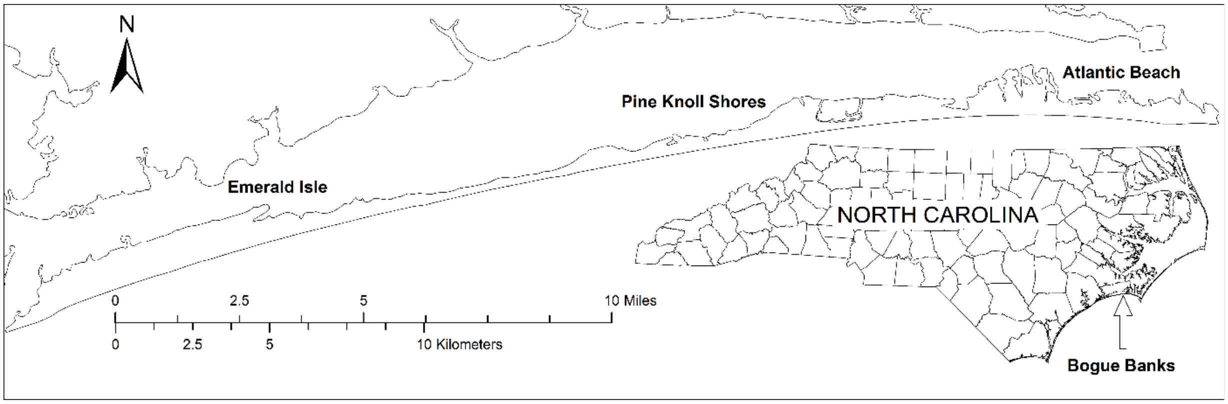

Figure 1: Map of Bogue Banks showing the towns of Emerald Isle, Pine Knoll Shores, and Atlantic Beach. Inset: Location of Bogue Banks off the coast of North Carolina.

Purpose and Scope

The goal of this study was to characterize the water table on Bogue Banks and evaluate how the shallow groundwater system may be affected by sea-level rise resulting from climate change. This study was also designed to determine the properties of the surficial aquifer and quantify the impact sea-level may have on Bogue Banks. The research sought to accomplish three primary objectives:

1. Derive hydrogeologic properties of the surficial aquifer
2. Simulate the water table on Bogue Banks
3. Assess the effect of sea-level rise on the water table on Bogue Banks

The data collected during the course of this research were used to test the hypothesis that rising sea levels will cause the water table to rise above the land surface causing groundwater inundation in >40% of the surface area on Bogue Banks.

Previous Research

Masterson et al. (2013-a) studied the impact of sea-level rise on Assateague Island, an undeveloped barrier island on the coast of Maryland and Virginia. This study investigated how increases in sea-level up to 60 cm would impact the groundwater system and what impact this would have on vegetation assemblages. Using Visual MODFLOW and the SEAWAT engine, this research showed that as sea-level rises, the thickness of the vadose zone decreases and the water table may rise above the land surface away from the shore, causing inland groundwater flooding.

Research performed by Sisco (2013) examined the relationship between the water table and storm events on Bogue Banks. Sisco (2013) focused on determining the hydrologic properties of the surficial aquifer and characteristics of the water table in the town of Emerald Isle, North Carolina. The goal of that study was to determine how the groundwater system affects storm-water runoff. This study found that during storm events, the water table may crest above the land surface and contribute to storm-water runoff. However, that study only characterized the water table for the westernmost part of the island.

Manda et al. (2014) determined the risk of impairment to OWTS on Bogue Banks due to rising sea-level and found that the rising water table and thinning vadose zone can lead to chronic impairment of OWTS. Sea-level rise was simulated for three scenarios: 0.2, 0.5, and 1.0 m. At the most extreme sea-level rise scenario, 20% of the study area was inundated and 54% was unsuitable for OWTS, defined as where the water table is within 0.3 m of the drainfield beneath the ground. This was set as the cutoff because a depth to the water table of 0.3 m or less may allow contaminants to enter the groundwater system (Humphrey and O’Driscoll, 2011-a, Humphrey and O’Driscoll, 2011-b). Current North Carolina regulations suggest that 0.45 m of separation exist between the drainfield and the seasonal high water table (15A NCAC 18A.

1900). These studies, taken together, examine potential issues faced by barrier island groundwater systems.

Hydrogeologic Setting and Conceptual Model

Lautier (2001) characterizes the hydrogeologic framework of the North Carolina Coastal Plain aquifer system as having eight significant aquifers separated by confining units. From oldest to youngest, these aquifers are: the Lower Cape Fear, the Upper Cape Fear, the Black Creek, the Peedee, the Beaufort, the Castle Hayne, the Yorktown, and the Surficial aquifers (Figure 2). Winner and Coble (1996) describe two aquifers in addition to the eight described by Lautier: the Pungo River aquifer, which is overlain by the Yorktown, and the Lower Cretaceous aquifer, which lies beneath the Lower Cape Fear aquifer. Most aquifers are predominantly sand, sometimes with interbedded clay, silt, or shell material with the notable exception of the Castle Hayne aquifer, which consists of limestone. These aquifers range in age from Early Cretaceous to Holocene (Lautier, 2001). The formations dip eastward at an average rate of 7 m per km and thicken in the same direction (Lautier, 2001). The resulting sediment wedge varies from 30 m thick in the western coastal plain to more than 2400 m thick under Cape Hatteras and sits on top of Paleozoic basement rock as shown in Figure 2 (Lautier, 2001; Winner and Coble, 1996).

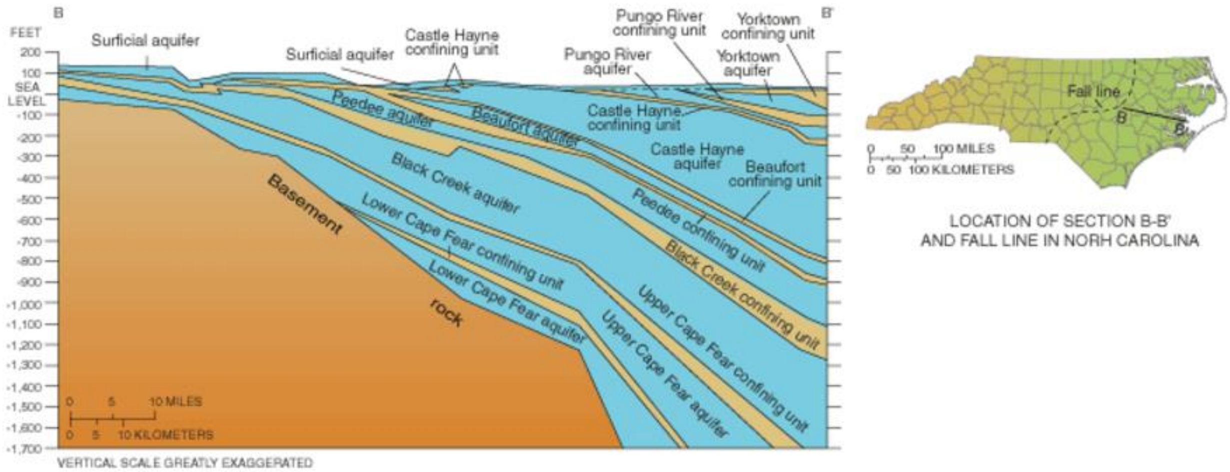

Figure 2: Hydrogeologic cross section of the North Carolina aquifer system (from Bales et al., 2004).

The surficial aquifer on Bogue Banks, or water table aquifer, is an unconfined, Quaternary aquifer composed mainly of sandy material with some beds of mud and clay typical of surficial aquifers present throughout the North Carolina Coastal Plain (Lautier, 2001). The predominant source of recharge to the surficial aquifers is precipitation. The average precipitation for a 10 year period from 1990 to 1999 in the North Carolina Coastal Plain was ~130 centimeters per year, but 52 to 92 % of annual precipitation is lost to runoff and evapotranspiration depending on soil infiltration capacity, land surface slope, and local evapotranspiration rates (Lautier, 2001). These estimates are for the entire coastal plain and may differ from local rates on a barrier island. The surficial aquifer has infiltration capacities of up to 50 cm per hour. Other possible sources of recharge are hydrologically connected units which allow lateral transmission of water from the mainland to offshore barrier islands (Lautier, 2001; Masterson et al., 2013-b).

A conceptual model of the groundwater system that may be impacted by sea-level rise on Bogue Banks is shown in Figure 3. In this conceptual model, only the surficial aquifer is considered. The dominant source of recharge for Bogue Banks is precipitation with additional artificial recharge coming from OWTS (Sisco, 2013). Not all the water from precipitation percolates to the water table as direct recharge. Some water is lost to the atmosphere through evapotranspiration, or the water may be lost as surface run-off (Sisco, 2013). Groundwater flows from areas of higher hydraulic head near the center of the island towards areas of lower hydraulic head near the coastlines (Sisco, 2013, Lautier, 2001). Groundwater levels are mainly driven by current sea-level and groundwater recharge. In most locations on the island, the water table is below the land surface. However, since the water table is close to or above the land surface in some of the low lying swales (e.g. where ponds and marshes exist), these areas are prone to present day temporary (e.g. after major precipitation events) or permanent groundwater inundation. As sea-level increases, magnitude and/or frequency of groundwater inundation is expected to increase because the elevation of the water table is expected to rise (Rotzoll and Fletcher, 2012). Although this issue has been studied in undeveloped barrier island settings (Masterson et al., 2013-a), this study seeks to understand the impact of groundwater inundation on a developed barrier island.

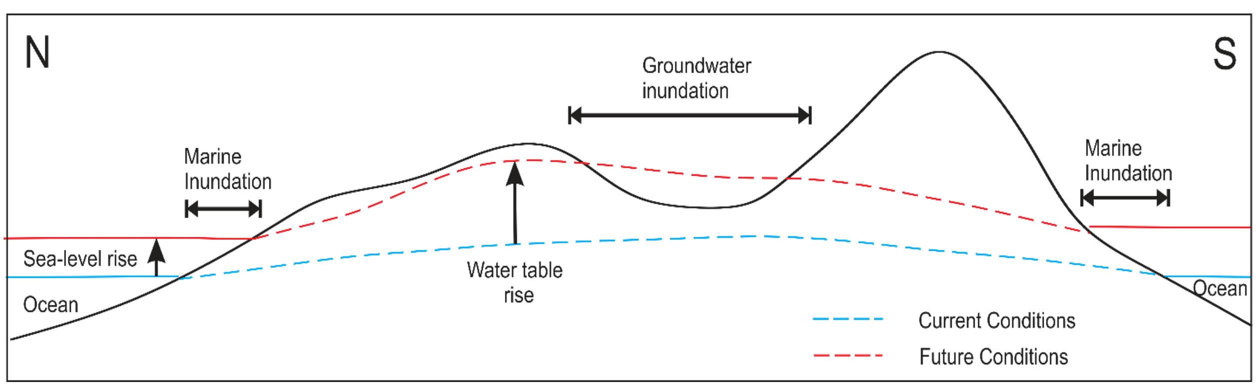

Figure 3- Conceptual model of the impact of sea-level rise on a barrier island water table.

METHODOLOGY

Well Installation

A total of 29 groundwater monitoring wells were installed in the surficial aquifer of Bogue Banks in the towns of Emerald Isle, Pine Knoll Shores, and Atlantic Beach (Figure 4) between 13 March, 2015 and 21 November, 2015. Locations were chosen based on accessibility and aerial coverage of the island. Wells were distributed in a variety of barrier island settings, including dunes, swales, ocean side, and sound side.

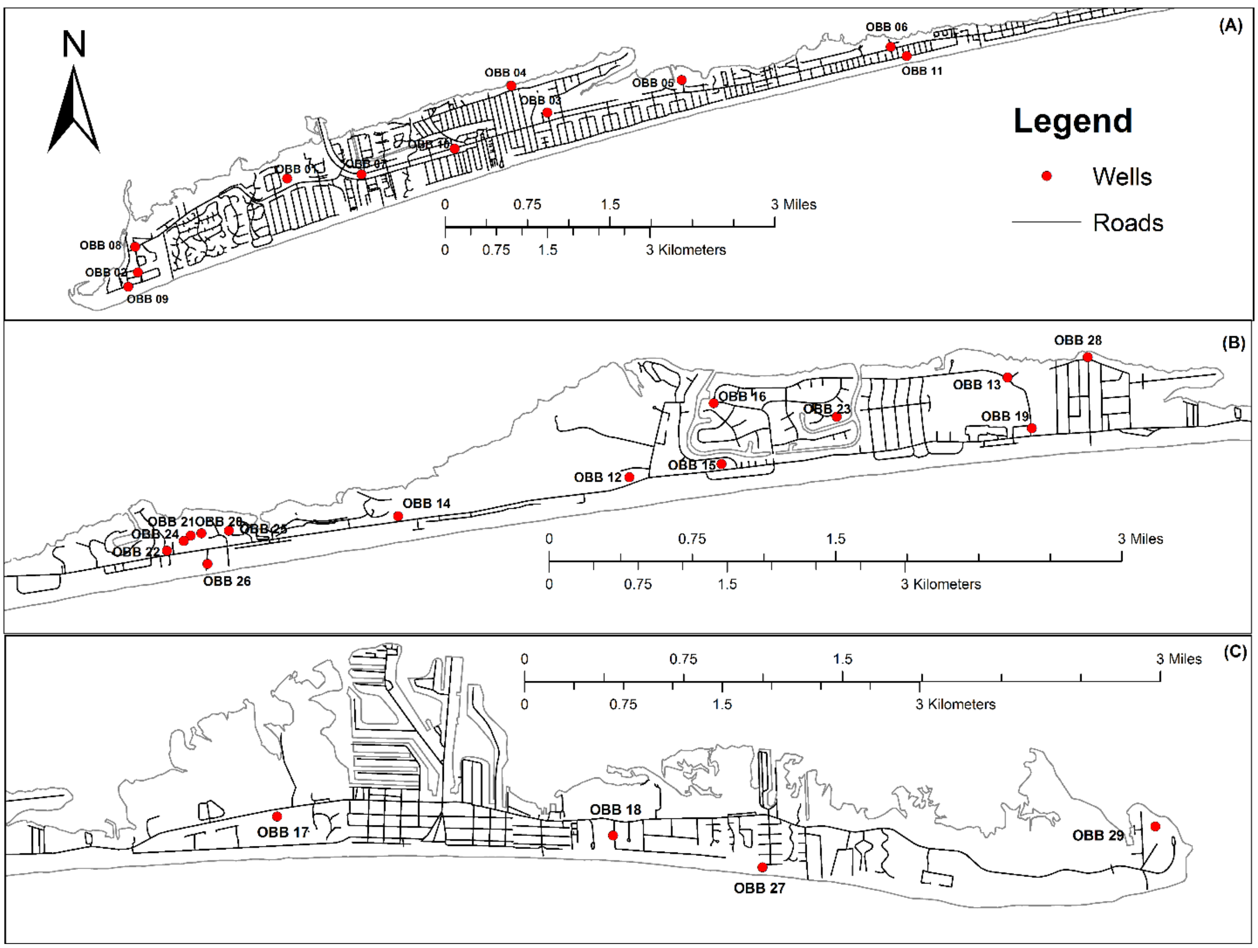

Figure 4: Map of the locations of the wells throughout (A) Emerald Isle, (B) Pine Knoll Shores, and (C) Atlantic Beach.

A direct push Geoprobe 540 UD drill rig was used to install all 29 monitoring wells (Figure 5). After using the Geoprobe to drill the desired depth, a 15 cm diameter hand auger was used to enlarge the first 0.6 m of the well to ensure compliance with state well construction standards. North Carolina monitoring well construction standards dictate the use of sand in the annular space between the well and the surrounding environment up to 0.45 m below the land surface, a bentonite clay seal up to 0.3 m below the land surface, and cement up to the land surface. The uppermost 1.5 m interval consists of a solid polyvinyl chloride (PVC) riser while the remaining sections of the well uses screened PVC pipe to allow free flow of water through the well (Figure 6).

Figure 5: The author (middle) installing a well using the Geoprobe.

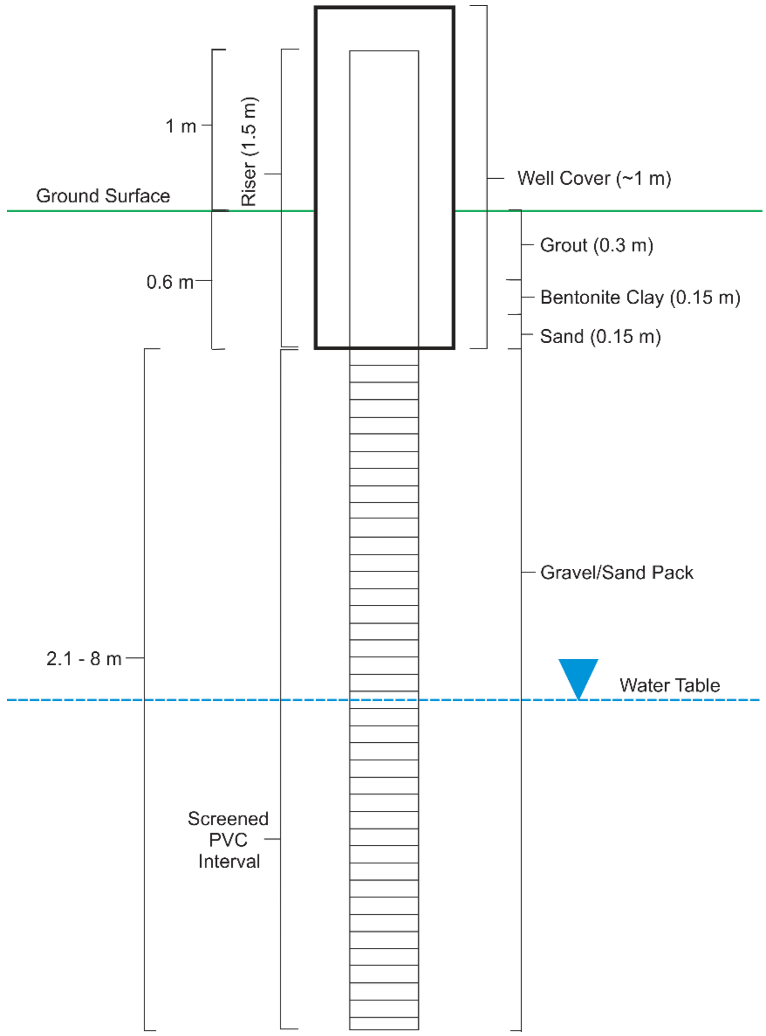

Figure 6: Diagram of an observation well.

Each completed well has a diameter of 1 inch (2.54 cm). The total depth was initially estimated based on the land surface elevation while later well depths were estimated based on existing data and previous experience. Wells ultimately varied in depth between 2.1 m and 8.0 m (Table 1). Each well was drilled below the water table to allow continued monitoring during water table fluctuations including the drier summer months when the water table drops.

Table 1: Monitoring well characteristics. Elevations are in reference to mean sea level

Well ID	Latitude	Longitude	Elevation of Top of Casing (m)	Elevation of Ground Surface (m)	Well Depth (m)	String and Logger length (m)	Logger Elevation (m)	Length of Casing Above Ground (m)
OBB 01	34.6596	-77.0685	4.423	3.563	5.486	6.2	-1.777	0.860
OBB 02	34.6478	-77.0928	1.852	1.242	2.438	2.91	-1.058	0.610
OBB 03	34.6677	-77.0268	1.824	0.937	5.131	5.417	-3.593	0.887
OBB 04	34.6714	-77.0324	2.810	1.893	3.658	4.451	-1.641	0.917
OBB 05	34.6717	-77.0052	2.307	1.390	2.134	2.935	-0.628	0.917
OBB 06	34.6757	-76.9718	3.638	2.729	3.606	3.542	0.096	0.908
OBB 07	34.6601	-77.0567	4.919	4.083	5.182	5.831	-0.912	0.835
OBB 08	34.6511	-77.0931	3.729	2.764	3.606	4.49	-0.761	0.965
OBB 09	34.6459	-77.0943	3.897	2.995	3.658	4.362	-0.465	0.902
OBB 10	34.6632	-77.0417	4.839	4.016	5.258	5.722	-0.883	0.823
OBB 11	34.6742	-76.9692	3.014	1.960	3.505	4.38	-1.366	1.055
OBB 12	34.6953	-76.8237	5.351	4.647	7.239	7.46	-2.109	0.704
OBB 13	34.7023	-76.7887	2.939	2.025	3.658	4.276	-1.337	0.915
OBB 14	34.6927	-76.8450	5.265	4.503	5.182	5.753	-0.488	0.762
OBB 15	34.6962	-76.8152	4.290	3.492	5.182	5.486	-1.196	0.799
OBB 16	34.7008	-76.8159	4.115	3.315	5.182	5.854	-1.739	0.801
OBB 17	34.7005	-76.7520	2.878	1.938	3.658	4.276	-1.398	0.939
OBB 18	34.6985	-76.7241	2.953	1.996	3.658	4.433	-1.480	0.957
OBB 19	34.6983	-76.7866	3.306	2.352	3.658	4.404	-1.098	0.954
OBB 20	34.6917	-76.8633	2.145	1.231	3.658	4.432	-2.287	0.914
OBB 21	34.6916	-76.8642	3.718	2.804	3.658	4.428	-0.710	0.914
OBB 22	34.6905	-76.8664	4.611	3.754	5.273	5.486	-0.875	0.856
OBB 23	34.6995	-76.8046	3.905	2.991	3.658	-	-	0.915
OBB 24	34.6911	-76.8648	3.571	2.669	3.658	4.264	-0.693	0.902
OBB 25	34.6919	-76.8607	2.515	1.643	3.658	4.296	-1.781	0.872
OBB 26	34.6894	-76.8628	7.660	6.749	8.001	8.326	-0.666	0.911
OBB 27	34.6961	-76.7118	4.311	3.397	3.658	4.254	0.057	0.915
OBB 28	34.7036	-76.7813	2.611	1.733	3.658	4.276	-1.665	0.878
OBB 29	34.6982	-76.6792	2.994	2.117	3.658	5.264	-2.270	0.878

Groundwater Monitoring

Water levels in 28 of the 29 monitoring wells were continuously monitored using Solinst Model 3001 and 3001 Junior Leveloggers (Figure 7). These water level loggers are pressure transducers which record absolute pressure (water pressure and barometric pressure), accurate to +/- 0.05% of full scale. However, water level readings must be corrected to account for barometric (atmospheric) pressure. At one well, a Solinst Model 3001 Barologger was deployed to record barometric pressure which was used to compensate the water level readings. One Barologger can be used to compensate readings for wells within about a 20 mile (30 km) radius because atmospheric pressure is not expected to change greatly in that area (https://www.solinst.com/products/data/ 3001.pdf). All loggers were set to collect readings at ten minute intervals, creating a time series of water levels ranging from 5 to 14 months (Appendix A). Manual water level measurements were taken at each well during data collection for the duration of the study using a water level meter. These readings were used to make sure the loggers were providing acceptable readings.

Figure 7- A Solinst levelogger used in the monitoring wells.

A Leica Builder 309 Total Station was used to survey the elevation of the top of the well casings using known elevations from National Geodetic Survey markers referenced to the North American Vertical Datum of 1988 (NAVD 88). A Real-Time Kinematic (RTK) Global Positioning System (GPS) was later used to confirm the elevations of previously surveyed wells and to survey wells which were too far from geodetic markers to be surveyed with the Total Station. Additionally, the RTK GPS was used to collect precise geographic coordinates of each well (Table 1).

Aquifer Properties

Hydraulic conductivity represents a volume of water transmitted through a one square unit length cross section of porous material at right angles to groundwater flow under a unit hydraulic gradient of 1:1 in a given amount of time (Heath, 1983). Acquiring an estimate of this property is essential to any study of an aquifer. Hydraulic conductivity was estimated using two methods: a falling head permeameter test and sieve analysis. Samples from ten well locations throughout Bogue Banks were selected for determining hydraulic conductivity at four foot intervals and the bottom of each well. The falling head permeameter test involves saturating a porous medium with water and measuring the time it takes for water in a tube to fall to a certain height (Fetter, 2001). The hydraulic conductivity can then be calculated by:

$$K = \frac{d_t^2 L}{d_c^2 t} \ln\left(\frac{h_0}{h}\right) \qquad \text{Eq. (1)}$$

where K is hydraulic conductivity (cm/s), L is sample length (cm), h_0 is the initial head in the falling tube (cm), h is the final head in the falling tube, t is the time needed to go from h_0 to h (s),

d_t is the inside diameter of the falling head tube (cm), d_c is the inside diameter of the sample chamber (cm).

In addition to the falling head permeameter test, sieve analyses were performed using a method set out by Driscoll **(**1986). Driscoll previously established the relationship between grain size and hydraulic conductivity. A dry sample is weighed then sent through a RoTap machine for two minutes. Cumulative weight percentages are recorded and a uniformity coefficient is calculated using the equation:

$$UC= (D_{40}/D_{90}) \qquad \text{Eq. (2)}$$

Where UC is the uniformity coefficient, D_{40} is the grain size representing the 40% retained size, and D_{90} is the grain size representing the 90% retained size. This is then graphed against D_{50} (which is the grain size representing the 50% retained size) grain size on previously published curves to determine permeability (it is assumed that the soil is of medium-density).

Although specific yield is not directly measured, a range of porosity values was determined using an Accupyc 1330 Pycnometer (Figure 8). This provides a theoretical range for specific yield if all water flows freely through pore spaces without being retained. The pycnometer is designed to measure density by giving the volume of a sample with a known mass. In order to estimate porosity, the sample chamber with a known volume must be completely filled with sample material. The resulting sample volume measurement will then be related to the total volume of the chamber and porosity can be calculated using the following equation:

$$n= (V_t-V_s)/ V_t \qquad \text{Eq. (3)}$$

where n is porosity, V_t is total volume of the sample chamber, and V_s is the sample volume. Care was taken not to compact the sample into the chamber due to the risk of compressing void space and artificially decreasing porosity. The sample chamber volume of the pycnometer was found to be 8.72 cm^3. Samples were taken from the bottom of each 4 foot sediment core for the same ten wells tested using the pycnometer. Each sample was measured five times (V1-V5) and deviations were given for each measurement (Appendix B).

Figure 8: Accupyc 1330 Pycnometer used to measure porosity.

Numerical Groundwater Modeling

The software program Visual MODFLOW was used to simulate groundwater flow in the surficial aquifer of Bogue Banks under steady-state conditions. Groundwater flow was simulated in a three-dimensional finite-difference model using the groundwater flow equation (Anderson et al., 2015). The model dimensions were 40,000 m x 10,000 m x 43.5 m discretized into 250 rows, 499 columns, and three layers (Figure 9). This results in a uniform cell size of 80 m x 40 m x 14.5 m (L x W x H). Since the water table was not expected to rise above the highest elevation of the island, the upper extent of the model was set to an elevation of 25 m to prevent interference with flow patterns at the top of the model. The lower extent of the model was set to -18.5 m based on the average depth to the first confining layer as determined using geophysical logs from the North Carolina Department of Environmental Quality (DEQ) Division of Water Resources. All cells which were not within the spatial extent of the island were set to inactive for computational efficiency.

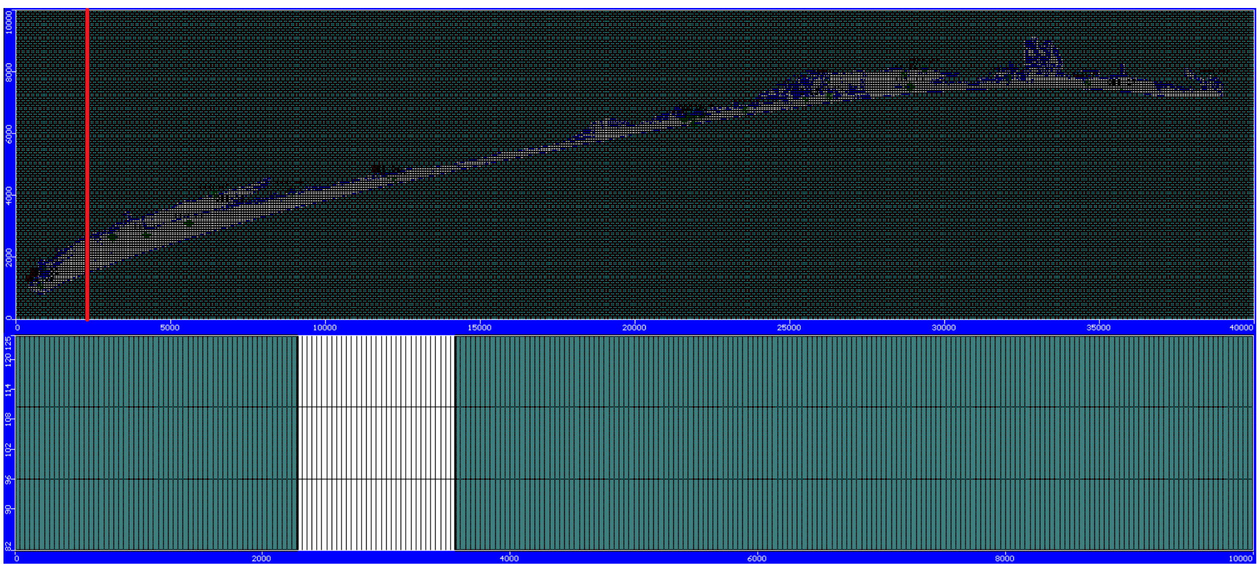

Figure 9- Model discretization in map view (top) and cross section (bottom).

A geospatial layer was used to represent the shoreline of Bogue Banks under present conditions. The mean high water elevation of 0.55 m was determined from a National Oceanographic and Atmospheric Administration (NOAA) tide gauge in nearby Beaufort, North

Carolina (https://tidesandcurrents.noaa.gov/sltrends/sltrends_station.shtml?stnid=8656483) and used as the baseline scenario. These measurements were taken for a standardized 19 year period from 1983 to 2001 used to measure values for tidal datums called the National Tidal Datum Epoch. In ArcGIS 10.3, the raster reclassify function was used to determine the trace of the shoreline at the mean high water level on the digital elevation model (DEM) of Bogue Banks. A shapefile of this outline was then created to represent base line (present day) conditions. This process was then repeated to create shapefiles that represented shorelines at sea-level increments of 0.2 to 1.4 m in 0.2 m intervals above the baseline. These outlines were then used as constant head boundaries in the groundwater modeling software. Separate outlines are required to properly simulate sea-level rise due to the fact that as sea-level rises, water will encroach landward in addition to moving up. Thus, the outline of Bogue Banks will be different at each scenario. This range of possible scenarios encompasses the likely best and worst case scenarios of sea-level rise by the year 2100 AD (Jevrejeva et al.; 2011, Rotzoll and Fletcher, 2013; Horton et al., 2014). Sea-level is assumed to change at a constant rate, though this may not be the case.

In a natural system, barrier islands move landward approximately 900 m for every one m of sea-level rise (Pilkey et al., 1980). However, Bogue Banks has been near its current position since about 1,100 years before present (BP) and has not exhibited marine transgression or regression and is assumed to remain stationary during the simulation time frame (Lazar et al., 2016). This lack of movement and a recent increase in relative sea-level rise rates (Kemp et al., 2009) may lead to more impairment of Bogue Banks by the year 2100 than in the previous several hundred years. Additionally, Bogue Banks would be assumed to remain stationary, both horizontally and vertically, due to anthropogenic influences. Subsidence at a rate of about 1 mm per year has been observed in Beaufort (Overton et al., 2015), but we are using conservative estimates and thus will not include subsidence. Aquifer properties derived from other aspects of this study were used as input parameters, including hydraulic conductivity, porosity, and specific yield estimates.

A geospatial layer obtained from Mew et al. (2002) was used to represent recharge to the surficial aquifer on Bogue Banks. Although initially containing hundreds of separate recharge zones, the layer was aggregated into categories by barrier island setting and location with recharge estimates ranging between 170 and 1209 mm/year (Table 2). Negative recharge (i.e. groundwater withdrawals) do not occur on a regular basis and are not included in the model. Evapotranspiration was applied to the model at a uniform rate of 223 mm/year (Sisco, 2013).

Table 2- Recharge zones on Bogue Banks

Zone	Setting	Recharge (mm/yr)
1	Inland Water	0.00
2	Atlantic Beach Urban	172.69
3	Pine Knoll Shores Urban	171.64
4	Emerald Isle Urban	170.00
5	Atlantic Beach Marshes	0.00
6	Pine Knoll Shores Marshes	0.00
7	Emerald Isle Marshes	0.00
8	Atlantic Beach Barrier Dunes	1209.18
9	Pine Knoll Shores Barrier Dunes	1199.83
10	Emerald Isle Barrier Dunes	1189.71
11	Atlantic Beach Back Barrier	287.53
12	Pine Knoll Shores Back Barrier	285.65
13	Emerald Isle Back Barrier	283.21
14	Back Barrier Water	0.00
15	Oceanside Dunes	1199.62

The model was run under steady-state conditions. Calibration is the process of changing one or more input parameters to minimize differences between observed and simulated data thus making the model match observed conditions. Calibration was achieved with the constant head boundary set at current sea-level (0 m). During the initial manual calibration phase, an anisotropic medium was assumed with equal K_x and K_y and K_z as one tenth of these values. Once the best possible manual calibration was achieved using a trial and error approach, parameter estimation (PEST) was used to refine hydraulic conductivity values leading to an anisotropic medium with different best possible value, leading to anisotropic K_x and K_y values. The initial calibration target was a normalized root mean square (NRMS) error of 10% or less, which is seen as an acceptable benchmark for model calibration (Lutz et al., 2009).

Geospatial Procedures

Geospatial modeling describes the process of using the results from Visual MODFLOW to calculate and visualize the impact of sea-level rise on Bogue Banks (Appendix C). Water level elevations were exported from Visual MODFLOW to ArcGIS and interpolated to form a water table surface (cell size=6.096 m^2). The resulting water table surfaces were then subtracted from the DEM to determine whether the water table was above or below the land surface. Positive values indicated that the water table was beneath the land surface while negative values indicated that the water table was above the land surface. The results were then combined with layers representing marine inundation derived from the DEM of Bogue Banks to determine which parts of the island were unimpaired, impaired by marine water, or impaired by groundwater. The proportion of land that was unimpaired, impaired by marine inundation or by groundwater inundation was then calculated under each sea-level rise scenario.

RESULTS AND DISCUSSION

Results from Groundwater Modeling

Calibration

The initial steady-state calibration target of a NRMS error of 10% was not achieved. The best NRMS error was about 20% (Figure 10).

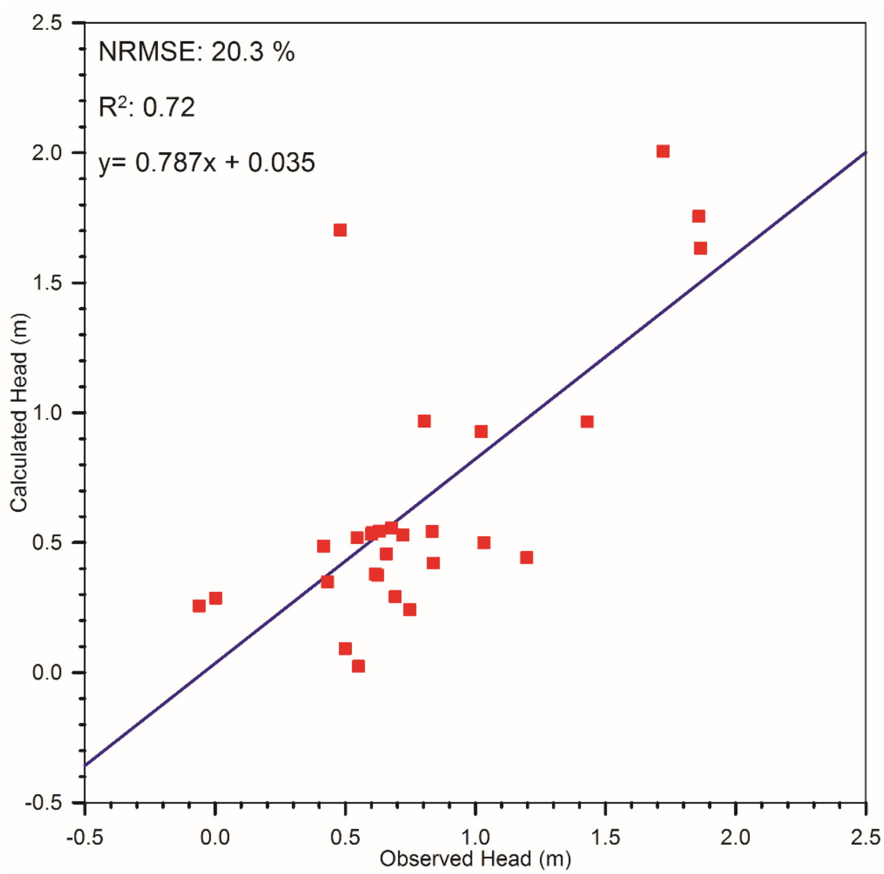

Figure 10- Observed vs simulated head for model with the best calibration (NRMS error=20%).

Residuals representing the difference between simulated and observed heads were plotted at each monitoring well throughout Bogue Banks (Figure 11). The residuals range from a low of 0.02 m to a maximum of 1.22 m. Ideally, the residuals should be as close to zero as possible as this indicates a better match between observed and simulated heads. High residuals are not limited to one area of Bogue Banks, indicating that no single area of the island is unreasonably modeled. The largest residuals are located at OBB 03 (1.22 m), OBB 18 (0.75 m), and OBB 22 (0.50 m) which are located in Emerald Isle, Atlantic Beach, and Pine Knoll Shores respectively. Higher residuals tend to be more concentrated on the eastern part of Bogue Banks while wells on the western portion of the island tend to have lower residuals. High residuals could occur as a result of heterogeneities in the aquifer or changes in storage, which is not considered in a steady-state model.

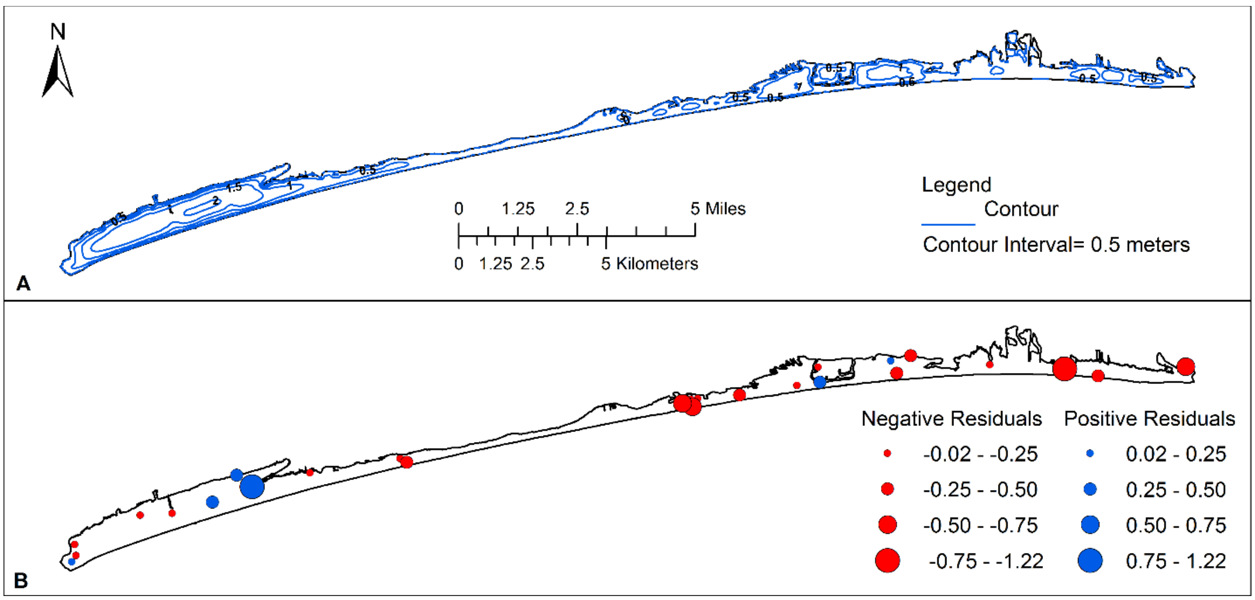

Figure 11- (A) Simulated water level contours for the calibrated model. (B) Residuals at well locations throughout Bogue Banks.

Sensitivity Analysis

Sensitivity analysis is performed to determine how changing input parameters will change the outcome of the model. This is necessary due to the fact that there are a range of possible values for many input parameters instead of one set value. After achieving calibration for current sea-level, recharge, hydraulic conductivity, and evapotranspiration were changed by plus and minus 25 and 50% individually. The mean and standard deviation of hydraulic head in each sensitivity run were then compared to the calibrated model statistics (Table 3). A mean head lower than that of the calibrated model implies that the average water table elevation is lower, indicating that more water is being taken out of the system and vice-versa. The greatest increase in mean water table elevation is caused by a 50% reduction in hydraulic conductivity while the greatest decrease is caused by a 50% decrease in recharge. The overall changes in mean water table elevation indicate that the model is equally sensitive to changes in hydraulic conductivity and recharge while not being as sensitive to changes in evapotranspiration.

Table 3- Sensitivity Analysis

Well ID	Calibrated	K+ 25%	K+ 50%	K- 25%	K- 50%	R +25%	R +50%	R- 25%	R- 50%	ET +25%	ET +50%	ET- 25%	ET- 50%
OBB 01	1.865	1.325	1.115	2.131	3.071	2.094	2.538	1.157	0.662	1.546	1.458	1.721	1.807
OBB 02	0.721	0.426	0.357	0.698	1.028	0.706	0.880	0.349	0.166	0.479	0.428	0.580	0.630
OBB 03	0.481	1.381	1.162	2.223	3.205	2.176	2.632	1.212	0.705	1.619	1.535	1.786	1.869
OBB 04	0.002	0.231	0.193	0.380	0.561	0.371	0.453	0.203	0.118	0.273	0.259	0.301	0.315
OBB 05	0.432	0.279	0.234	0.460	0.681	0.455	0.561	0.239	0.129	0.325	0.302	0.371	0.393
OBB 06	0.602	0.434	0.364	0.709	1.038	0.690	0.839	0.383	0.225	0.514	0.490	0.562	0.586
OBB 07	1.858	1.424	1.198	2.290	3.301	2.262	2.751	1.231	0.686	1.649	1.543	1.861	1.966
OBB 08	0.631	0.439	0.367	0.717	1.052	0.717	0.887	0.367	0.188	0.500	0.456	0.588	0.631
OBB 09	0.416	0.392	0.329	0.641	0.941	0.638	0.785	0.333	0.176	0.452	0.416	0.522	0.557
OBB 10	1.722	1.630	1.374	2.610	3.745	2.564	3.100	1.426	0.821	1.900	1.795	2.111	2.215
OBB 11	0.838	0.340	0.284	0.556	0.817	0.541	0.659	0.300	0.176	0.403	0.384	0.440	0.459
OBB 12	1.022	0.750	0.629	1.218	1.773	1.193	1.451	0.656	0.376	0.880	0.832	0.975	1.023
OBB 13	0.803	0.783	0.657	1.269	1.844	1.240	1.504	0.688	0.400	0.922	0.875	1.014	1.060
OBB 14	0.833	0.438	0.367	0.715	1.047	0.695	0.843	0.388	0.230	0.520	0.497	0.566	0.588
OBB 15	-0.061	0.207	0.173	0.340	0.500	0.330	0.402	0.183	0.108	0.246	0.235	0.268	0.279
OBB 16	0.624	0.302	0.253	0.495	0.730	0.481	0.586	0.267	0.158	0.359	0.343	0.391	0.407
OBB 17	0.615	0.304	0.254	0.500	0.739	0.504	0.629	0.249	0.119	0.343	0.307	0.413	0.448
OBB 18	1.197	0.356	0.298	0.582	0.855	0.573	0.703	0.307	0.170	0.415	0.388	0.468	0.495
OBB 19	1.429	0.780	0.655	1.267	1.844	1.246	1.520	0.676	0.379	0.910	0.855	1.021	1.076
OBB 20	0.545	0.418	0.351	0.684	1.004	0.665	0.808	0.371	0.220	0.497	0.475	0.541	0.563
OBB 21	0.601	0.430	0.360	0.703	1.031	0.683	0.829	0.381	0.225	0.511	0.488	0.556	0.578
OBB 22	1.033	0.403	0.338	0.659	0.967	0.640	0.778	0.357	0.212	0.479	0.458	0.521	0.542
OBB 24	0.678	0.448	0.375	0.732	1.073	0.711	0.864	0.397	0.235	0.532	0.509	0.579	0.602
OBB 25	0.658	0.369	0.309	0.603	0.885	0.586	0.712	0.327	0.194	0.438	0.419	0.477	0.496
OBB 26	0.747	0.195	0.163	0.321	0.476	0.311	0.380	0.172	0.102	0.232	0.222	0.253	0.263
OBB 27	0.692	0.234	0.196	0.385	0.569	0.379	0.466	0.203	0.112	0.274	0.257	0.309	0.326
OBB 28	0.499	0.075	0.063	0.123	0.182	0.120	0.147	0.066	0.038	0.089	0.084	0.098	0.102
OBB 29	0.550	0.019	0.016	0.031	0.046	0.040	0.055	0.008	-0.008	0.014	0.004	0.034	0.044
Mean	0.787	0.529	0.444	0.859	1.250	0.843	1.027	0.461	0.261	0.619	0.583	0.690	0.726
Standard Deviation	0.470	0.420	0.354	0.672	0.963	0.660	0.798	0.367	0.212	0.490	0.462	0.544	0.571

Uncertainty

Due to the inherent uncertainty in future conditions, all models should include estimates of uncertainty (Tartakovsky, 2012). One method of characterizing uncertainty is a process called scenario modeling in which several forecasts are made representing a range of possible outcomes (Anderson et al., 2015). In this study, this is accomplished by performing seven sea-level rise forecasts from the best case scenario of 0.2 m to the worst case scenario of 1.4 m above the baseline.

Forecasts of Groundwater and Marine Inundation

Increasing sea-level causes progressively greater groundwater impairment from 28.02% to 48.22% of the total area of Bogue Banks (Table 4).

Table 4- Groundwater impairment of Bogue Banks due to changes in sea-level

Change in sea-level	Impaired Area (Km^2)	Unimpaired Area (Km^2)	Impaired %	Unimpaired %
0.2 m	6.92	16.52	28.02	71.98
0.4 m	8.04	14.05	32.55	67.45
0.6 m	9.95	12.14	40.28	59.72
0.8 m	10.35	10.03	41.90	58.10
1.0 m	10.45	8.25	42.31	57.69
1.2 m	11.83	6.87	47.89	52.11
1.4 m	11.91	5.20	48.22	51.78

Although the focus of this research is on groundwater inundation, the problems of sea-level rise are compounded when the influence of marine inundation is included. Marine inundation accounts for 5.11% impairment at 0.2 m of sea-level rise to 30.73% inundation at 1.4 m of sea-level rise (Table 5).

Table 5- Marine impairment of Bogue Banks due to changes in sea-level

Change in sea-level	Impaired Area (Km^2)	Unimpaired Area (Km^2)	Impaired %	Unimpaired %
0.2 m	1.26	23.44	5.11	94.89
0.4 m	2.61	22.09	10.58	89.42
0.6 m	2.61	22.09	10.58	89.42
0.8 m	4.32	20.38	17.49	82.51
1.0 m	6.00	18.70	24.29	75.71
1.2 m	6.00	18.70	24.29	75.71
1.4 m	7.59	17.11	30.73	69.27

When marine and groundwater inundation are combined, the baseline impairment is 33.13% increasing progressively to 78.95% total impairment at 1.4 m sea-level rise (Table 6). Inundation maps of Bogue Banks under each sea-level rise scenario can be seen in Figure 12.

Table 6- Combined marine and groundwater impairment due to changes in sea-level

Change in sea-level	Impaired Area (Km^2)	Unimpaired Area (Km^2)	Impaired %	Unimpaired %
0.2 m	8.18	16.52	33.13	66.87
0.4 m	10.65	14.05	43.13	56.87
0.6 m	12.56	12.14	50.86	49.14
0.8 m	14.67	10.03	59.39	40.61
1.0 m	16.45	8.25	66.60	33.40
1.2 m	17.83	6.87	72.18	27.82
1.4 m	19.50	5.20	78.95	21.05

When calculating groundwater impairment, the total area of Bogue Banks is used as the benchmark from which to calculate percent impairment. For example, in the first scenario (0.2 m change in sea-level), Bogue Banks has a total area of 24.7 km^2. Of that, 1.26 km^2 is impaired by marine inundation. Groundwater inundation impairs 6.92 km^2 out of 24.7 km^2, accounting for 28.02% of the island.

The results indicate that groundwater inundation will impair more land than marine inundation in each scenario. Groundwater inundation accounts for between 4.45 to 7.34 km^2 more inundated area than marine water (Appendix D). This study, one of few to examine the influence of sea-level rise on groundwater inundation, indicates that groundwater inundation may be more problematic than marine inundation as sea level reaches moderate or high levels. Even under the most optimistic sea-level rise projection (0.2 m above baseline), almost 30% of Bogue Banks is impaired by groundwater and 33% is impaired by both marine and groundwater inundation. Therefore, local governments and residents should consider the effects of groundwater inundation in addition to marine inundation as a consequence of sea-level rise.

Governments and residents of Bogue Banks are concerned about the potential impact of inundation on preexisting infrastructure. If current population trends continue, Bogue Banks may see as many as 8,600 permanent residents by the year 2100, potentially leading to more developed area and more infrastructure impairment (http://www.census.gov). It is therefore prudent to quantify what percentage of currently developed areas are inundated in each scenario. Bogue Banks has three development categories based on percent of impervious cover: low intensity has 20-29%, medium intensity has 50-79%, and high intensity has 80 to 100%. Groundwater inundation would impair between 22.5% and 61.7% in lightly developed areas (Table 7), 17% and 62.2% in moderately developed areas (Table 8), and 29.5% and 63.5% of heavily developed areas of Bogue Banks under sea-level rise scenarios of 0.2- 1.4m above present conditions (Table 9). The results indicate that the proportion of developed land impaired by groundwater is generally smaller than the proportion of undeveloped land that is impaired by groundwater (Table 10).

Table 7- Proportion of lightly developed areas that are impaired by groundwater inundation on Bogue Banks due to changes in sea-level

Change in Sea-Level	Unimpaired %	Groundwater %
0.2 m	77.55	22.45
0.4 m	69.34	30.66
0.6 m	61.47	38.53
0.8 m	55.44	44.56
1.0 m	50.49	49.51
1.2 m	43.76	56.24
1.4 m	38.26	61.74

Table 8- Proportion of moderately developed areas that are impaired by groundwater inundation on Bogue Banks due to changes in sea-level

Change in Sea-Level	Unimpaired %	Groundwater %
0.2 m	82.97	17.03
0.4 m	71.87	28.13
0.6 m	63.32	36.68
0.8 m	56.71	43.29
1.0 m	52.20	47.80
1.2 m	44.23	55.77
1.4 m	37.79	62.21

Table 9- Proportion of heavily developed areas that are impaired by groundwater inundation on Bogue Banks due to changes in sea-level

Change in Sea-Level	Unimpaired %	Groundwater %
0.2 m	70.54	29.46
0.4 m	56.79	43.21
0.6 m	48.56	51.44
0.8 m	46.38	53.62
1.0 m	44.78	55.22
1.2 m	38.36	61.64
1.4 m	36.45	63.55

Table 10- Proportion of land that is impaired by groundwater inundation on Bogue Banks due to changes in sea-level based on developed and undeveloped land

	Developed Land		Undeveloped Land	
Change in Sea-Level	Unimpaired %	Groundwater Inundation%	Unimpaired %	Groundwater Inundation %
0.2 m	78.71	21.29	69.78	30.22
0.4 m	69.56	30.44	61.06	38.94
0.6 m	61.50	38.50	51.90	48.10
0.8 m	55.49	44.51	45.35	54.65
1.0 m	50.76	49.24	39.78	60.22
1.2 m	43.73	56.27	32.27	67.73
1.4 m	38.10	61.90	27.69	72.31

0.4 m

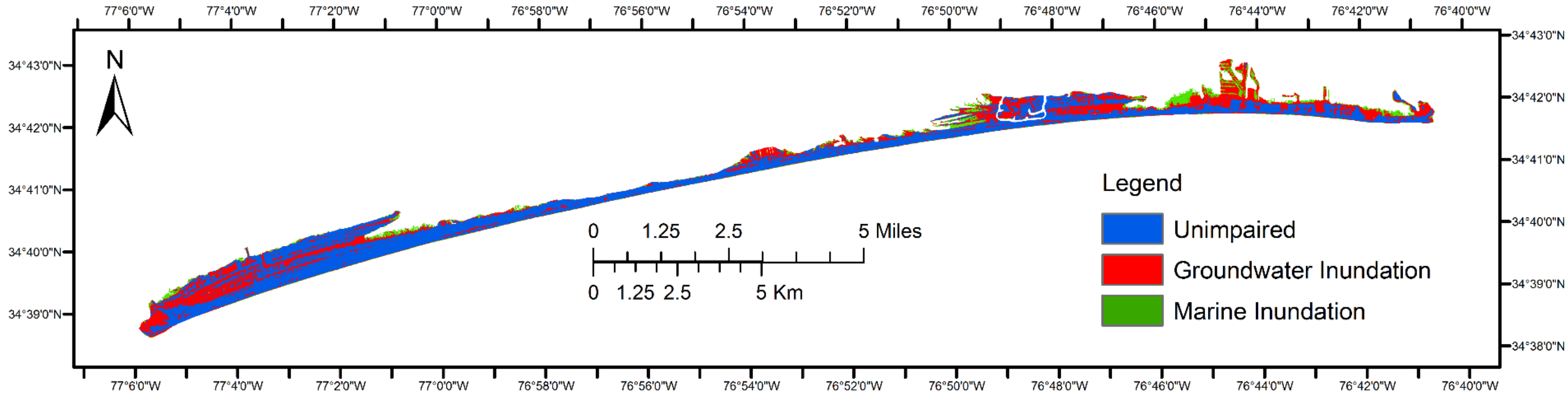

0.6 m

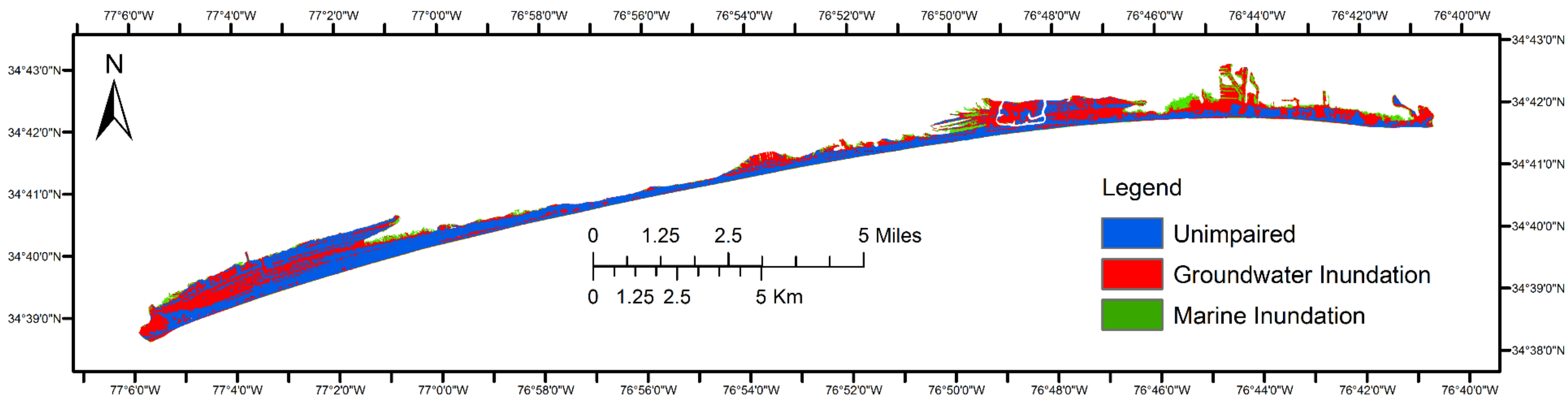

Figure 12- Examples of inundation maps from 0.4 and 0.6 m of sea-level rise. Other maps can be seen in Appendix E.

Total impairment of Bogue Banks could be underestimated due to the estimation of aquifer properties throughout Bogue Banks. The aquifer was assumed to be homogeneous and anisotropic with values: Kx= 14.25 m/d, Ky= 9.00 m/d, and Kz= 0.11 m/d. Previous studies on Bogue Banks found hydraulic conductivities of between 0.1 and 6.4 meters per day (m/d), although these values were estimated using a different method (Sisco, 2013). These conductivities were found in less permeable material in swales in Emerald Isle. Lower conductivities would mean that water moves more slowly through the aquifer, which would lead to a higher water table and more inundated area. It is important to note that as hydraulic conductivity can vary over 12 orders of magnitude, so a difference of less than 10 m/d is not considered significant (Heath, 1983).

In addition to recharge from precipitation, recharge could be provided by effluent from OWTS systems and package treatment plants. Average monthly flows from seven package treatment plants are between 1,015 and 32,597 gallons per day (Mahoney, 2016). As observed in the sensitivity analysis, the surficial aquifer is sensitive to increases in recharge. The primary source of usable water on Bogue Banks is the Castle Hayne aquifer and water withdrawn from the Castle Hayne may ultimately become effluent through OWTS systems. The impact of OWTS systems on Bogue Banks could be simulated similar to stormwater infiltration basins (e.g. Carleton, 2010) to determine if there is a significant impact on the water table due to groundwater mounding under these systems.

From 1950 to 2012, an increase in nuisance flooding was seen at the NOAA gauge in nearby Beaufort, North Carolina (Sweet et al., 2014). As sea-level rise increases in severity, the impact of groundwater inundation outpaces the impact of marine inundation. Groundwater impairs between 4.32 and 7.34 km^2 more area of the island than marine inundation. Thus, in each sea-level rise scenario, groundwater inundation could be a bigger concern than marine inundation on Bogue Banks unless the flooding is managed or mitigated. In the context of this study, impairment is defined as where the water table crests above the land surface. However, infrastructure degradation may occur long before this occurs. OWTS are impaired when the water table is within 0.3 m of the drainfield, which may be 0.45 or 0.9 m below ground (Manda et al., 2014). Therefore, impairment may be higher than noted above because a greater percentage of Bogue Banks may not be suitable for further development unless other means are developed, e.g., centralized sewer systems. This demonstrates the need for proactive planning regarding the impacts of sea-level rise on low-lying coastal regions worldwide. Continued public education and outreach is one avenue that may be taken to addressing the potential impacts of sea-level rise. In the future, residents may need to consider whether to stay on the island or not. If many residents stay, it may not be too early to start considering preserving undeveloped land to accommodate infiltration, stormwater runoff, and permanent inundation. Adapting infrastructure to address rising sea-levels and increased flooding should be considered as a long term solution. In the event of permanent land degradation, migration off of Bogue Banks may be an attractive solution. In this scenario, the financial burden on individuals, families, and businesses could be eased by government intervention through the provision of incentives, buybacks, or catastrophe relief funds.

Further research studies on the groundwater flow systems on Bogue Banks should include efforts to move from a steady-state to a transient state model. Transient models would incorporate more hydrogeologic parameters, such as storage and seasonal variability. Research on mitigation methods based on this and a transient model would entail a more solution based approach to inundation on Bogue Banks. Sisco (2013) using a steady state model examined the impact of pumping 500 and 1000 m^3 per day from the surficial aquifer and found that there was a high probability of drawing salt water from nearby surface water bodies. Future studies should address this problem by using transient models to examine how groundwater withdrawals may be a suitable mitigation strategy to lessen the effects of groundwater inundation under varying environmental conditions on the island.

Impact of Tidal Fluctuations

Previous studies have examined how tides influence the height of a water table in coastal settings (Carol et al., 2009). This necessitates a quantification of the impact tides have on the Bogue Banks water table.

Data from 23 wells were examined for tidal influences and oscillations were observed in ten wells ranging from 0.008 m to 0.03 m (Figure 13). While the results indicate that oscillations tend to decrease farther from the nearest shoreline, several wells not showing tidal influence were closer to the shore than wells that did show tidal influence. There is no apparent relationship between magnitude of tidal fluctuation and residuals from the calibrated model. Also, the outlier at OBB 08 with an oscillation of 0.03 m has one of the lowest residuals while the lowest oscillation seen at OBB 25 has a residual of 0.2 m. Due to the low magnitude of the oscillations relative to sea-level rise, tidal influence was not included in the forecasting models.

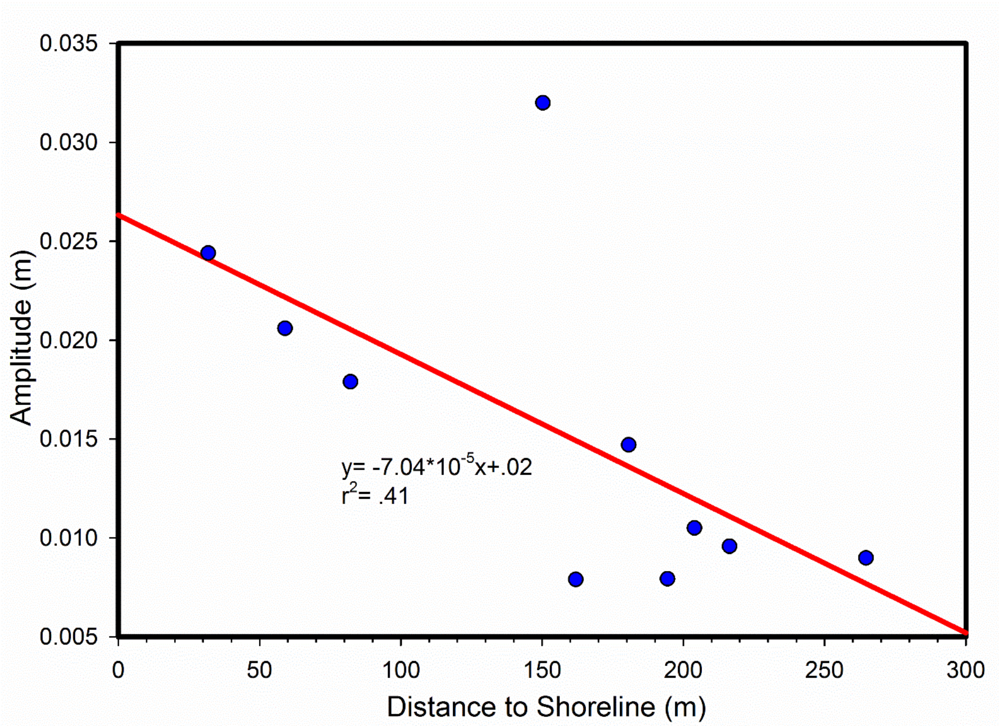

Figure 13- Relationship between distance to shoreline and water table amplitude.

Assumptions and Limitations

There are several limitations inherent in this model. Many of these are due to parameter assumptions which do not accurately represent the surficial aquifer. Several parameters are assumed to be constant throughout the entire model or a large area therein. These include evapotranspiration, which changes based on the type of vegetation, wind speed, water and energy availability, and may change as a result of climate change due to the increase in water at or near the land surface. Hydraulic conductivity is assumed to be a uniform, representative value throughout the entire study area despite a known range of values. Since the thickness of the surficial aquifer is assumed to be uniform, this implies that transmissivity is also uniform.

Resolution of the visual MODFLOW grid could be problematic in this model. While there is no limit to the number of rows and columns in MODFLOW, Visual MODFLOW limits the number to 500 each. This creates a minimum grid size of 80 meters. Therefore, some water level data may be generalized due to the grid size.

Sea-level is assumed to rise under a constant rate. However, sea-level rise rates have changed in the recent past (Lavelle-Levinson et al., 2017) and as climate changes, sea-level may change at varying rates between now and the year 2100. Any potential change in the rate of sea-level rise is not accounted for in a steady-state model. Another potential consequence of climate change may be a change in precipitation rates. Sayemuzzaman and Jha (2014) found that precipitation rates in the North Carolina coastal plain vary seasonally. In this study, changes in precipitation were only accounted for in the sensitivity analysis phase. In a transient state model, the water table fluctuation method may be used to obtain local recharge estimates from water level data. This would also allow future researchers to account for seasonal variability in recharge rates. A transient model will also allow future researchers to account for seasonal changes in the water table, temperature, precipitation, and evapotranspiration.

Another limitation inherent in steady-state models is that there is no change in storage. Storage is the amount of water taken into or out of pore spaces per unit surface area per unit head change (Heath, 1983). In an unconfined aquifer, like the surficial aquifer on Bogue Banks, water is released from gravity drainage, meaning that the water source is specific yield. However, neither storage nor specific yield have any effect on the steady-state model. This does not accurately represent the surficial aquifer and could be a significant source of error. Finally, transient models allow researchers to collect data from intermediate points in simulations. For example, data forecasting inundation in the year 2050 may be collected and used, whereas the current steady-state model only allows for final projections to the year 2100.

In a natural system, barrier islands move landward approximately 1000 feet for every one foot of sea-level rise (Pilkey et al., 1980). However, Bogue Bank is assumed to remain at its current location due to anthropogenic influences. This implies that there is no lateral or vertical movement for the next 83 years.

SUMMARY AND CONCLUSIONS

This study is one of few that seeks to understand the impact of sea-level rise on a groundwater system on a barrier island. The goals of this study were to derive the hydrogeologic properties of the surficial aquifer, simulate the water table, and assess the effect of sea-level rise on the water table on Bogue Banks. A three-dimensional finite-difference model was constructed in Visual MODFLOW to simulate the location of the water table under seven sea-level rise scenarios between 0.2 and 1.4 m above current mean high water.

Hydraulic conductivity of the surficial aquifer on Bogue Banks was found to range between 3.3 m/d and 54.4 m/d with an average of 24.0 m/d. Values of porosity were found to range between 0.29% and 0.40% with an average of 0.34% (Appendix B). These values agree with previous research on materials like the ones comprising the surficial aquifer and were used as input parameter ranges for the numerical groundwater model (Heath, 1983).

The model generated in this study has issues which may affect the forecasting of the effects of sea-level rise. The surficial aquifer is assumed to be homogeneous and anisotropic throughout the study area, though a range of possible conductivities has been established. Sea-level is assumed to rise under a constant rate to levels forecast to be present in the year 2100, though sea-level rise changes at variable rates (Kemp et al., 2009).

The results of this study show that sea-level rise causes the water table to rise, cresting above the land surface in even the least severe circumstances. These results support the hypothesis- that rising sea levels will cause the water table to rise above the land surface and that increasing sea-level will cause groundwater inundation greater than 40%. The results support the hypothesis for changes in sea-level of 0.6 m and greater. Forecasts show that increasing sea-level will cause groundwater inundation between 28.0% and 48.2% of the total area of Bogue Banks. When combined with the impacts of marine impairment, this number increases to between 33.1% and 78.9% of Bogue Banks. According to the results, groundwater inundation is more severe than marine inundation for each sea-level rise scenario. Local and state governments should consider proactive flood management or mitigation strategies which may include public outreach, migration, undeveloped land preservation, adapting to changing conditions, or financial incentives.

REFERENCES

Anderson, M. P., Woessner, W.H., and Randall J., 2015, Applied groundwater modeling: Simulation of flow and advective transport. Academic Press: San Diego, 2015, 384 p.

Bales, J.D., Chapman, M.J., Oblinger, C.J., Robbins, J.C., 2004, North Carolina District Science Plan Science Goals for 2003-2008, U.S. Geological Survey OFR 2004-1025, https://nc.water.usgs.gov/reports/ofr041025/report.html.

Carleton, G.B., 2010, Simulation of Groundwater Mounding Beneath Hypothetical Stormwater Infiltration Basins, U.S. Geological Survey Scientific Investigations Report 2010-5102, 64 p.

Carol, E.S., Kruse, E.E., Pousa, J.L., and Roig, A.R., 2009, Determination of heterogeneities in the hydraulic properties of a phreatic aquifer from tidal level fluctuations: a case in Argentina: Hydrogeology, v. 17, p. 1727-1732, doi: 10.1007/s10040-009-0478-3.

Driscoll, F.G., 1986, Groundwater and wells, Second Edition. Johnson Division: St. Paul, Minnesota, 1986, 31 p.

Fetter, C.W. 2001, Applied hydrogeology, Fourth Edition, Prentice Hall: Upper Saddle River, NJ, 190 p.

Ferguson, G., and Gleeson, T., 2012, Vulnerability of coastal aquifers to groundwater use and climate change: Nature Climate Change, v. 2, p. 342-345.

Guha, H., and Panday, S., 2012, Impacts of sea-level rise on groundwater salinity in a coastal community of south Florida: Journal of American Water Resources Association, v. 48, p. 510-529.

Horton B.P., Rahmstorf, S., Engelhart, S.E., and Kemp, A.C., 2014, Expert assessment of sea-level rise by AD 2100 and AD 2300: Quaternary Science Reviews, v. 84, p. 1–6.

Heath, R.C., 1983, Basic Ground-Water Hydrology: USGS Water-Supply Paper 2220, 86p.

Humphrey Jr, C.P., O'Driscoll, M., 2011a, Cumulative saturation of low chroma soil colors and shallower depths: International Journal of Soil Science, v. 6, p. 249-258.

Humphrey Jr, C.P., O'Driscoll, M., 2011b, Evaluation of soil colors as indicators of the seasonal high water table in coastal North Carolina: International Journal of Coastal Science, v. 6, p. 103-113.

Jevrejeva, S., Moore, J.C., and Grinsted, A., 2012, Sea level projections to AD2500 with a new generation of climate change scenarios, Global and Planetary Change, v. 80–81. p. 14–20.

Kemp, A.C., Horton, B.P., Culver, S.J., Corbett, D.R., Plassche, O., Gehrels, W.R., Douglas, B.C., Parnell, A.C., 2009, Timing and magnitude of recent accelerated sea-level rise (North Carolina, United States): Geology, v. 37, p. 1035-1038, doi: 10.1130/G30352A.1.

Kopp, R.E., Horton, B.P., Kemp, A.C., Tebaldi, C., 2014, Past and future sea-level rise along the coast of North Carolina, USA: Climate Change, 17 p. DOI: 10.1007/s10284-015-1451-x.

Lavelle-Levinson, A., Dutton, A., Martin, J.B., 2017, Spatial and temporal variability of sea level rise hot spots over the eastern United States: Geophysical Research Letters, v.44, p. 7876-7882, doi: 10.1002/2017GLO73926.

Langevin, C.D., and Zygnerski, M., 2013, Effect of sea-level rise on salt water intrusion near a coastal well field in southeastern Florida: Ground Water. v. 51, p. 801-803.

Lautier, J. C., 2001, Hydrogeologic framework and ground water condition in the North Carolina Central Coastal Plain: North Carolina Department of Environment and Natural Resources, Division of Water Resources.

Lazar, K. B., Mallinson, D. J., and Culver, S. J., 2016, Late Quaternary development of the Croatan Beach Ridge Complex, Bogue Sound, Bogue Banks, NC, USA and implications for coastal evolution: Estuarine, Coastal, and Shelf Science, v. 174(2016), p. 49-64.

Lutz, A., Thomas, J. M., Pohll, G., Keita, M., and McKay, W.A., 2009, Sustainability of groundwater in Mali, West Africa: Environmental Geology, v. 58, p.1441-1450.

Mahoney, R.N., 2016, Nutrient and bacteria dynamics of package treatment plants in coastal Carteret County, North Carolina, [M.S. thesis]: Greenville, NC, East Carolina University.

Masterson, J.P., and Garabedian, S.P., 2007, Effects of sea-level rise on ground water flow in a coastal aquifer system: Ground Water, v. 45, p. 20,209-217.

Manda, A.K., Sisco, M.S., Mallinson, D.J., Griffin, M.T., 2014, Relative role and extent of marine and groundwater inundation on a dune-dominated barrier island under sea-level rise scenarios: Hydrological Processes, 11p. DOI: 10.1002/hyp.10303.

Masterson, J.P., Fienen, M.N., Thieler, E.R., Gesch, D. B., Gutierrez, B.T., and Plaint, N.G., 2013a, Effects of sea level rise on barrier island groundwater system dynamics- Ecohydrological implications: Ecohydrology, v.7, 1064–1071. doi: 10.1002/eco.1442

Masterson, J.P, Fienen, M.N., Gesch, D.B., and Carlson, C.S., 2013b, Development of a numerical model to simulate groundwater flow in the shallow aquifer system of Assateague Island, Maryland and Virginia, U.S. Geological Open-File Report 2013-1111. http://pubs.usgs.gov/of/2013/1111/.

Mew Jr., H.E., Hirth, D.K., Lewis, D.V., Daniels, R.B., Keysworth, A.J., 2002, Methodology for Compiling Ground Water Recharge Maps in the Piedmont and Coastal Plain Provinces of North Carolina: NC DENR Groundwater Bulletin Number 25, 76 p.

National Oceanographic and Atmospheric Administration, 2013, NOAA Tides and Currents Station Selection: https://tidesandcurrents.noaa.gov/datums.html?units=1&epoch=0&id=8656483&name=Beaufort&state=NC (accessed December, 2015).

National Oceanographic and Atmospheric Administration, 2013, Mean Sea Level Trend, Beaufort, North Carolina: https://tidesandcurrents.noaa.gov/sltrends/sltrends_station.shtml?stnid=8656483 (accessed September 2017).

Nicholls, R.J., and Cazenave, A., 2010. Sea-level rise and its impact on coastal zones: Science, v. 328, p. 1517-1520.

Oude Essink, P.H.P., van Baaren, E.S., and de Louw, P.G.B., 2010, Effects of climate change on coastal groundwater systems: a modeling study in the Netherlands: Water Resources Research. 49. DOI: 10.1029/2009/WR008719.

Overton, M., Birkemeier, W., Benton, S., Cleary, W., Jarrett, T., Peterson, C., Riggs, S.R., Rogers, S., Rudolph, G., Sciaudone, E.J., 2015, North Carolina sea level rise assessment report: N.C. Coastal Resources Commission Science Panel (accessed September, 2017).

Pilkey Jr., O.H., Neal, W.J., Pilkey Sr., Orrin H., and Riggs, S.R., 1980, From Currituck to Calabash: Living with North Carolina's barrier islands, Second Edition. North Carolina Science and Technology Research Center.

Rotzoll, K., and Fletcher, C.H., 2012, Assessment of groundwater inundation as a consequence of sea-level rise: Nature Climate Change. DOI: 10.1038/NCLIMATE1725.

Sayemuzzaman, M., Jha, M.K., 2014, Seasonal and annual precipitation time series trend analysis in North Carolina, United States: Atmospheric Research, v. 137, p.183-194, https://doi.org/10.1016/j.atmosres.2013.10.012

Sisco, M.S., 2013, Assessing the shallow groundwater system as a potential factor in generating storm-water runoff on a North Carolina barrier island, [M.S. thesis]: Greenville, NC, East Carolina University.

Stoll, S., Franssen, H.J. Hendricks, Barthel, R., and Kinzelbach, W., 2011, What can we learn from long-term groundwater data to improve climate change impact studies?: Hydrology and Earth System Sciences, v. 15, p. 3861-3875. DOI: 10.5194/hess-15-3861-2011.

Stutz, M.L., and Pilkey, O.H., 2011. Open-ocean barrier islands: Global influence of climatic, oceanographic, and depositional settings: Journal of Coastal Research, v. 27, p. 207-222.

Sweet, W., Park, J., Marra, J., Zervas, C., and Gill, S., 2014. Sea level rise and nuisance flood frequency changes around the United States: NOAA Technical Report NOS CO-OPS 073.

Tartakovsky, D.M., 2013. Assessment and management of risk in subsurface hydrology: A review and perspective: Advances in Water Resources, v. 51, p.247-260. http://dx.doi.org/10/1016/j.advwatres.2012.04.007.

Timmons, E.A., Rodriguez, A.B., Mattheus, C.R., and Dewitt, R., 2010, Transition of a regressive to a transgressive barrier island due to back-barrier erosion, increased storminess, and low sediment supply: Bogue Banks, North Carolina, USA: Marine Geology, v. 278, p. 100-114.

United States Census Bureau, Population Division, Annual Estimates of the Resident Population: April 1, 2010 to July 1, 2016: https://factfinder.census.gov/faces/tableservices/jsf/pages/productview.xhtml?src=bkmk (accessed October 2017).

Winner Jr, M.D., and Coble, R.W., 1996. Hydrogeologic framework of the North Carolina coastal plain. U.S. Geological Survey Professional Paper 1401-1.

Appendix A- Water Level Time Series

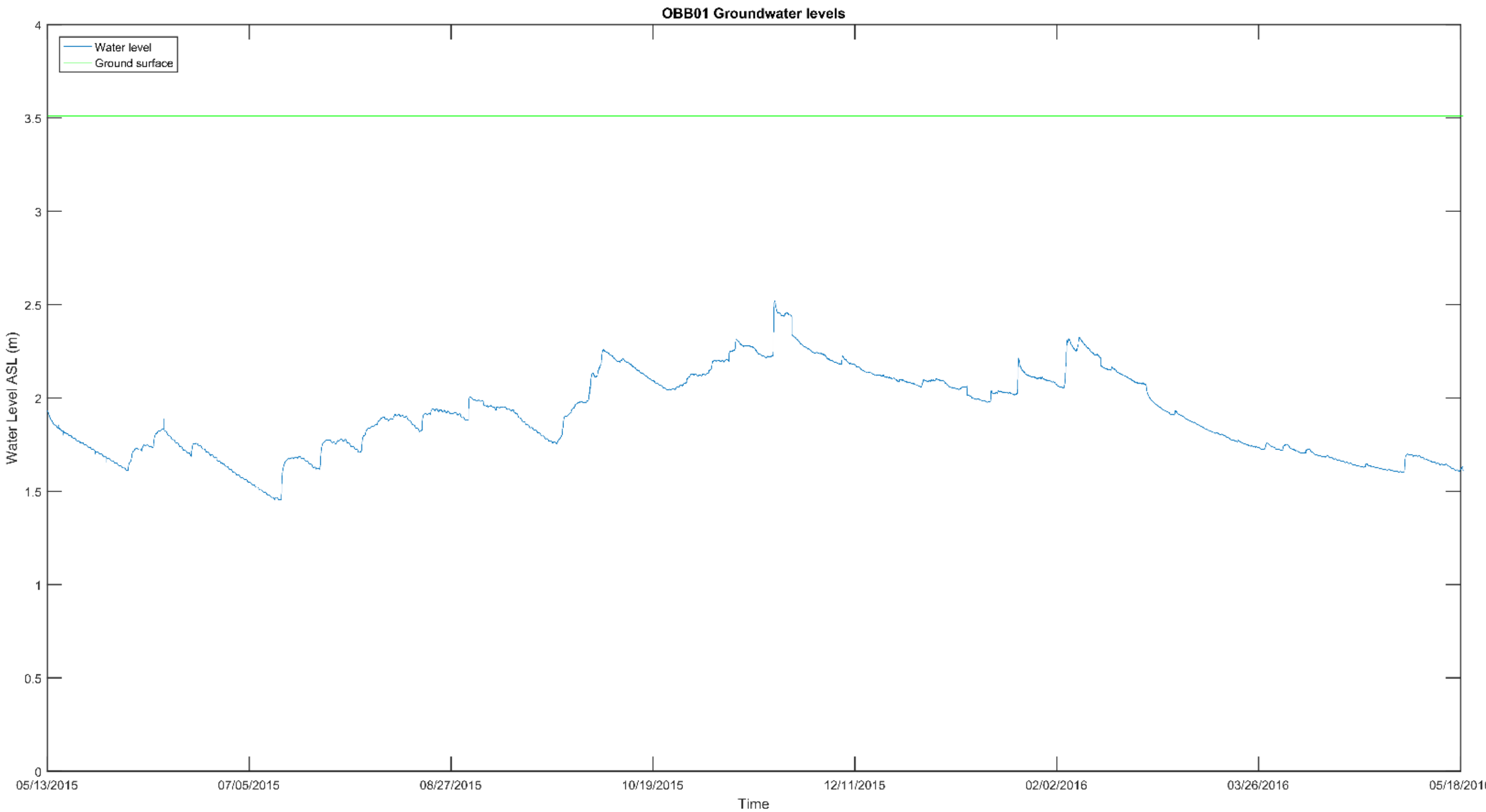

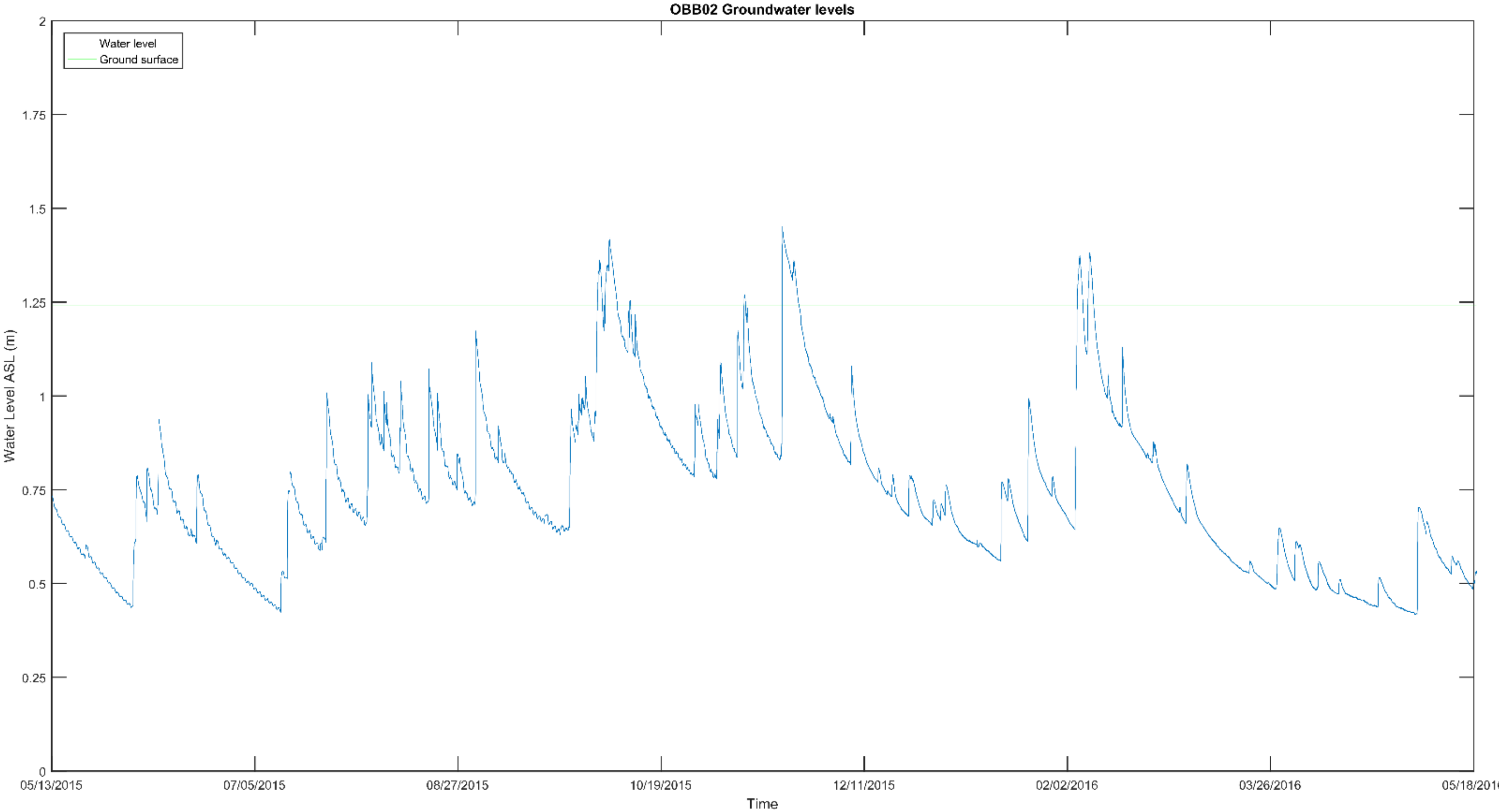
OBB02 Groundwater levels
Water level
Ground surface
Water Level ASL (m)
2
1.75
1.5
1.25
1
0.75
0.5
0.25
0
05/13/2015
07/05/2015
08/27/2015
10/19/2015
12/11/2015
02/02/2016
03/26/2016
05/18/2016
Time

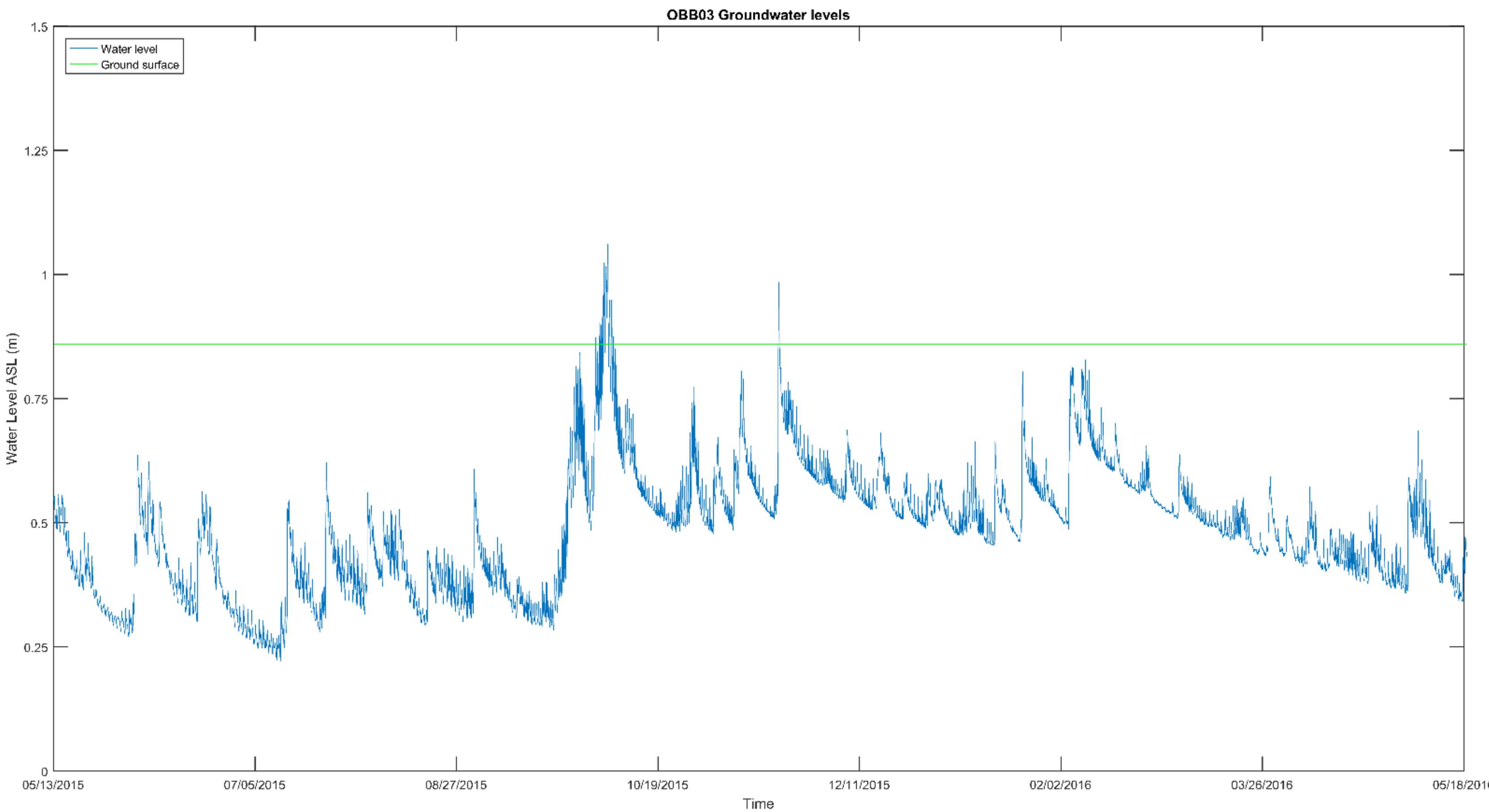
OBB03 Groundwater levels
Water level
Ground surface
Water Level ASL (m)
1.5
1.25
1
0.75
0.5
0.25
0
05/13/2015
07/05/2015
08/27/2015
10/19/2015
12/11/2015
02/02/2016
03/26/2016
05/18/2016
Time

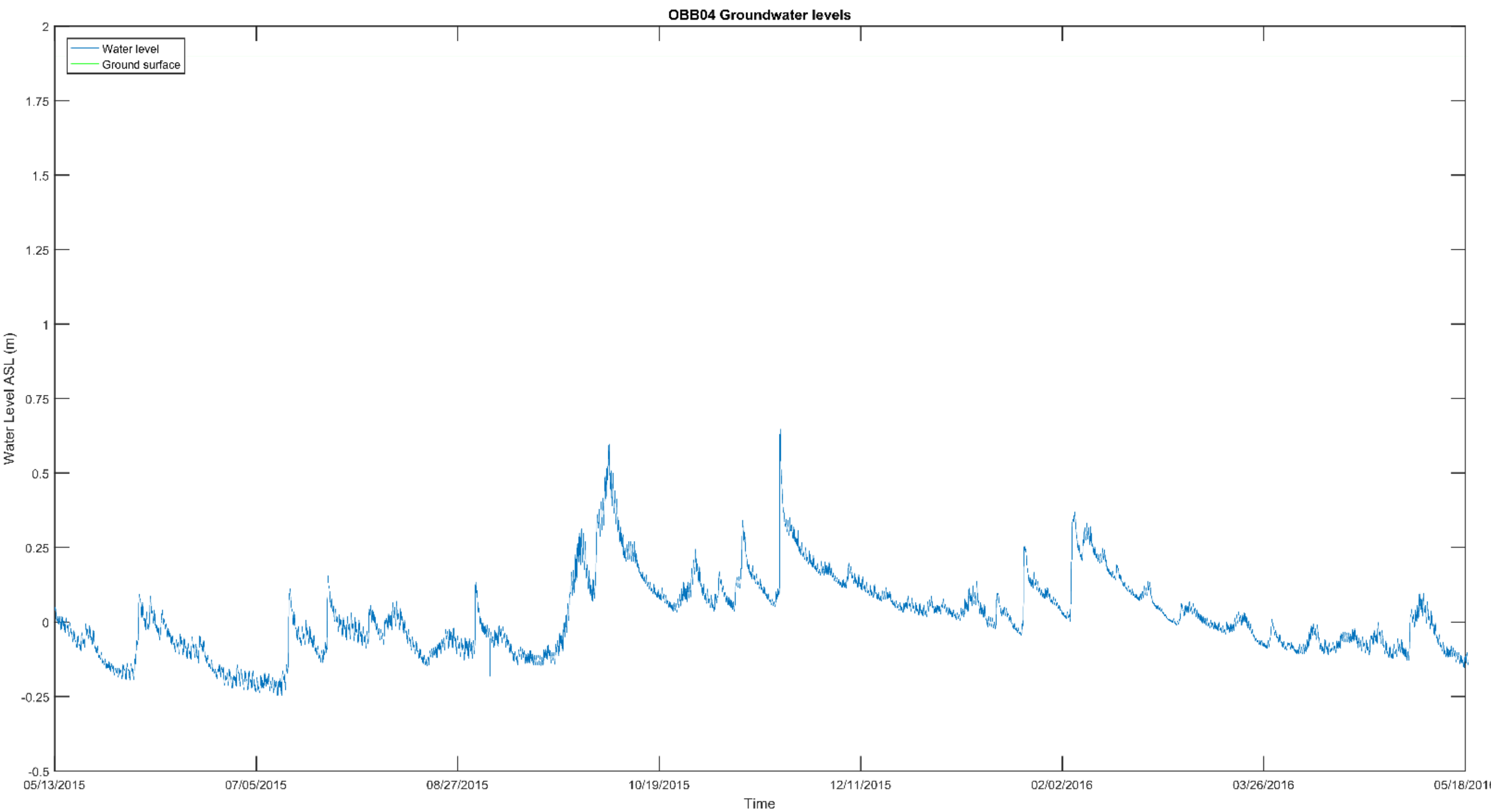
OBB04 Groundwater levels
Water level
Ground surface
Water Level ASL (m)
2
1.75
1.5
1.25
1
0.75
0.5
0.25
0
-0.25
-0.5
05/13/2015
07/05/2015
08/27/2015
10/19/2015
12/11/2015
02/02/2016
03/26/2016
05/18/2016
Time

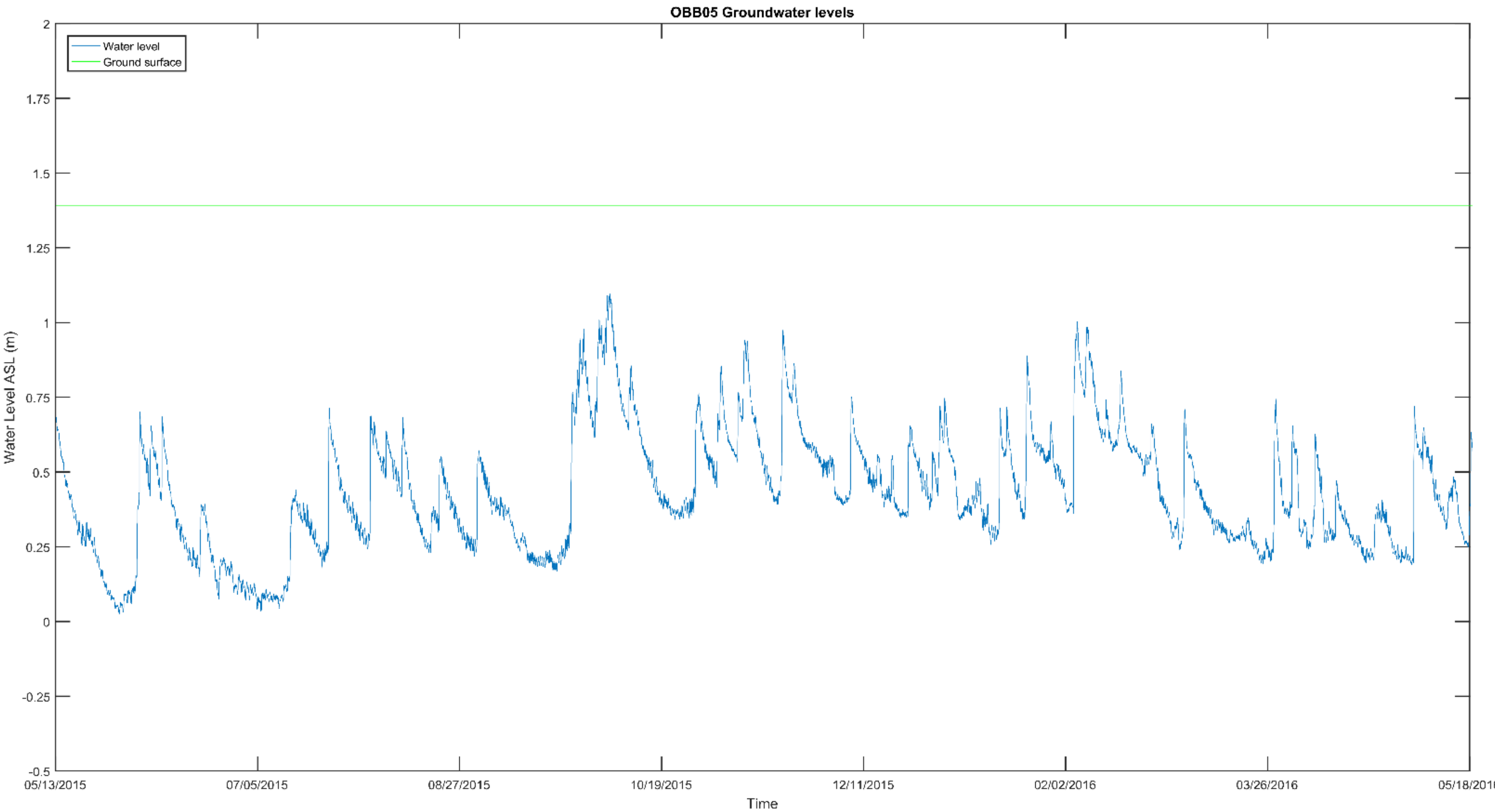
OBB05 Groundwater levels
Water level
Ground surface
Water Level ASL (m)
2
1.75
1.5
1.25
1
0.75
0.5
0.25
0
-0.25
-0.5
05/13/2015
07/05/2015
08/27/2015
10/19/2015
12/11/2015
02/02/2016
03/26/2016
05/18/2016
Time

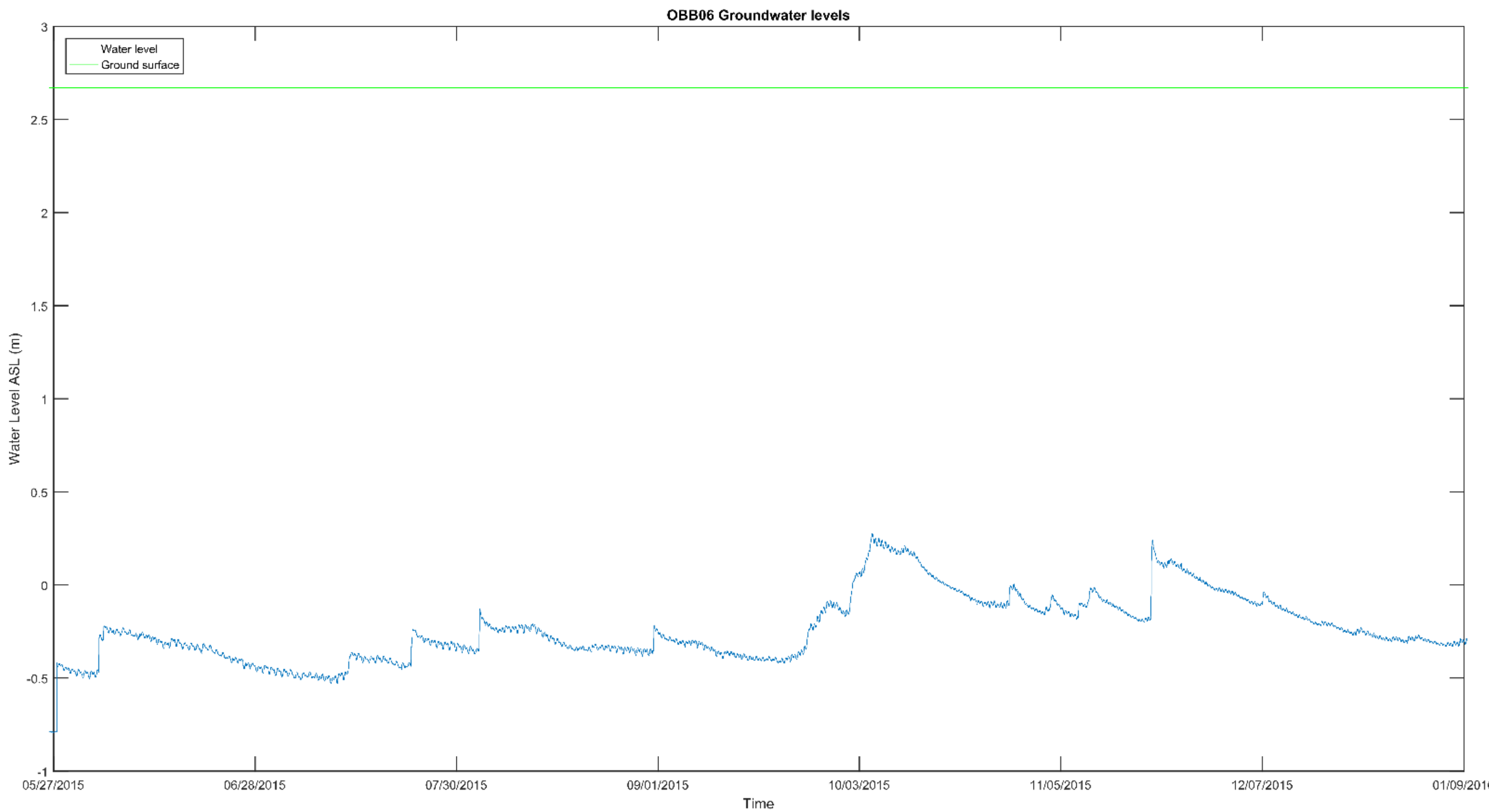

OBB06 Groundwater levels
Water level
Ground surface
Water Level ASL (m)
3
2.5
2
1.5
1
0.5
0
-0.5
-1
05/27/2015
06/28/2015
07/30/2015
09/01/2015
10/03/2015
11/05/2015
12/07/2015
01/09/2016
Time

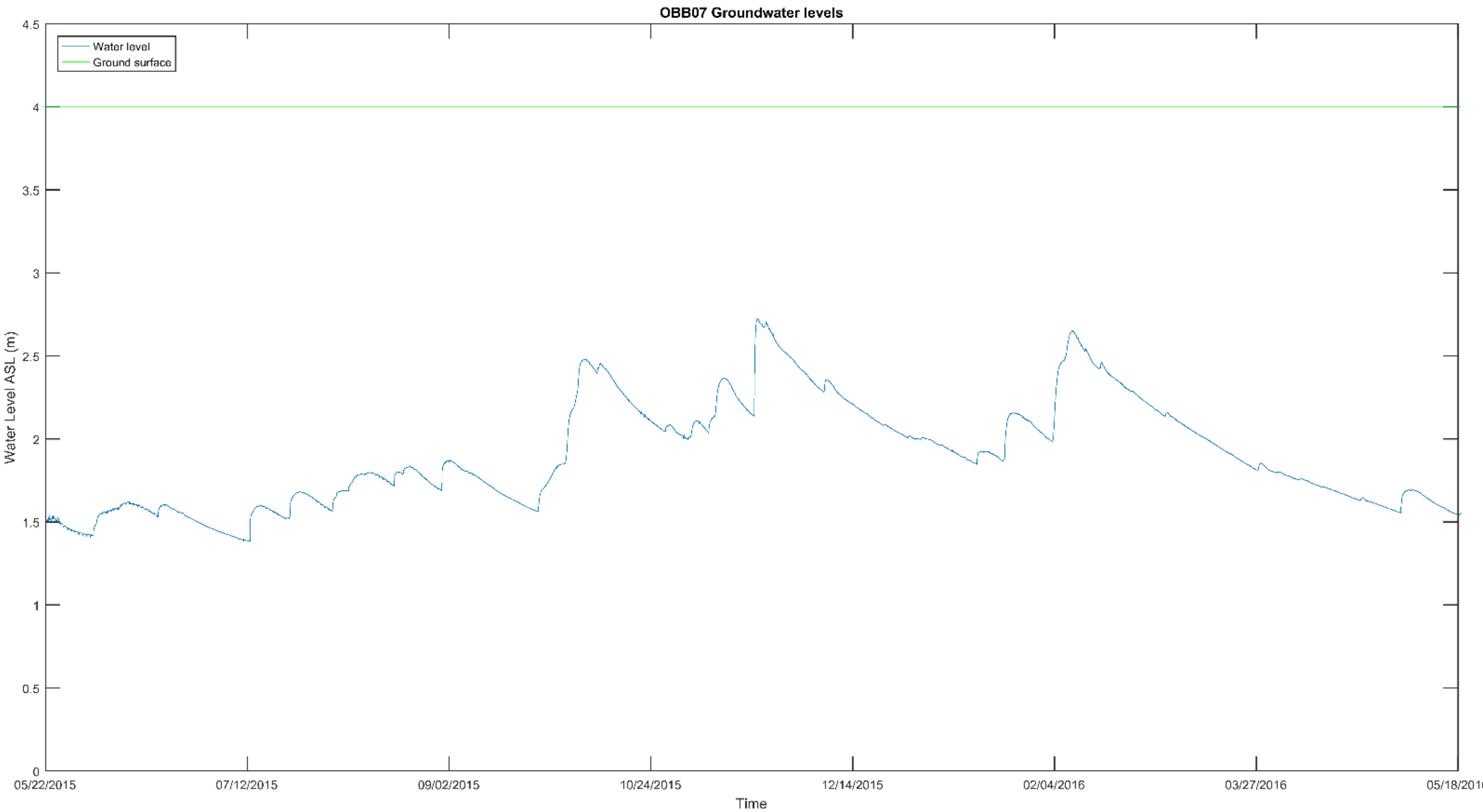
OBB07 Groundwater levels
Water level
Ground surface
Water Level ASL (m)
0
0.5
1
1.5
2
2.5
3
3.5
4
4.5
05/22/2015
07/12/2015
09/02/2015
10/24/2015
12/14/2015
02/04/2016
03/27/2016
05/18/2016
Time

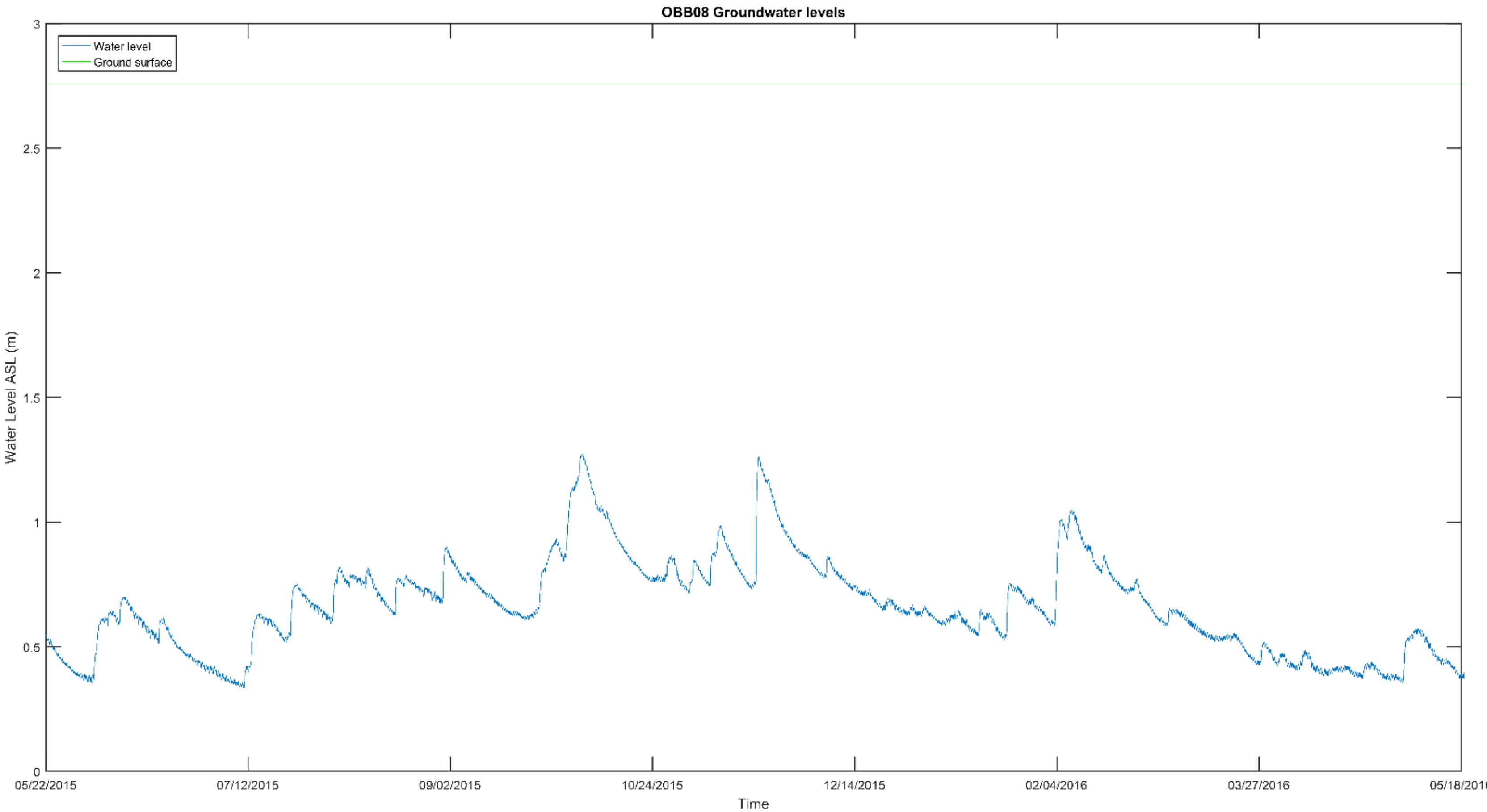

OBB08 Groundwater levels
Water level
Ground surface
Water Level ASL (m)
0
0.5
1
1.5
2
2.5
3
05/22/2015
07/12/2015
09/02/2015
10/24/2015
12/14/2015
02/04/2016
03/27/2016
05/18/2016
Time

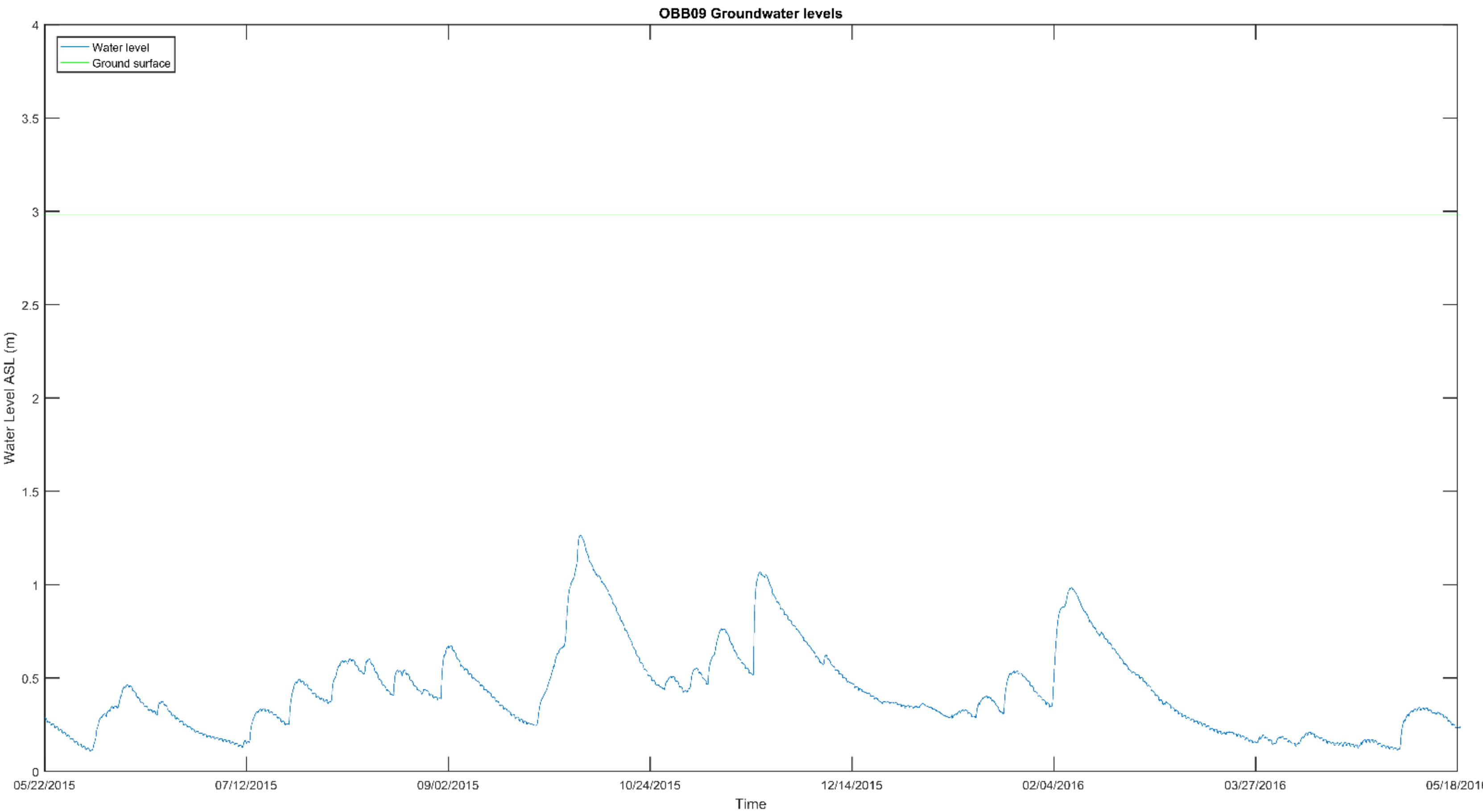
OBB09 Groundwater levels
Water level
Ground surface
Water Level ASL (m)
0
0.5
1
1.5
2
2.5
3
3.5
4
05/22/2015
07/12/2015
09/02/2015
10/24/2015
12/14/2015
02/04/2016
03/27/2016
05/18/2016
Time

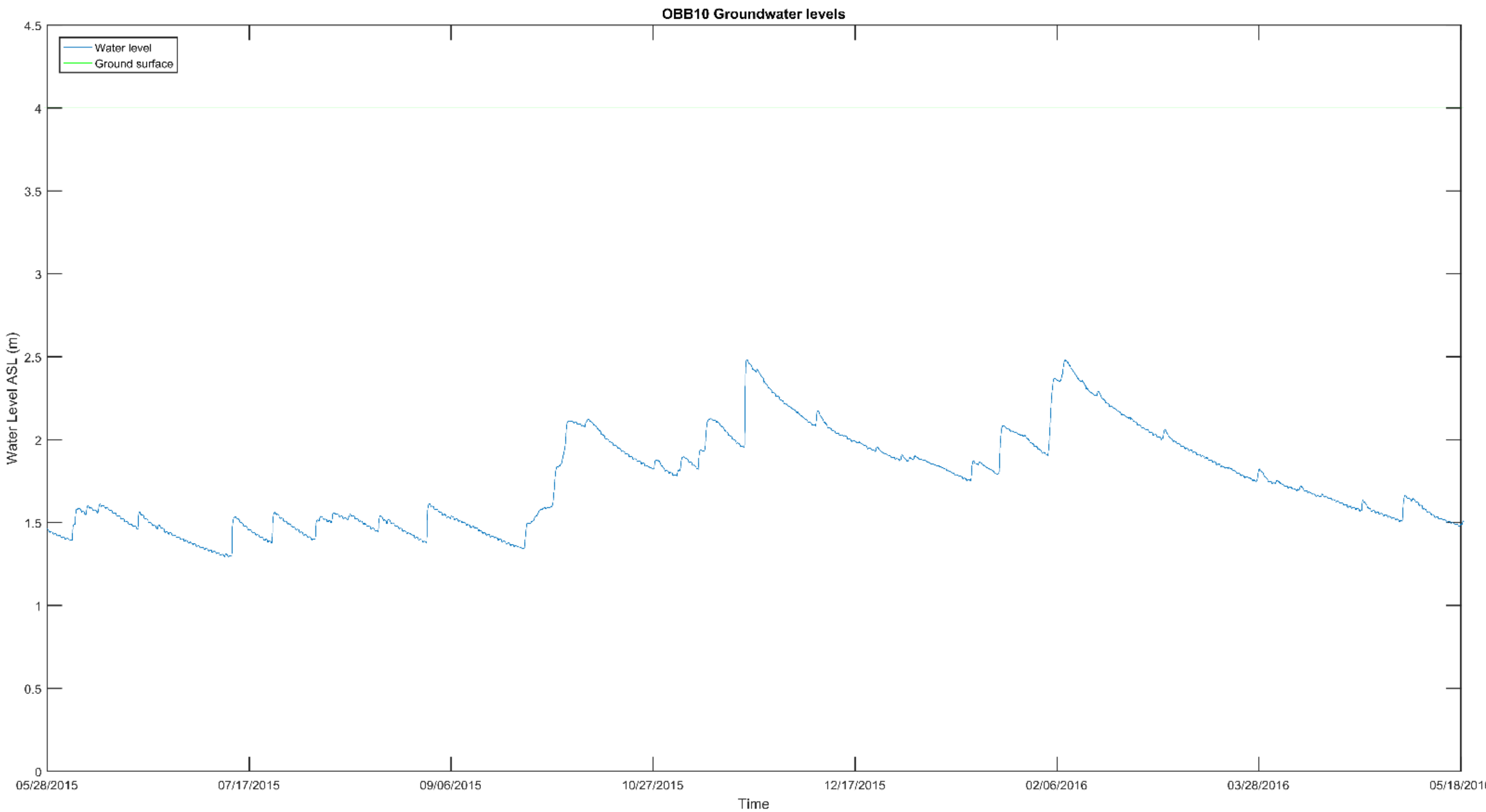

OBB10 Groundwater levels
Water level
Ground surface
Water Level ASL (m)
4.5
4
3.5
3
2.5
2
1.5
1
0.5
0
05/28/2015
07/17/2015
09/06/2015
10/27/2015
12/17/2015
02/06/2016
03/28/2016
05/18/2016
Time

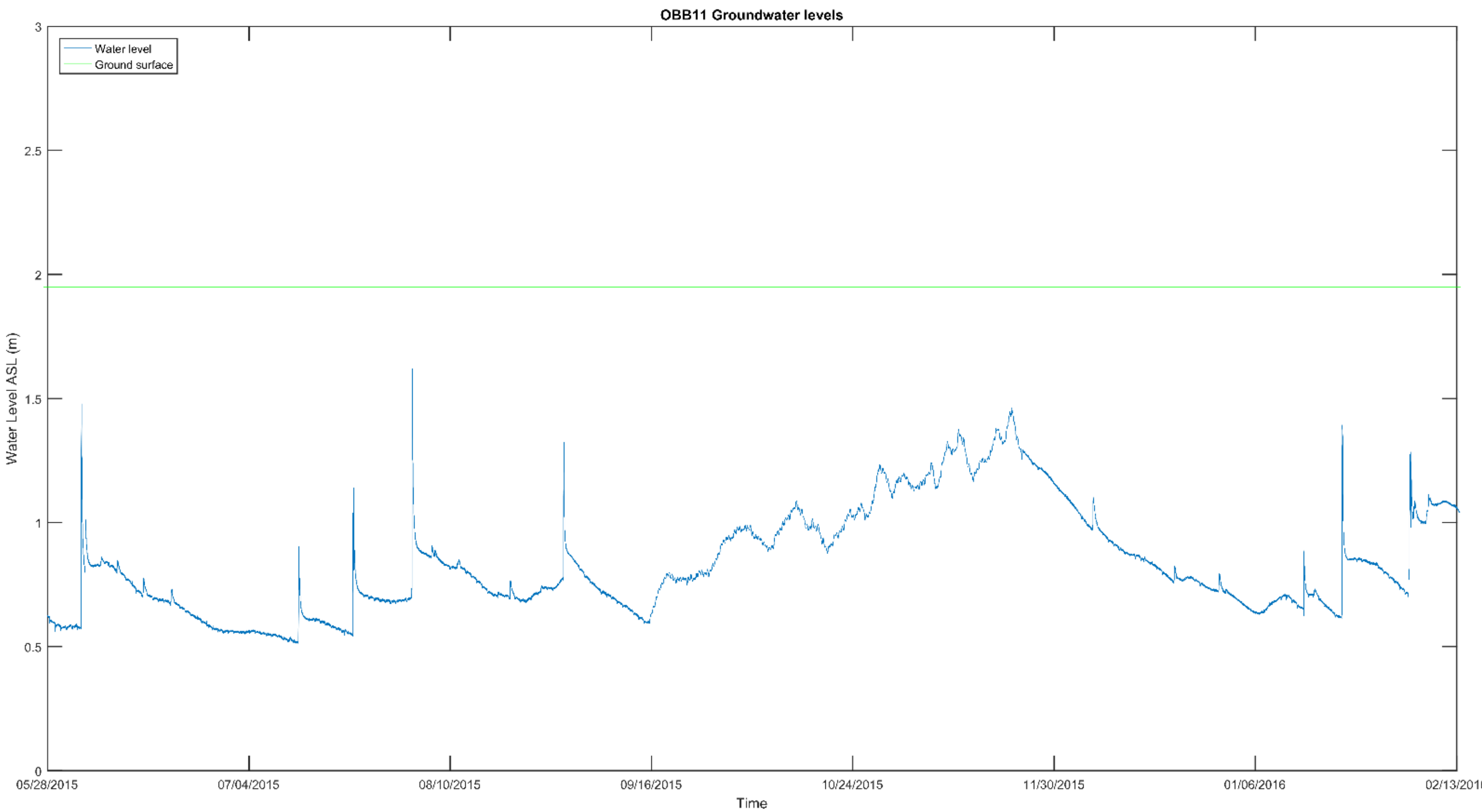
OBB11 Groundwater levels
Water level
Ground surface
Water Level ASL (m)
3
2.5
2
1.5
1
0.5
0
05/28/2015
07/04/2015
08/10/2015
09/16/2015
10/24/2015
11/30/2015
01/06/2016
02/13/2016
Time

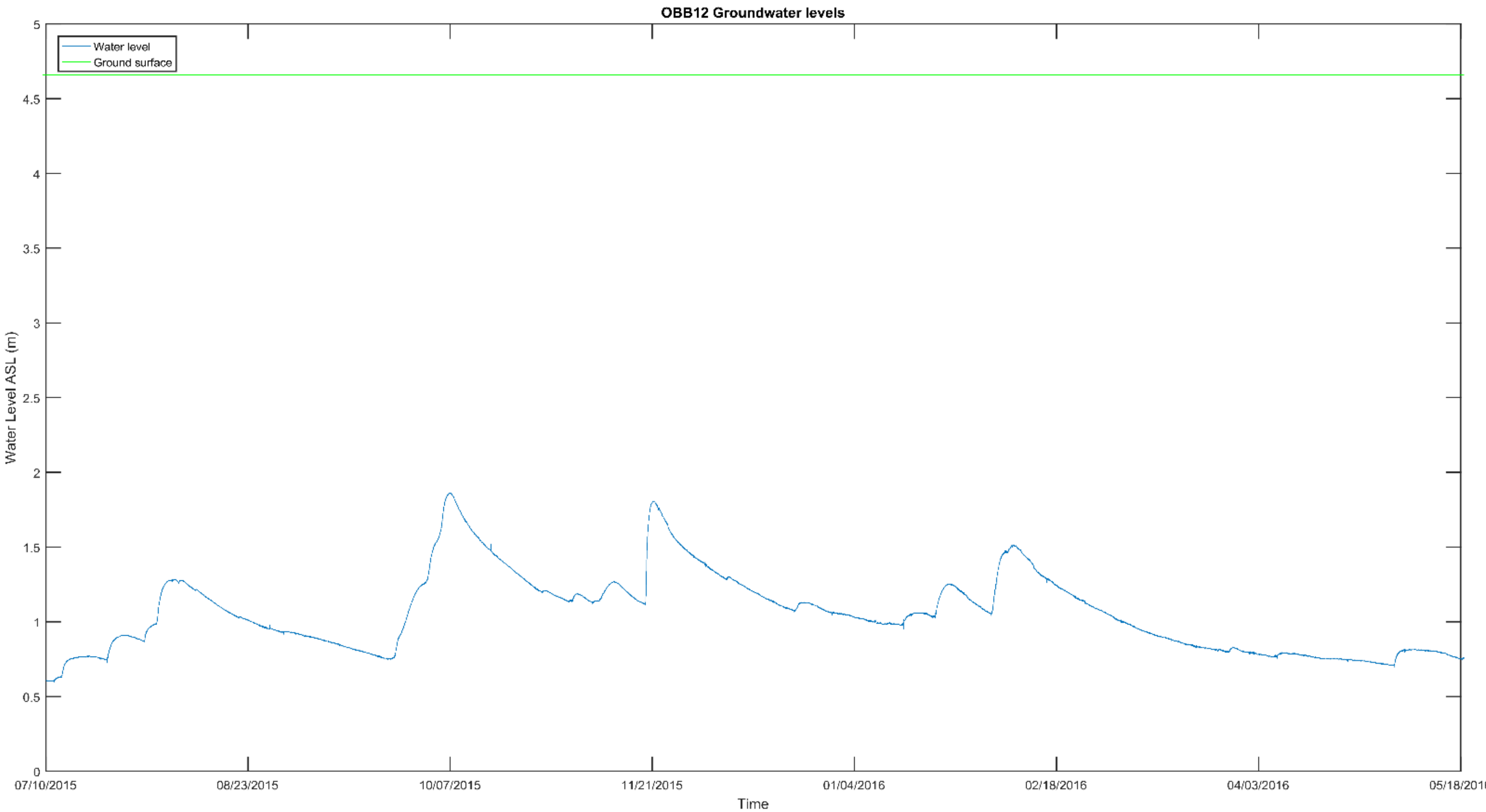
OBB12 Groundwater levels
Water level
Ground surface
Water Level ASL (m)
0
0.5
1
1.5
2
2.5
3
3.5
4
4.5
5
07/10/2015
08/23/2015
10/07/2015
11/21/2015
01/04/2016
02/18/2016
04/03/2016
05/18/2016
Time

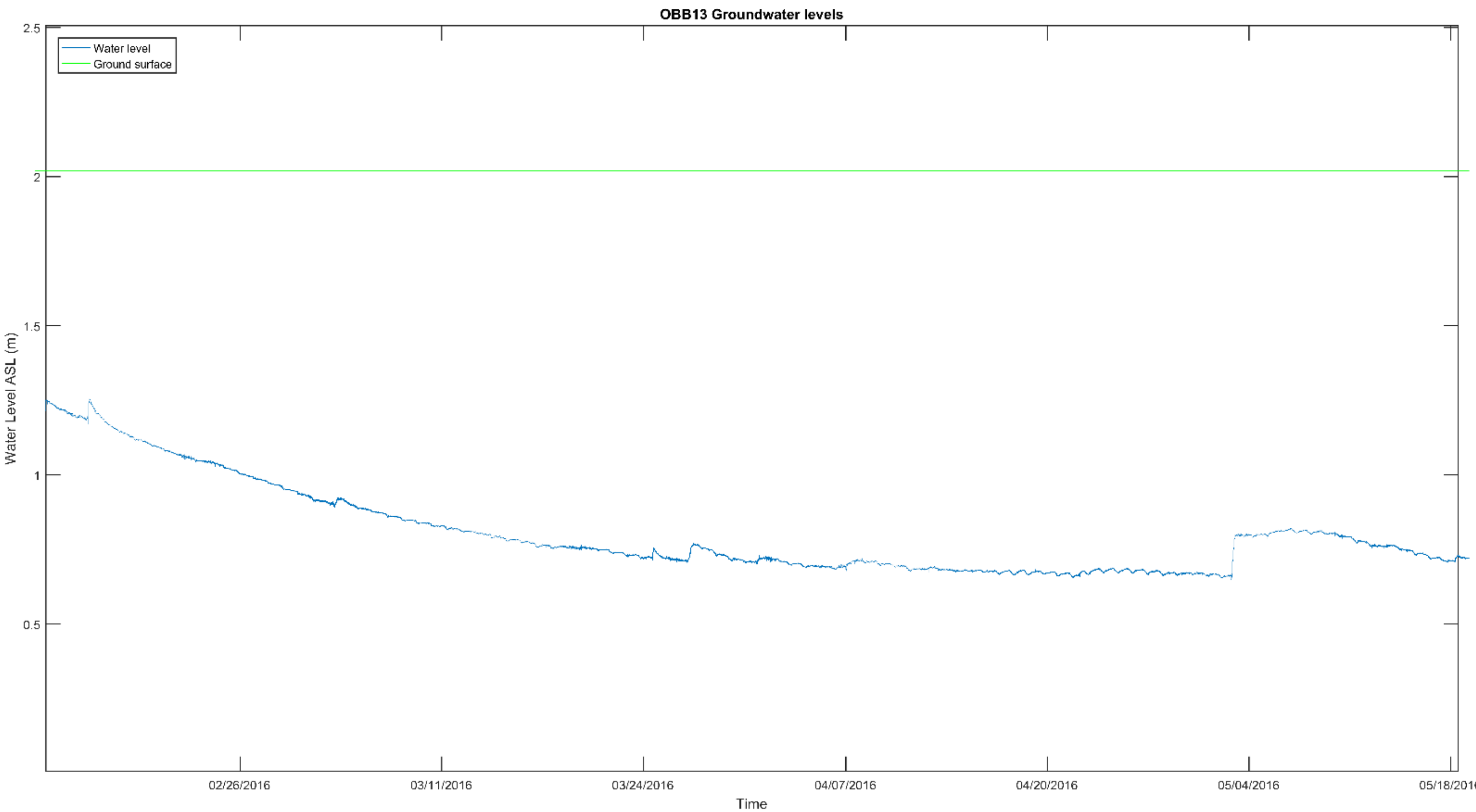
OBB13 Groundwater levels
Water level
Ground surface
Water Level ASL (m)
2.5
2
1.5
1
0.5
02/26/2016
03/11/2016
03/24/2016
04/07/2016
04/20/2016
05/04/2016
05/18/2016
Time

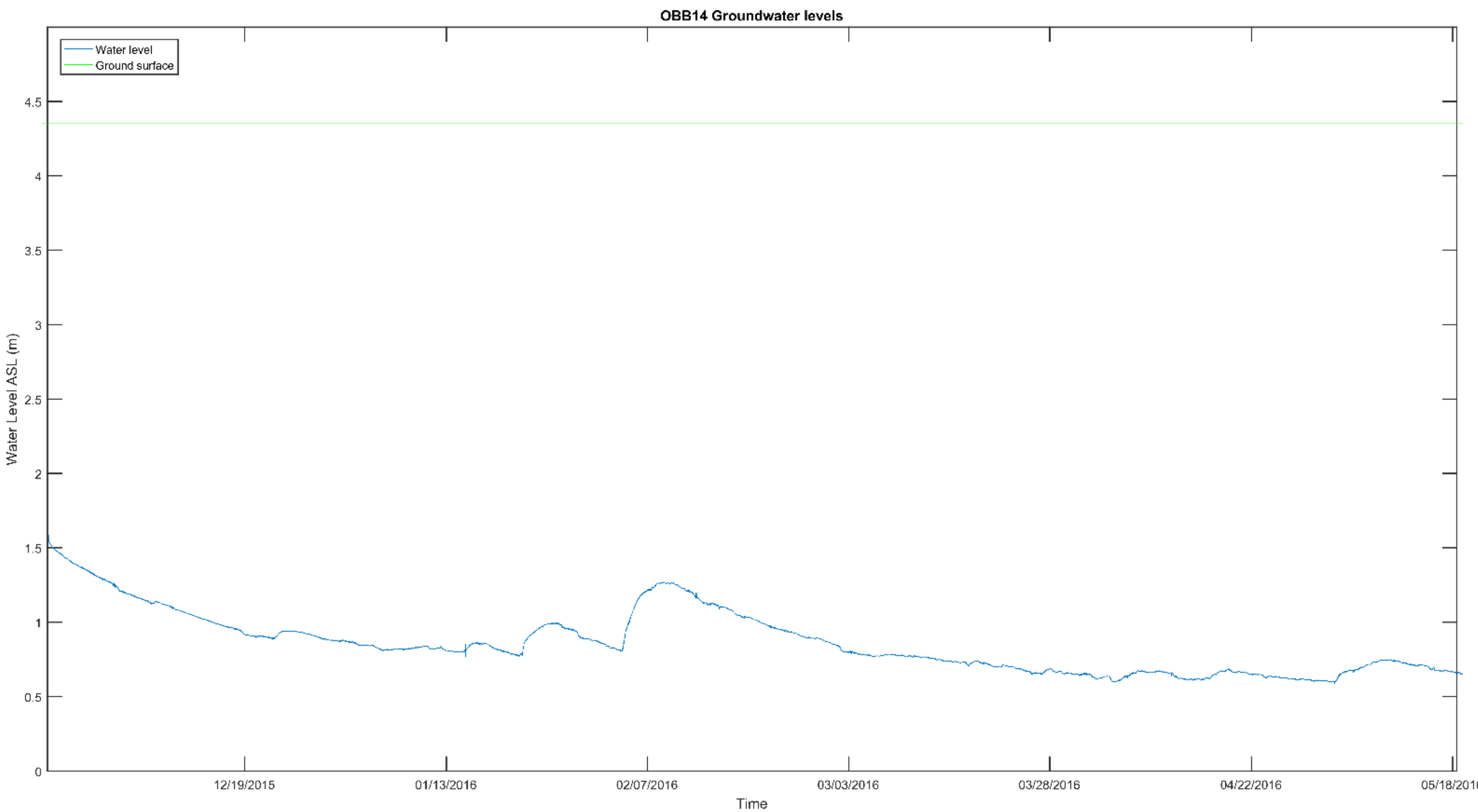
OBB14 Groundwater levels
Water level
Ground surface
Water Level ASL (m)
4.5
4
3.5
3
2.5
2
1.5
1
0.5
0
12/19/2015
01/13/2016
02/07/2016
03/03/2016
03/28/2016
04/22/2016
05/18/2016
Time

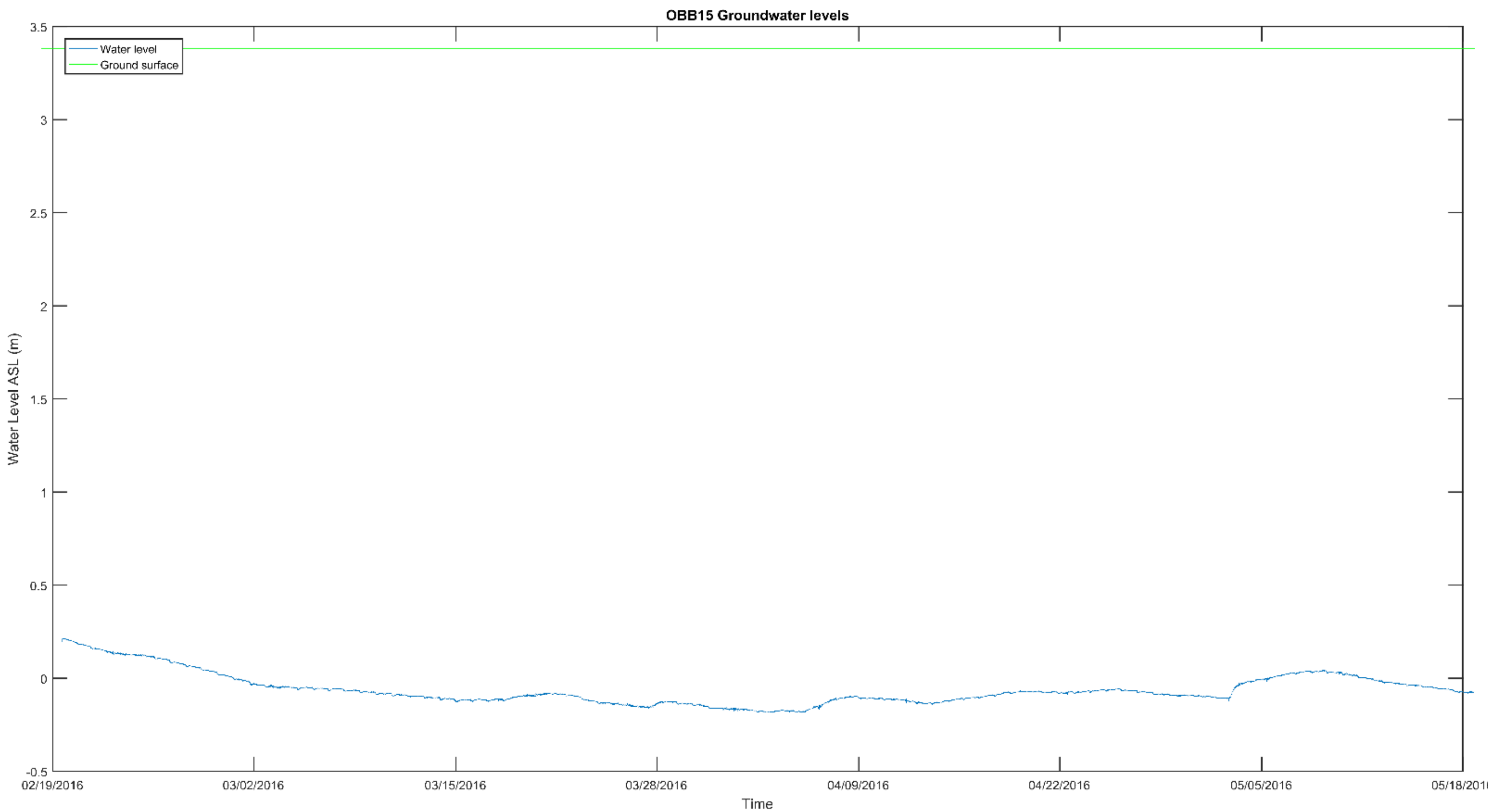
OBB15 Groundwater levels
Water level
Ground surface
Water Level ASL (m)
3.5
3
2.5
2
1.5
1
0.5
0
-0.5
02/19/2016
03/02/2016
03/15/2016
03/28/2016
04/09/2016
04/22/2016
05/05/2016
05/18/2016
Time

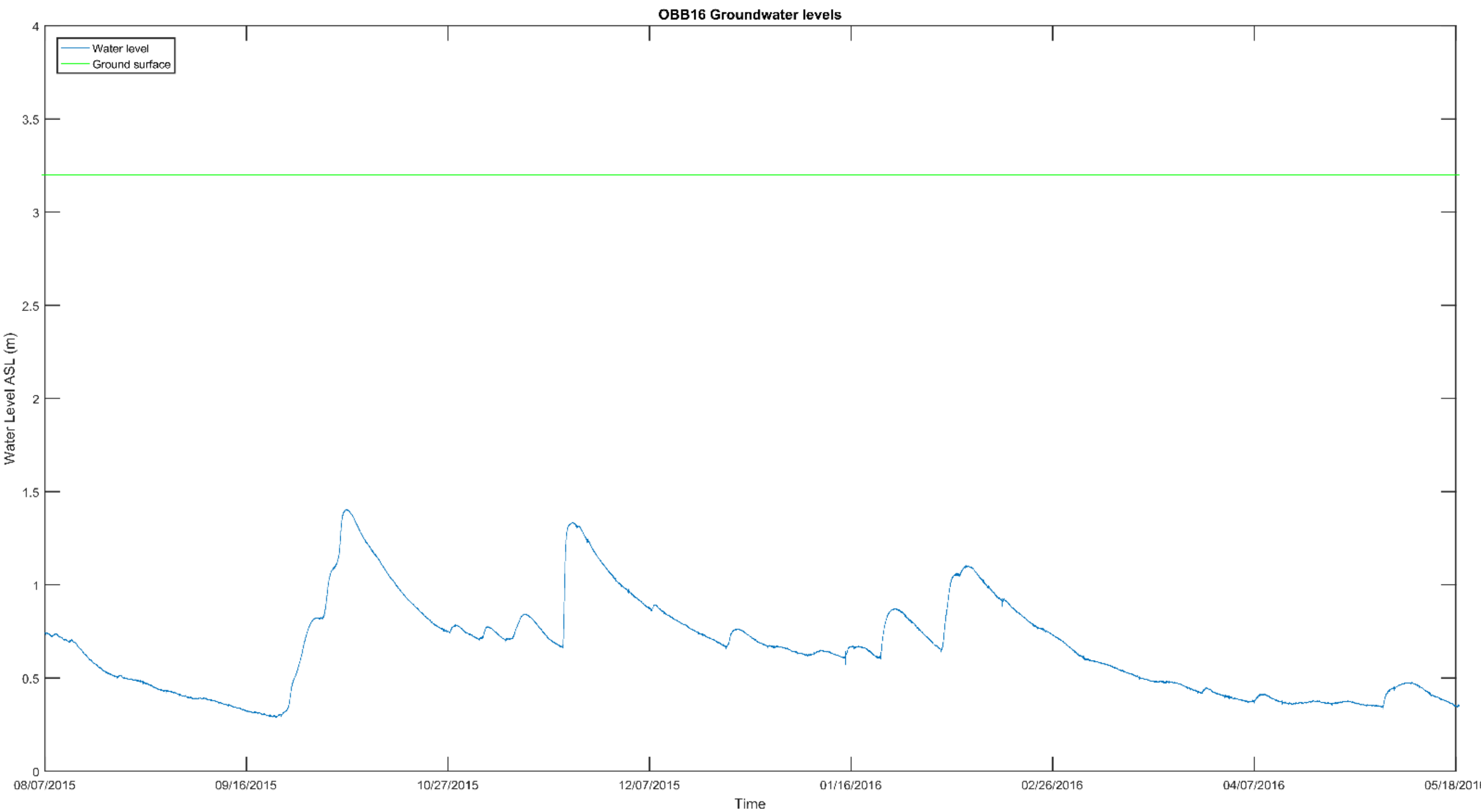
OBB16 Groundwater levels
Water level
Ground surface
Water Level ASL (m)
Time
0
0.5
1
1.5
2
2.5
3
3.5
4
08/07/2015
09/16/2015
10/27/2015
12/07/2015
01/16/2016
02/26/2016
04/07/2016
05/18/2016

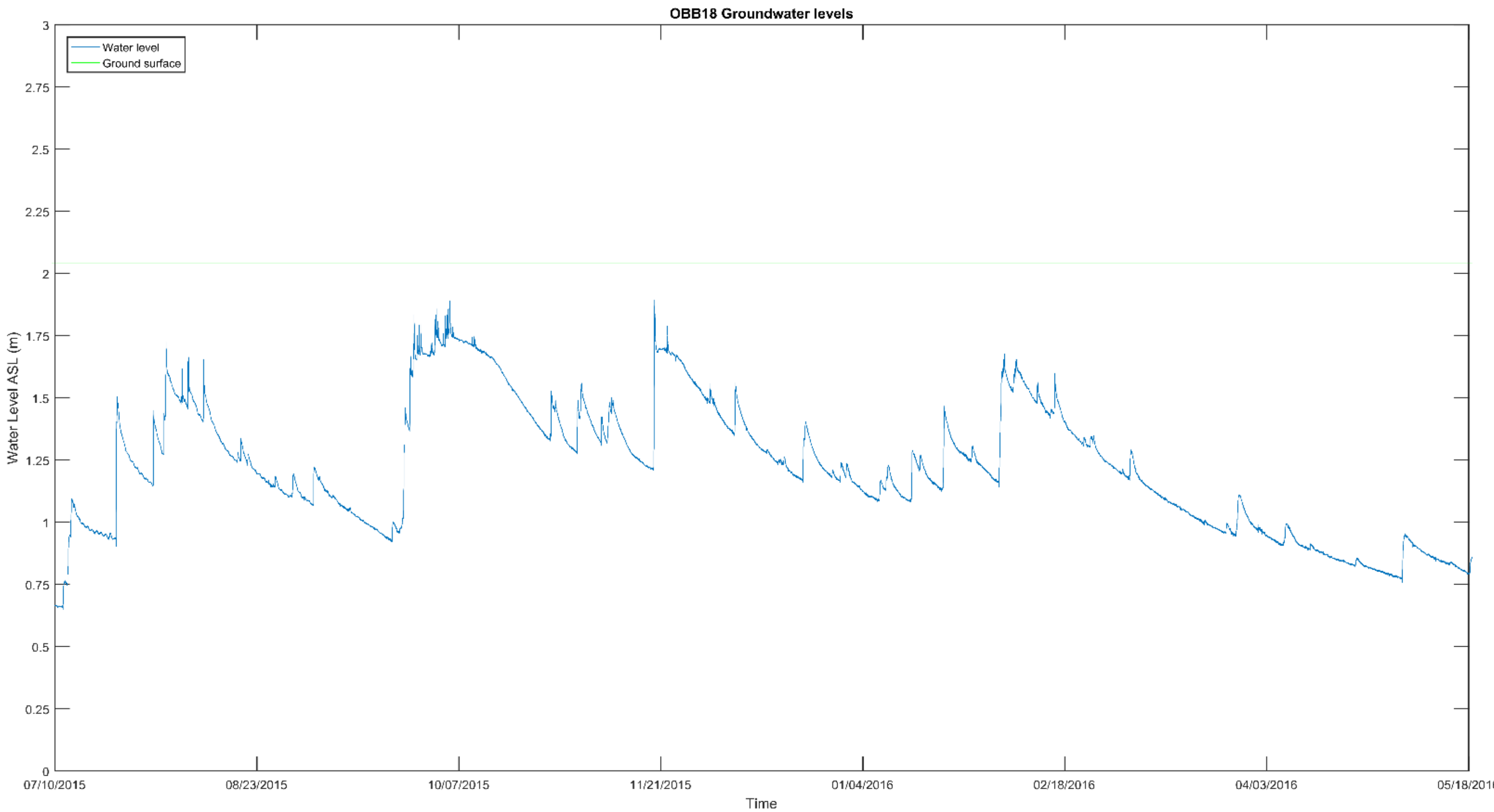
OBB18 Groundwater levels
Water level
Ground surface
Water Level ASL (m)
Time
3
2.75
2.5
2.25
2
1.75
1.5
1.25
1
0.75
0.5
0.25
0
07/10/2015
08/23/2015
10/07/2015
11/21/2015
01/04/2016
02/18/2016
04/03/2016
05/18/2016

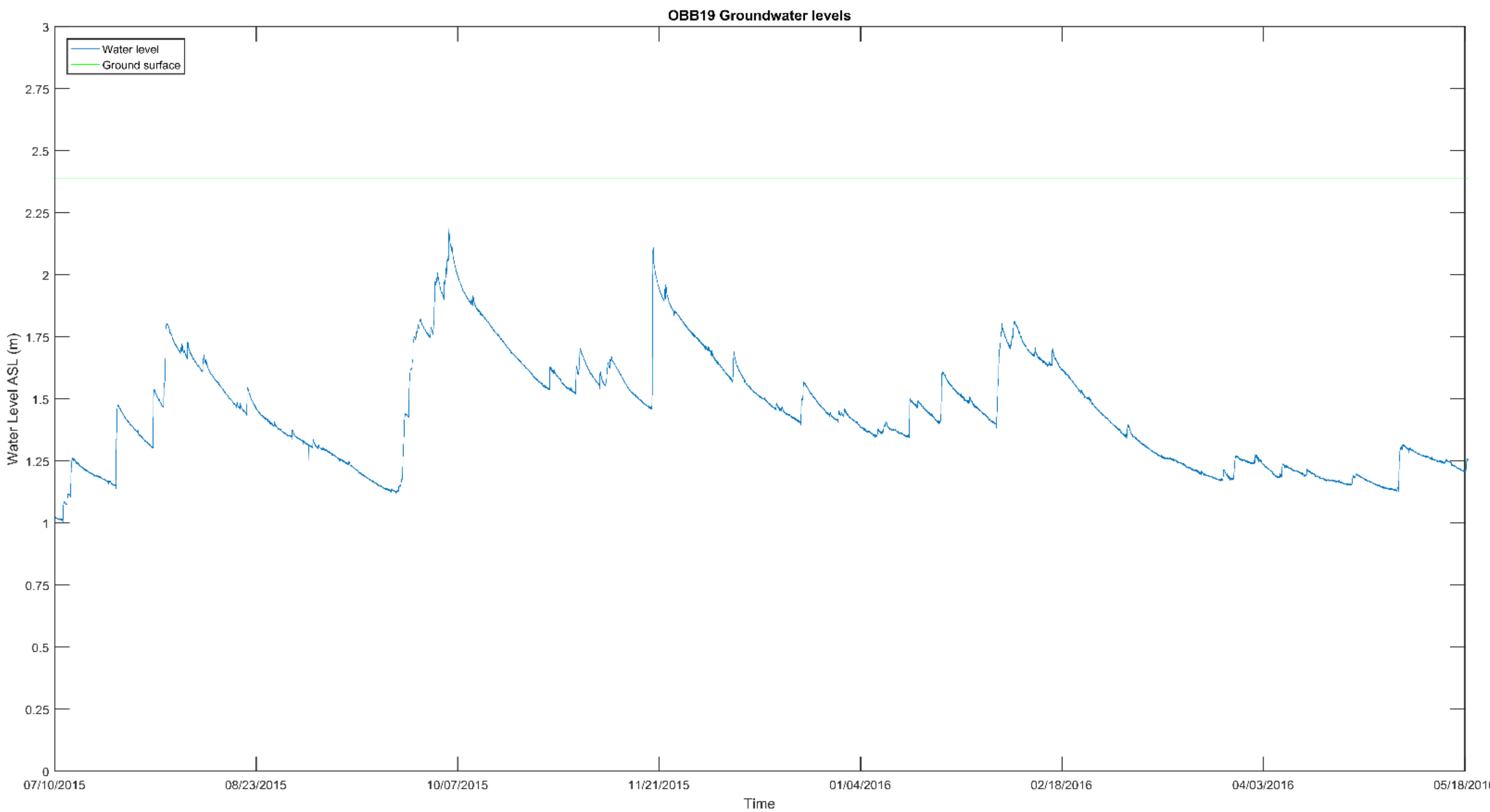
OBB19 Groundwater levels
Water level
Ground surface
Water Level ASL (m)
3
2.75
2.5
2.25
2
1.75
1.5
1.25
1
0.75
0.5
0.25
0
07/10/2015
08/23/2015
10/07/2015
11/21/2015
01/04/2016
02/18/2016
04/03/2016
05/18/2016
Time

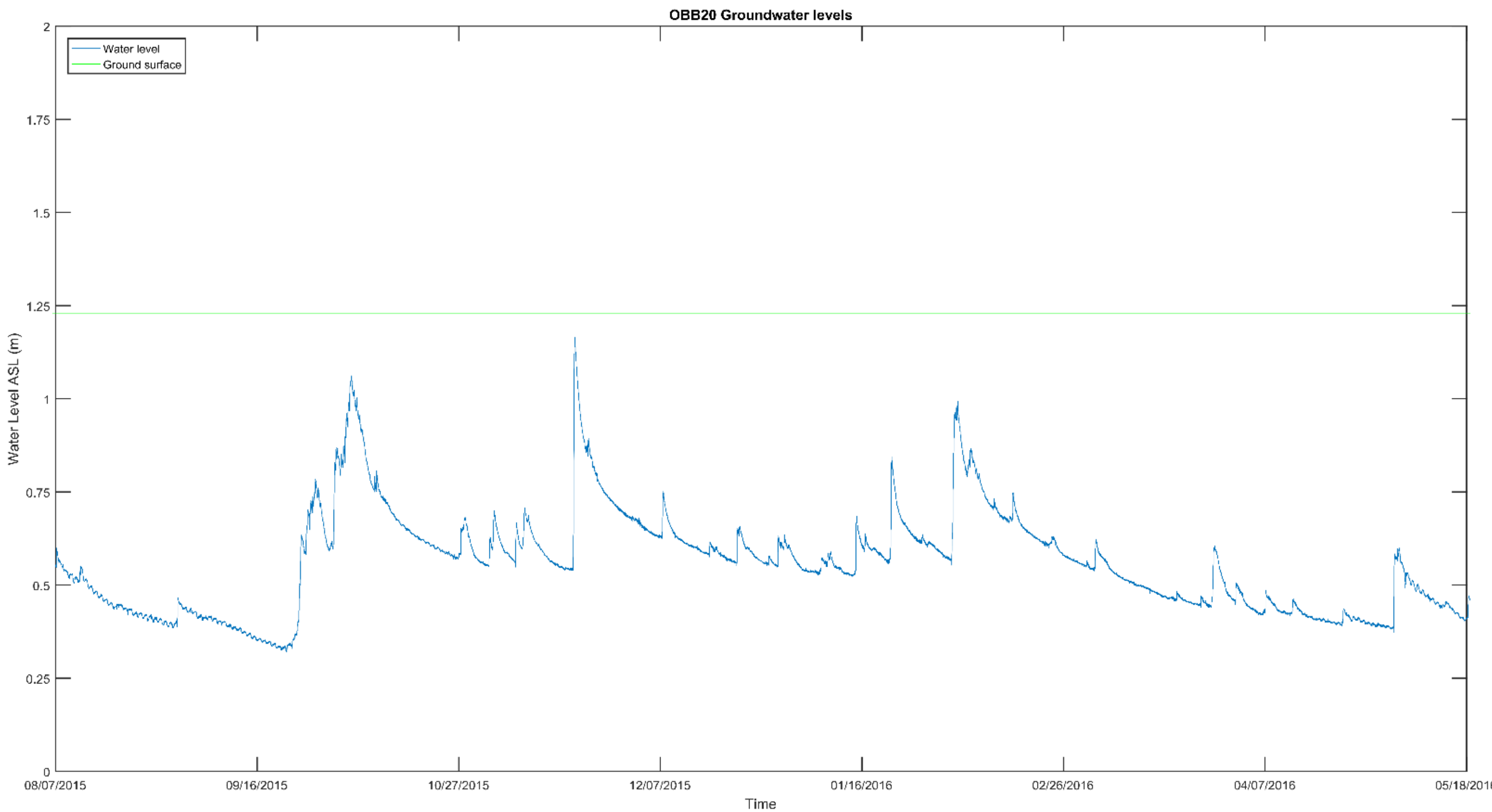
OBB20 Groundwater levels
Water level
Ground surface
Water Level ASL (m)
2
1.75
1.5
1.25
1
0.75
0.5
0.25
0
08/07/2015
09/16/2015
10/27/2015
12/07/2015
01/16/2016
02/26/2016
04/07/2016
05/18/2016
Time

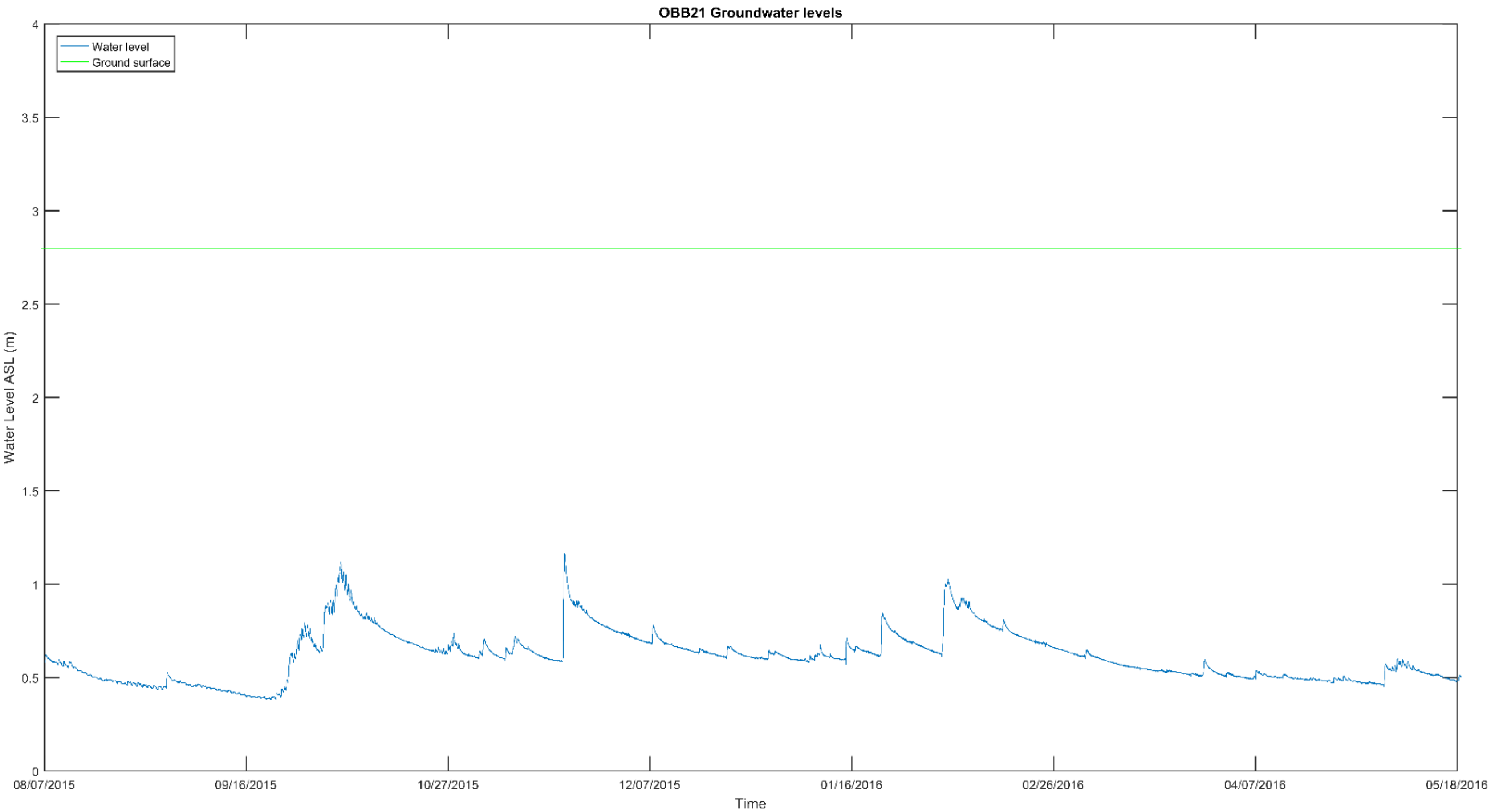
OBB21 Groundwater levels
Water level
Ground surface
Water Level ASL (m)
Time
0
0.5
1
1.5
2
2.5
3
3.5
4
08/07/2015
09/16/2015
10/27/2015
12/07/2015
01/16/2016
02/26/2016
04/07/2016
05/18/2016

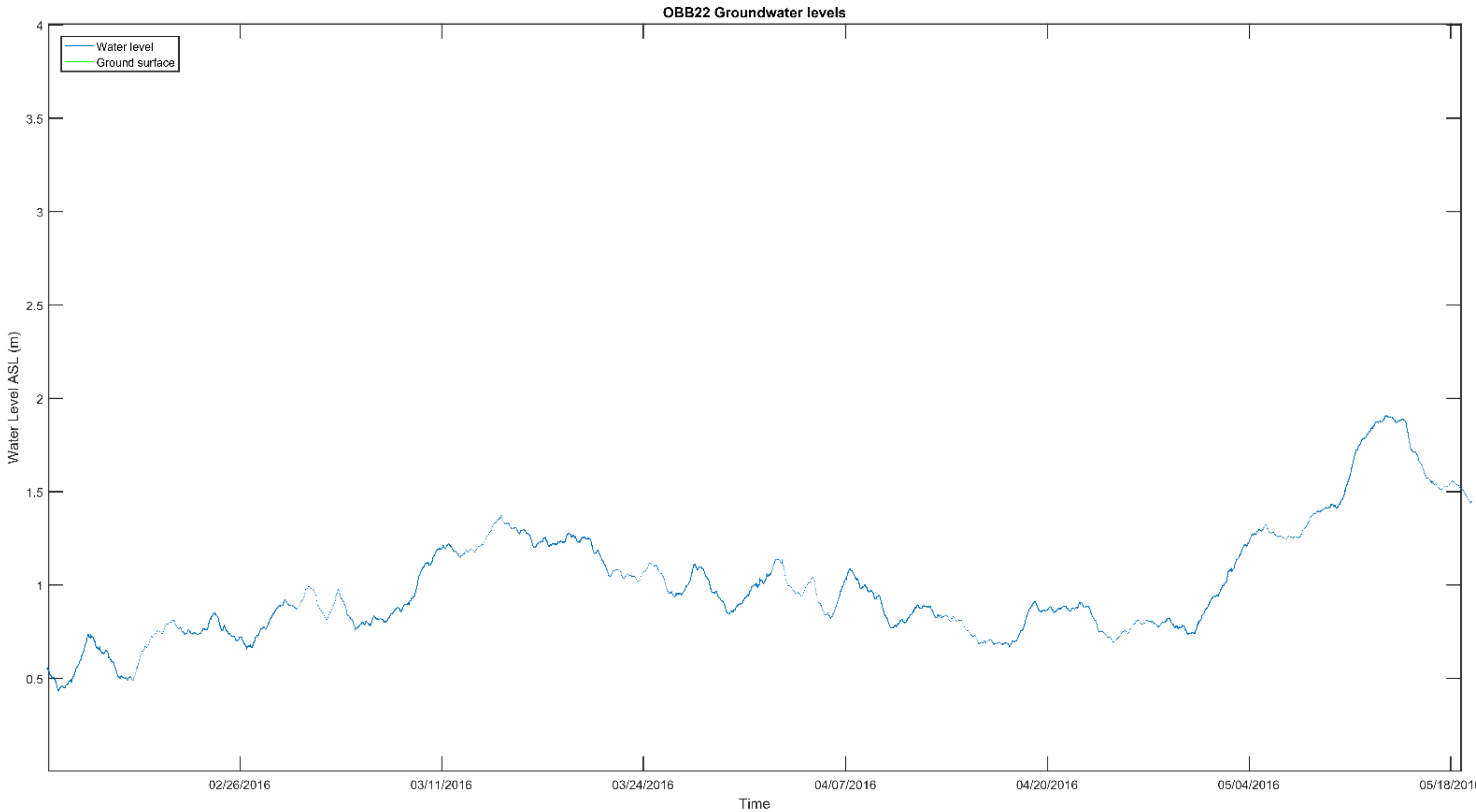
OBB22 Groundwater levels
Water level
Ground surface
Water Level ASL (m)
4
3.5
3
2.5
2
1.5
1
0.5
02/26/2016
03/11/2016
03/24/2016
04/07/2016
04/20/2016
05/04/2016
05/18/2016
Time

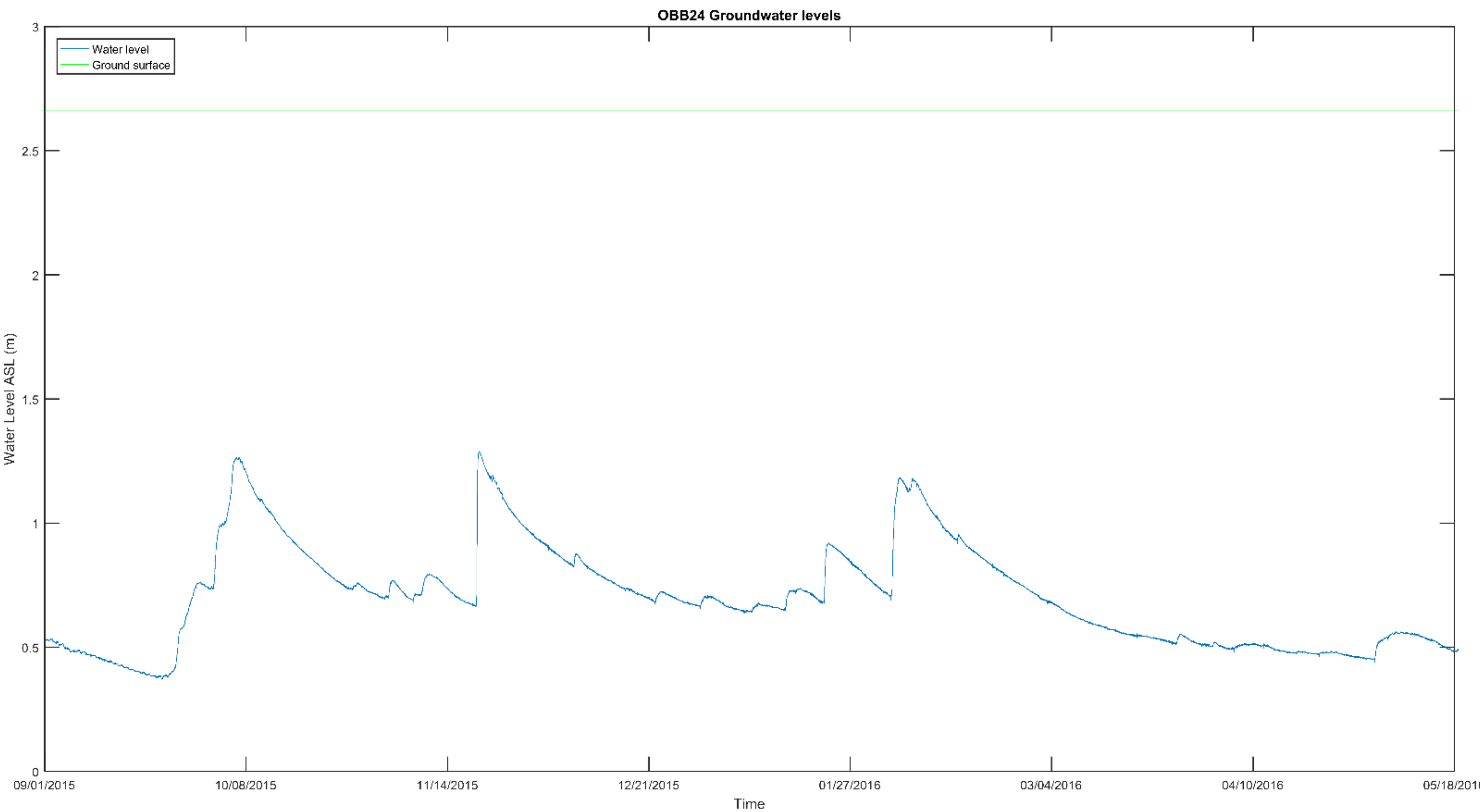
OBB24 Groundwater levels
Water level
Ground surface
Water Level ASL (m)
0
0.5
1
1.5
2
2.5
3
09/01/2015
10/08/2015
11/14/2015
12/21/2015
01/27/2016
03/04/2016
04/10/2016
05/18/2016
Time

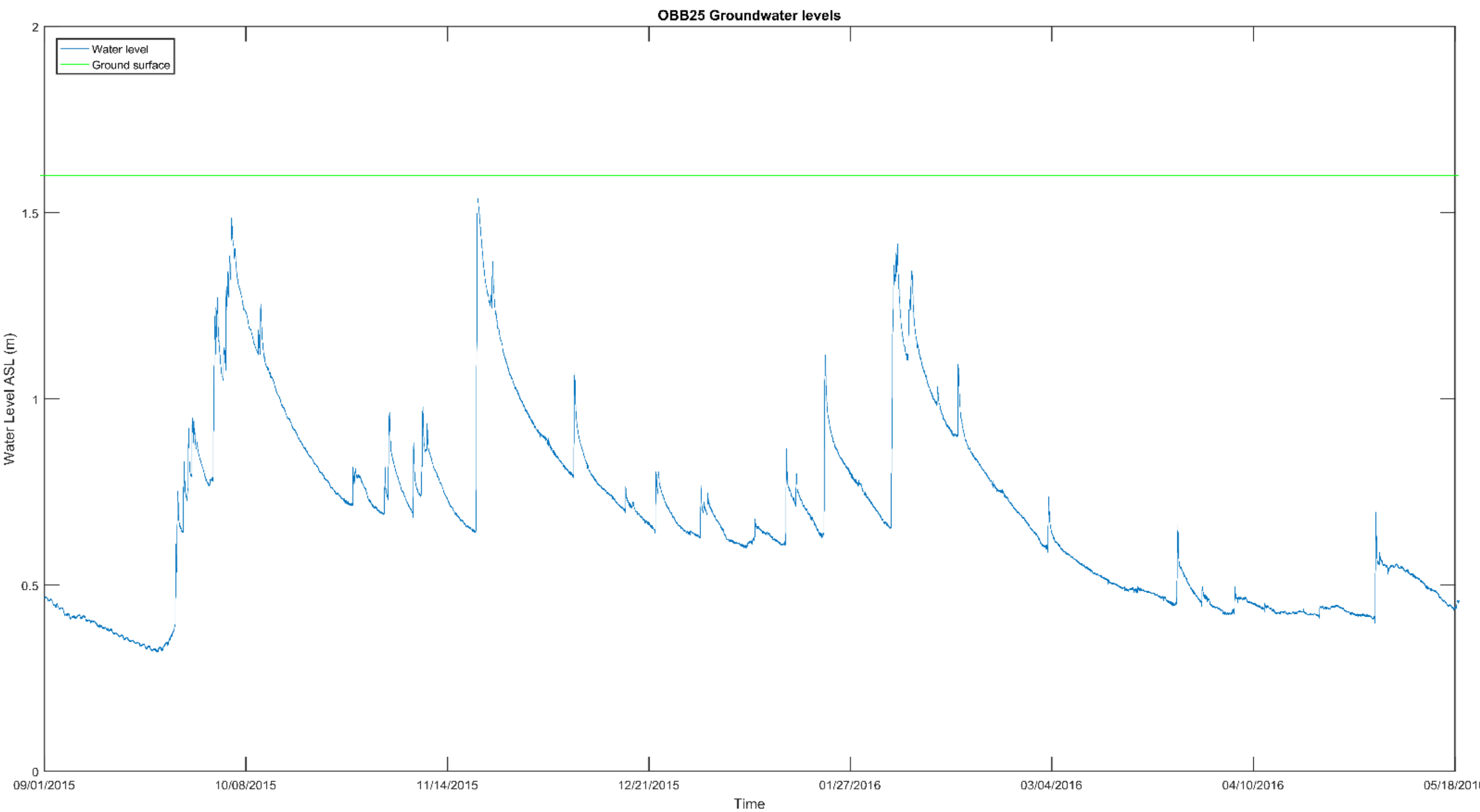
OBB25 Groundwater levels
Water level
Ground surface
Water Level ASL (m)
2
1.5
1
0.5
0
09/01/2015
10/08/2015
11/14/2015
12/21/2015
01/27/2016
03/04/2016
04/10/2016
05/18/2016
Time

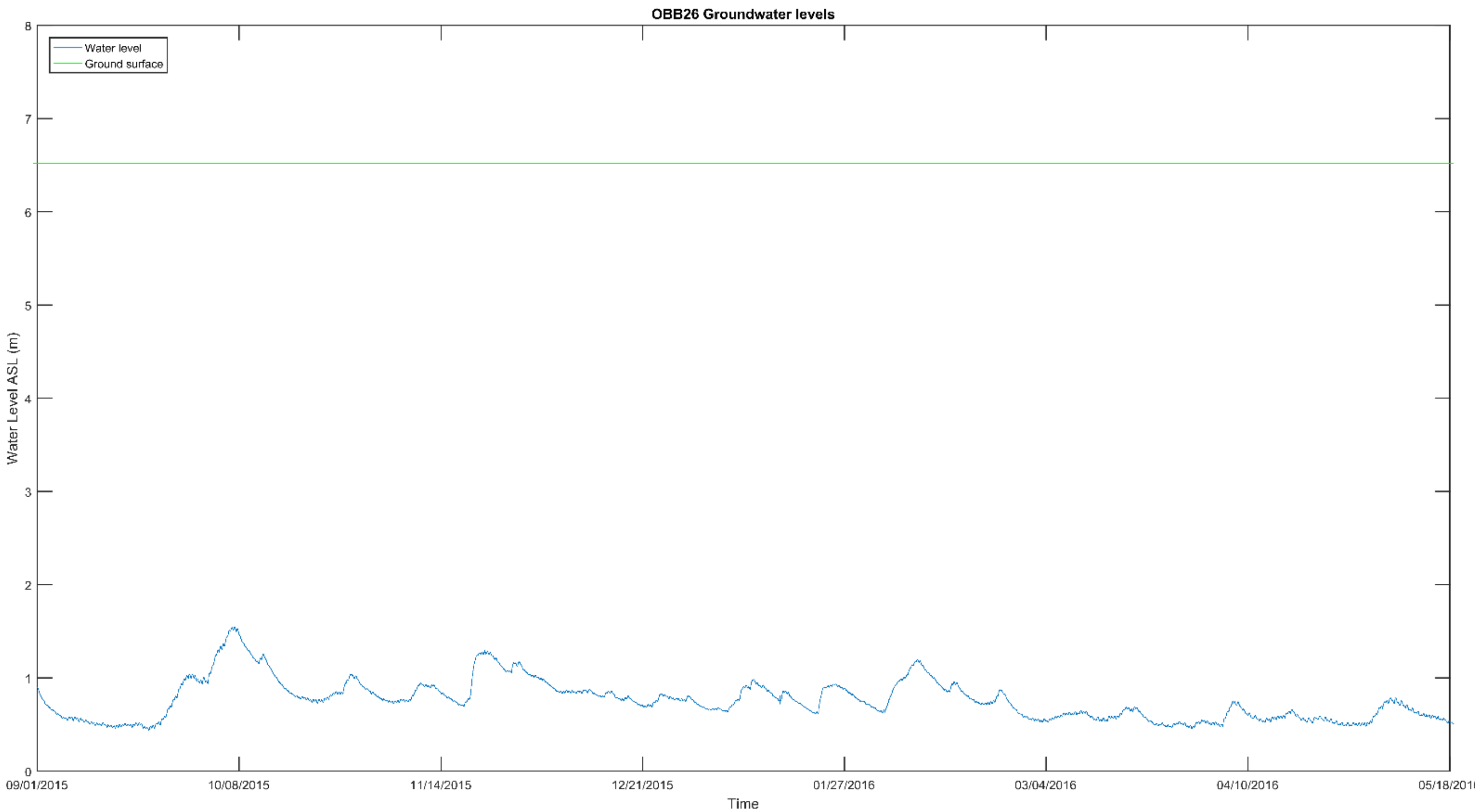
OBB26 Groundwater levels
Water level
Ground surface
Water Level ASL (m)
Time
0
1
2
3
4
5
6
7
8
09/01/2015
10/08/2015
11/14/2015
12/21/2015
01/27/2016
03/04/2016
04/10/2016
05/18/2016

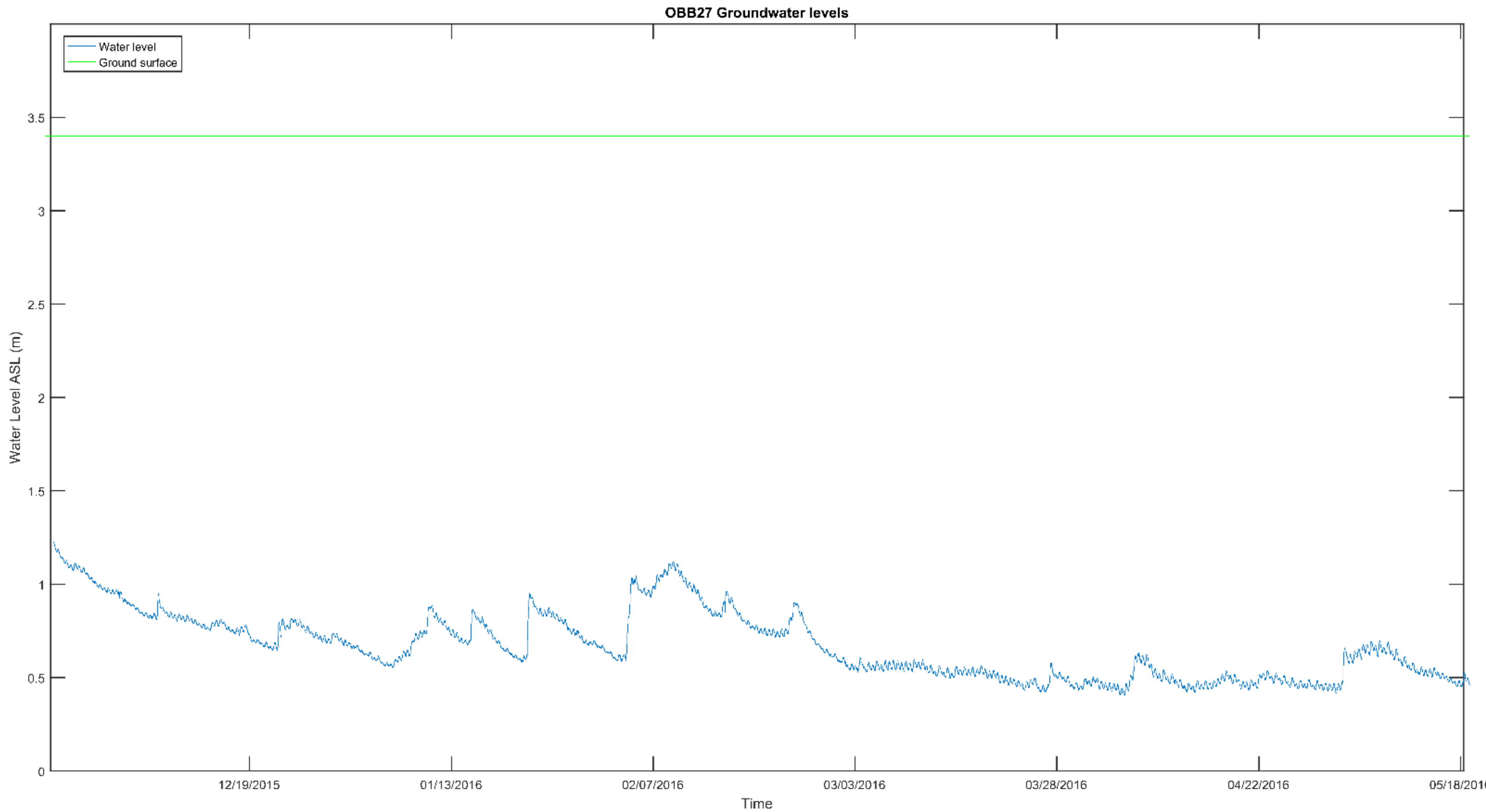
OBB27 Groundwater levels
Water level
Ground surface
Water Level ASL (m)
0
0.5
1
1.5
2
2.5
3
3.5
12/19/2015
01/13/2016
02/07/2016
03/03/2016
03/28/2016
04/22/2016
05/18/2016
Time

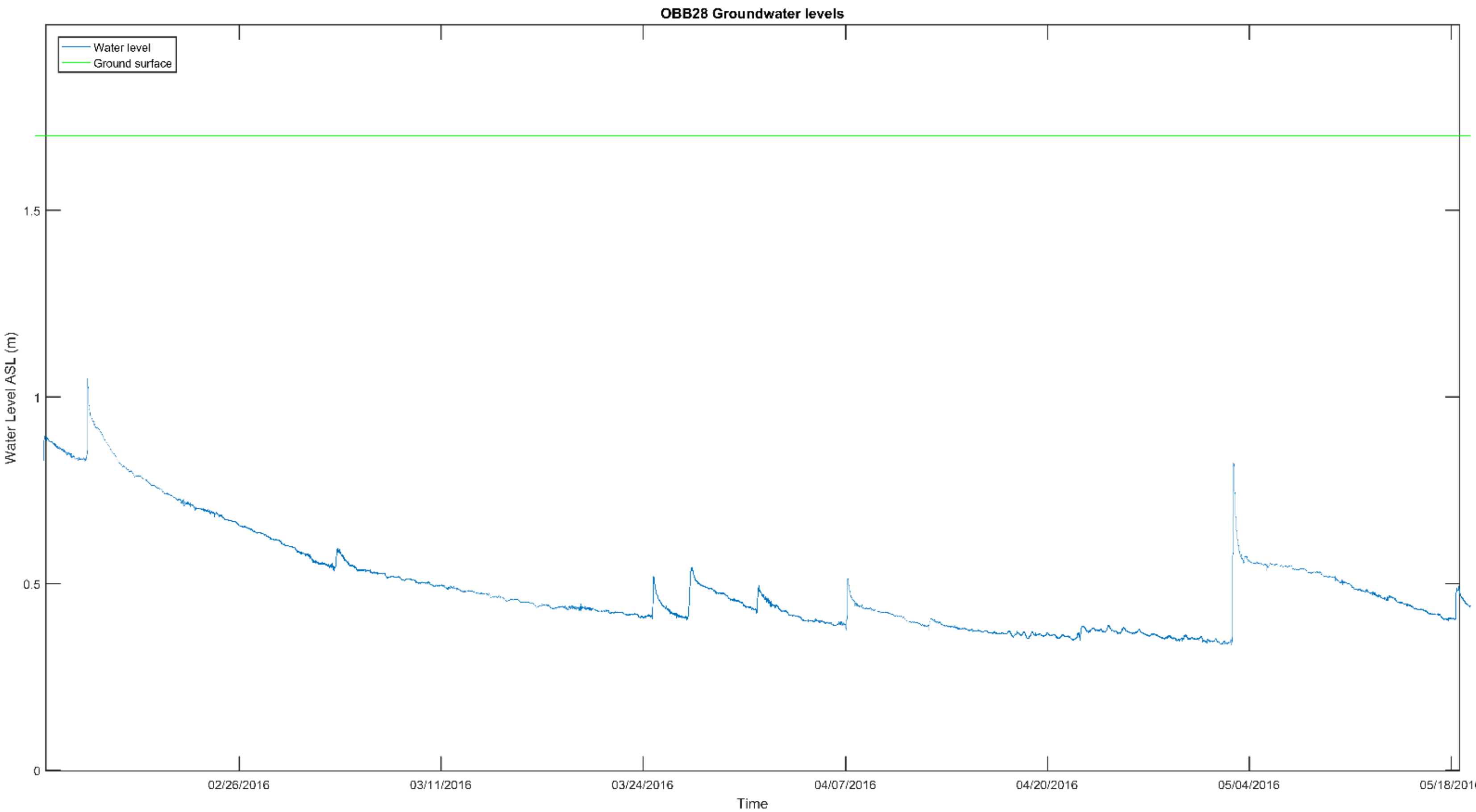

OBB28 Groundwater levels
Water level
Ground surface
Water Level ASL (m)
0
0.5
1
1.5
02/26/2016
03/11/2016
03/24/2016
04/07/2016
04/20/2016
05/04/2016
05/18/2016
Time

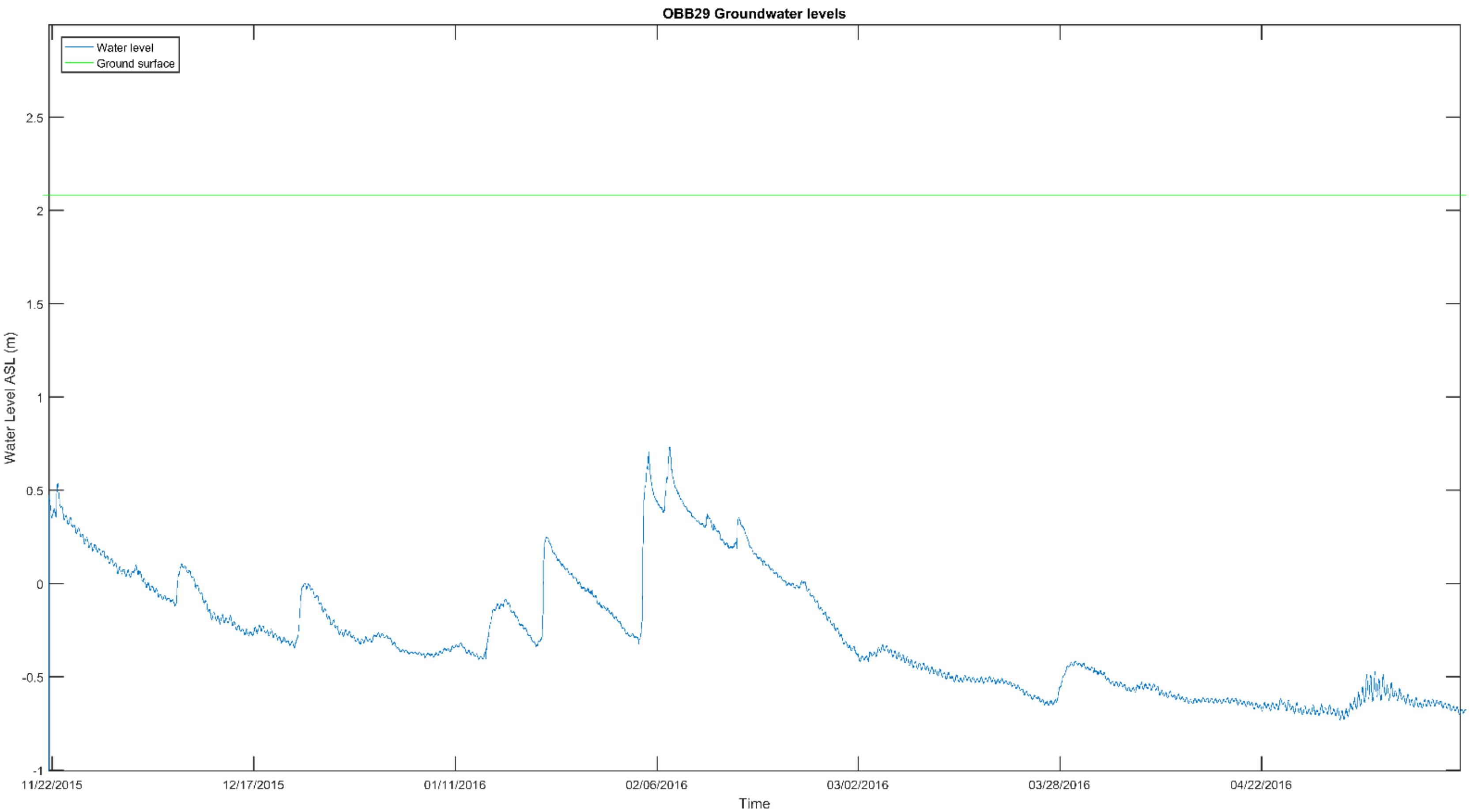

OBB29 Groundwater levels
Water level
Ground surface
Water Level ASL (m)
2.5
2
1.5
1
0.5
0
-0.5
-1
11/22/2015
12/17/2015
01/11/2016
02/06/2016
03/02/2016
03/28/2016
04/22/2016
Time

Appendix B: Aquifer Properties

Hydraulic Conductivity

Hydraulic conductivity as measured by the permeameter ranged from 3.30 m/d to a maximum of 30.25 m/d with an average of 14.75 m/d (Table 11). Sieve analysis gives a low conductivity of 10.37 m/d and a maximum of 54.43 m/d with an average of 27.70 m/d. Combined these two methods give an average of 24.0 m/d. These values are consistent with values seen in silty to clean sand typical of the surficial aquifer (Heath, 1983, Lautier, 2001). These value are not consistent with those seen in previous research on Bogue Banks. Sisco (2013) found much lower hydraulic conductivities ($7x10^{-4}$). However, Sisco was studying low-lying swales where lower conductivity materials are expected.

Table 11- Falling head permeameter readings

Core Number	dt (cm)	dc (cm)	L (cm)	h_0 (cm)	h_1 (cm)	t_1 (s)	h_2 (cm)	t_2 (s)	K (m/d)
3S	1.27	4.128	85.6	70	60	283.6	37	1014.6	4.10
3I	1.27	4.128	75.4	80.5	70.5	33.9	48	130.7	24.25
3D	1.27	4.128	87	72	62	38.3	40	127.7	30.25
4S	1.27	4.128	62.3	97	87	31.9	63	116.7	17.90
4I	1.27	4.128	60.6	99	88	175.3	65	634.1	3.30
4D	1.27	4.128	85.4	73.5	63.5	109.1	40	438.6	9.55
7S	1.27	4.128	76.8	79	69	52.4	47	176.4	17.35
8S	1.27	4.128	82.5	72	62	67.3	38	268.5	15.55
12-1	1.27	4.128	65	93	83	22.6	61	87.8	26.23
12-2	1.27	4.128	82	76.5	66	60.65	44	230	16.17
12-3	1.27	4.128	85.6	73	63	145	39.5	584.7	7.25
12-4	1.27	4.128	77	79	69	47.2	46	174.1	18.85
12-6	1.27	4.128	43	114	104	30.1	81	168.8	10.83
19S	1.27	4.128	82	74	64	107.1	40	420.2	9.45
19I	1.27	4.128	73.2	80	70	69.2	47	256.5	12.00
19D	1.27	4.128	55.7	96	86	38.3	63	149.9	12.95

Table 12- Driscoll Sieve Analysis.

Sample ID	Sample weight (g)	Weight retained at <0.63 mm (g)	Weight retained at 0.63 mm (g)	Weight retained at 0.125 mm (g)	Weight retained at 0.18 mm (g)	Weight retained at 0.25 mm (g)	Weight retained at 1 mm (g)	Weight retained at 2 mm (g)
3-1	18.771	0.003	0.211	4.851	7.185	6.505	0.016	0.000
3-2	30.951	0.014	0.723	9.761	9.214	10.991	0.191	0.057
3-3	25.235	0.011	0.169	6.554	8.388	8.803	0.758	0.552
3-4	28.059	0.004	1.713	8.661	13.178	4.498	0.005	0.000
3-5	25.503	0.005	0.937	7.817	12.191	4.547	0.006	0.000
4S	25.786	0.005	1.277	12.626	10.773	1.074	0.016	0.015
4I	30.434	0.014	0.966	14.297	10.102	4.878	0.157	0.020
4D	17.486	0.026	0.312	8.304	6.424	2.410	0.010	0.000
7-1	30.459	0.001	0.267	7.062	15.928	7.199	0.002	0.000
7-2	46.639	0.005	0.328	13.051	22.272	10.983	0.000	0.000
7-3	52.751	0.013	1.261	22.278	19.877	9.321	0.001	0.000
7-4	49.437	0.060	0.625	14.617	17.543	16.522	0.061	0.009
7-5	33.896	0.000	0.534	8.027	10.444	14.781	0.110	0.000
8S	20.875	0.005	0.592	10.021	9.916	0.341	0.000	0.000
8I	29.207	0.002	0.278	10.749	13.421	4.730	0.027	0.000
8D	17.09	0.000	0.345	7.921	8.660	0.164	0.000	0.000
11S	36.708	0.001	0.178	1.821	14.849	19.670	0.083	0.106
11I	26.801	0.002	0.124	0.773	3.584	15.532	3.034	3.752
11D	28.508	0.003	0.200	1.586	8.654	17.912	0.106	0.047
12-1	26.932	0.000	0.068	2.920	15.040	8.896	0.008	0.000
12-2	34.201	0.001	0.321	6.181	18.204	9.494	0.000	0.000
12-3	27.253	0.000	0.134	5.102	15.738	6.279	0.000	0.000
12-4	38.893	0.002	0.431	4.536	15.598	18.293	0.033	0.000
12-5	36.85	0.112	0.581	6.074	13.213	16.861	0.009	0.000
12-6	26.593	0.006	0.194	2.697	7.406	15.724	0.406	0.160

Table 12 continued.

Sample ID	Sample weight (g)	Weight retained at <0.63 mm (g)	Weight retained at 0.63 mm (g)	Weight retained at 0.125 mm (g)	Weight retained at 0.18 mm (g)	Weight retained at 0.25 mm (g)	Weight retained at 1 mm (g)	Weight retained at 2 mm (g)
17S	53.24	0.013	0.424	7.855	24.638	20.296	0.014	0.000
17I	57.524	0.065	0.946	17.688	22.544	16.240	0.030	0.011
17D	25.003	0.008	0.320	4.749	11.099	8.789	0.018	0.020
19S	25.43	0.007	0.251	3.167	12.335	9.670	0.000	0.000
19I	26.333	0.002	0.078	0.352	3.287	22.558	0.056	0.000
19D	126.708	0.047	0.274	5.003	19.379	91.526	8.340	2.139
26-1	26.995	0.003	0.115	3.785	12.708	10.381	0.003	0.000
26-2	39.871	0.001	0.067	1.126	11.663	27.005	0.009	0.000
26-3	26.659	0.004	0.218	4.132	11.164	11.139	0.002	0.000
26-4	38.554	0.007	0.171	1.438	12.914	24.018	0.006	0.000
26-5	34.69	0.011	0.152	1.671	11.417	21.434	0.005	0.000
26-6	31.135	0.005	0.207	2.514	10.210	18.196	0.003	0.000
26-7	175.399	0.458	2.267	36.373	60.858	74.647	0.530	0.266
28S	26.446	0.004	0.809	17.666	7.659	0.307	0.001	0.000
28I	2.459	0.001	0.013	0.055	0.120	0.199	0.194	1.877
28D	117.918	0.189	18.689	58.772	39.436	0.670	0.040	0.122

Cumulative weight percent retained

The following graphs correspond to Table 12. These were then used in conjunction with Equation 2 to find a value for hydraulic conductivity of the surficial aquifer based on the Driscoll method.

3-1

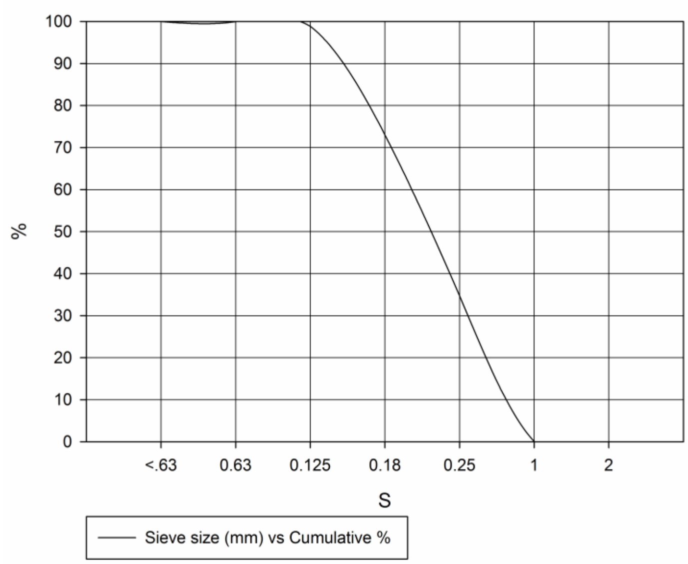

3-2

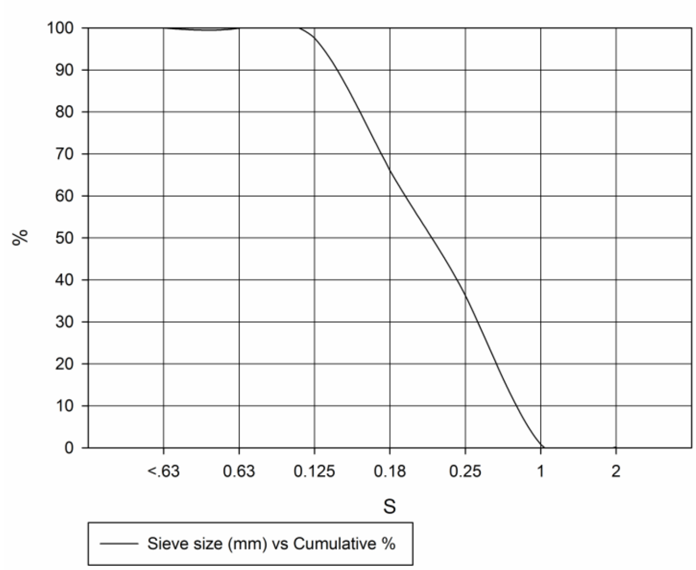

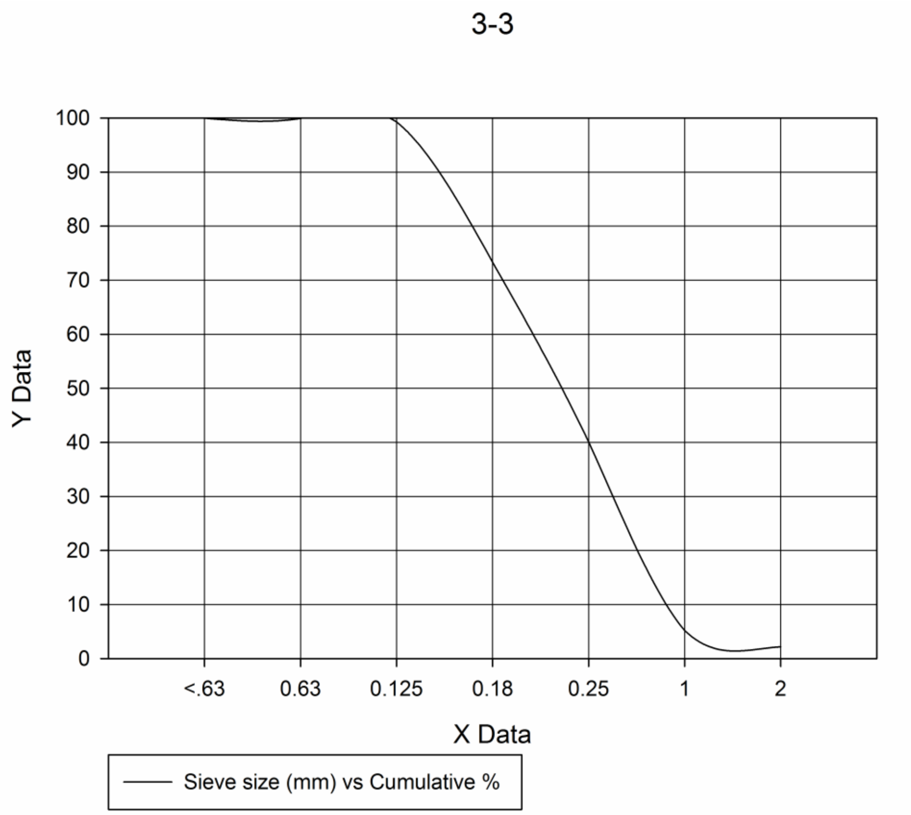
3-3
100
90
80
70
60
50
40
30
20
10
0
Y Data
<.63
0.63
0.125
0.18
0.25
1
2
X Data
Sieve size (mm) vs Cumulative %

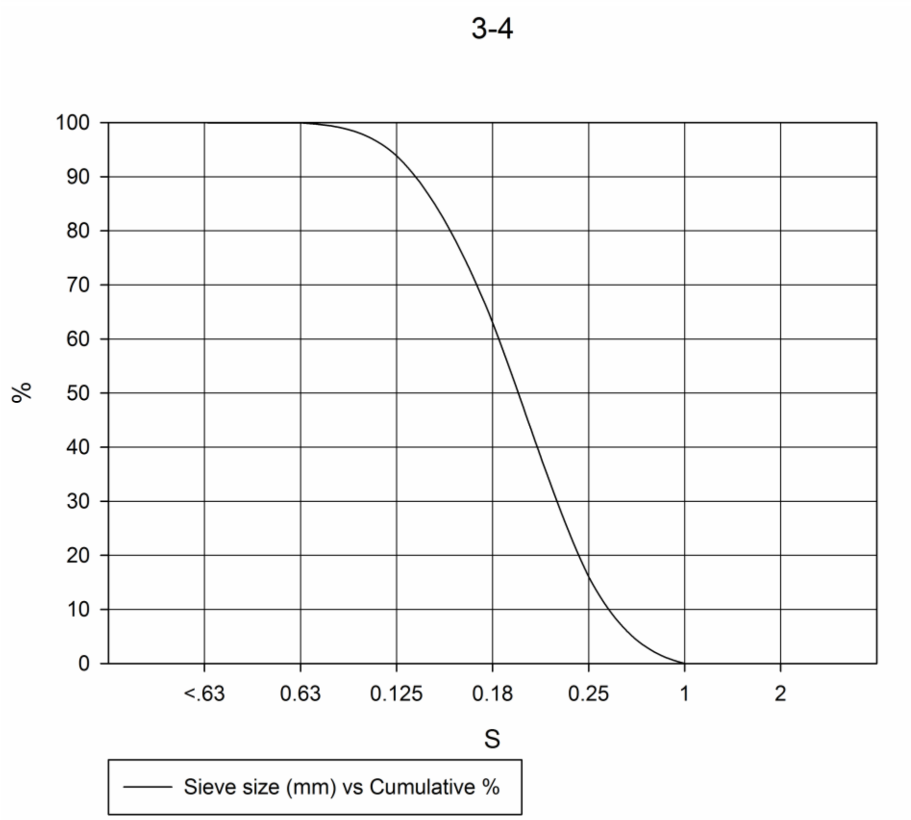
3-4
100
90
80
70
60
50
40
30
20
10
0
%
<.63
0.63
0.125
0.18
0.25
1
2
S
Sieve size (mm) vs Cumulative %

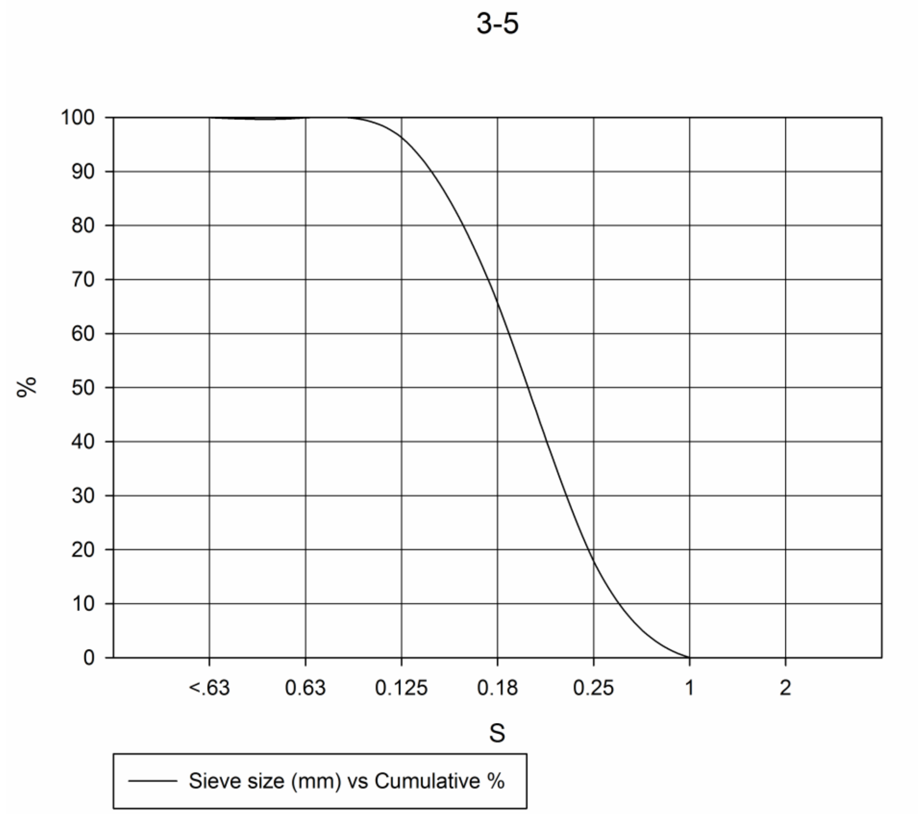
3-5
100
90
80
70
60
50
40
30
20
10
0
%
<.63
0.63
0.125
0.18
0.25
1
2
S
Sieve size (mm) vs Cumulative %

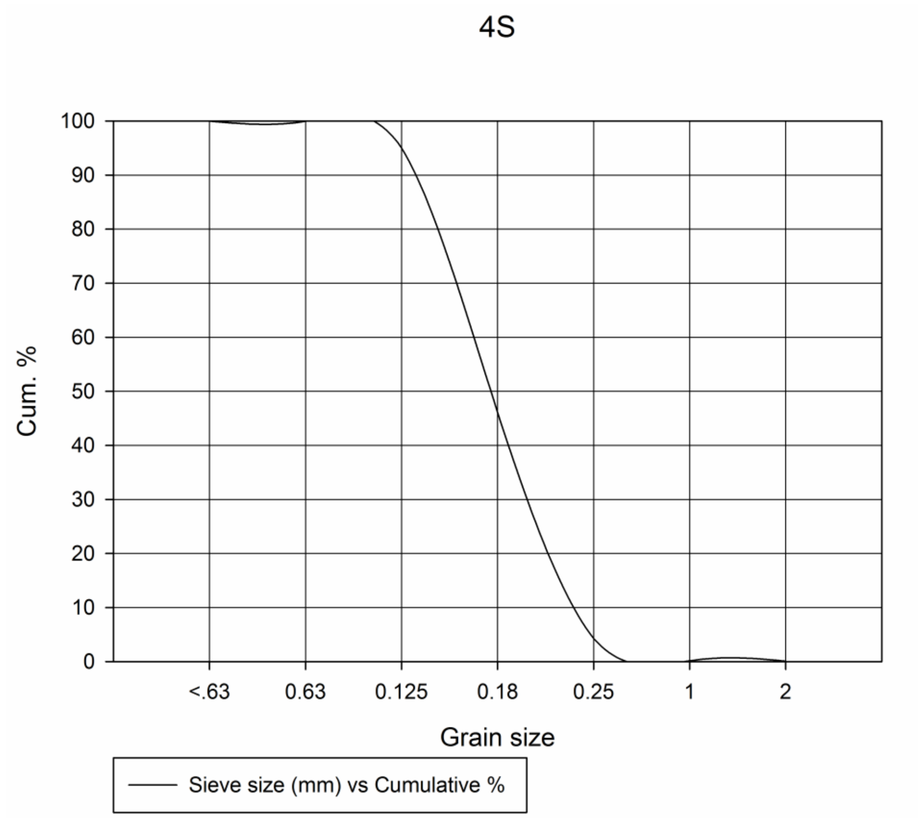
4S
100
90
80
70
60
50
40
30
20
10
0
Cum. %
<.63
0.63
0.125
0.18
0.25
1
2
Grain size
Sieve size (mm) vs Cumulative %

4I

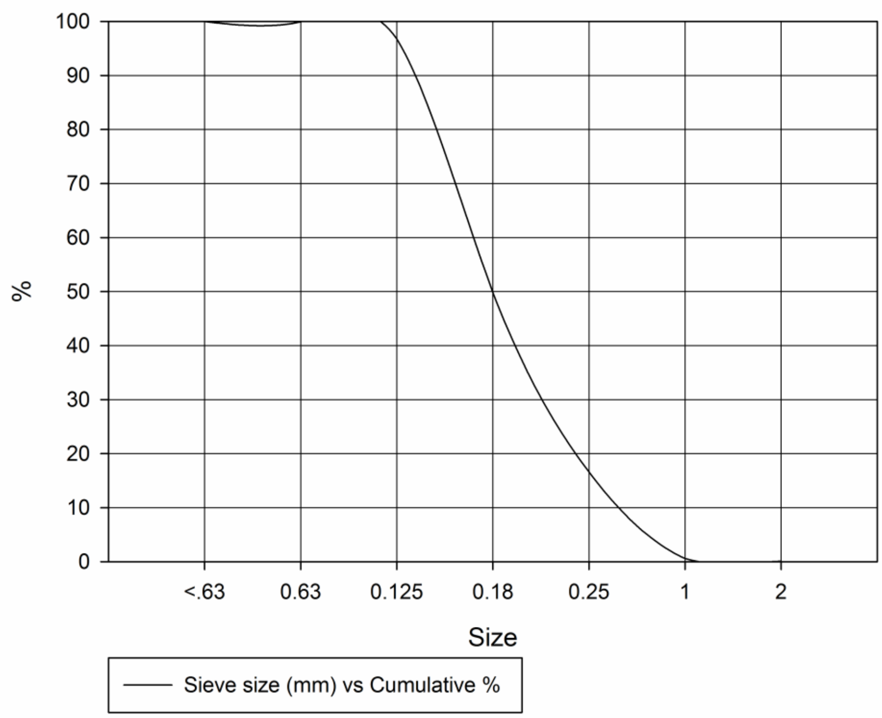
100
90
80
70
60
50
40
30
20
10
0
%
<.63
0.63
0.125
0.18
0.25
1
2
Size
Sieve size (mm) vs Cumulative %

4D

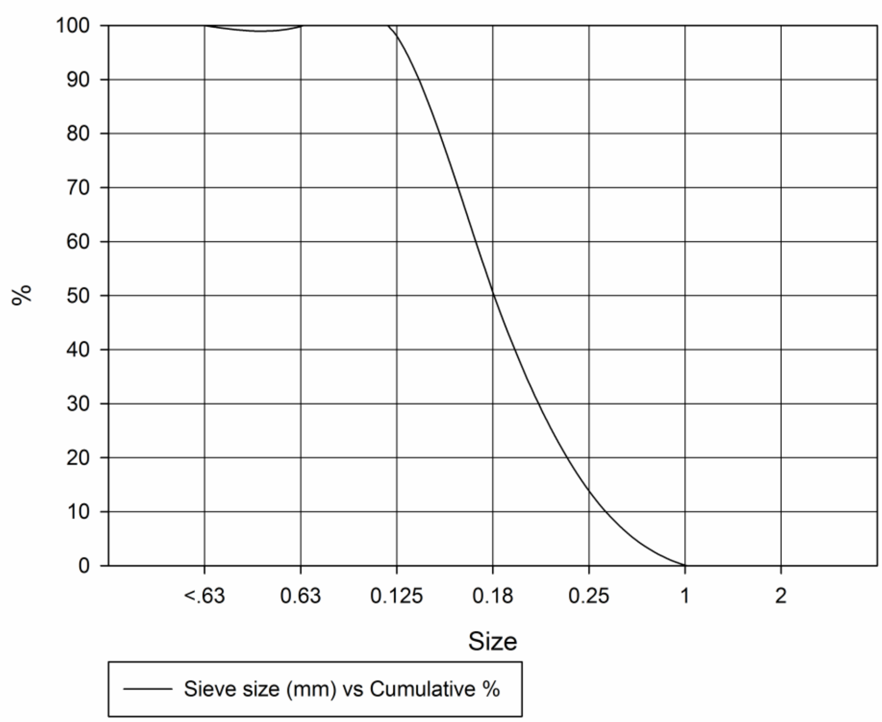
100
90
80
70
60
50
40
30
20
10
0
%
<.63
0.63
0.125
0.18
0.25
1
2
Size
Sieve size (mm) vs Cumulative %

7-1

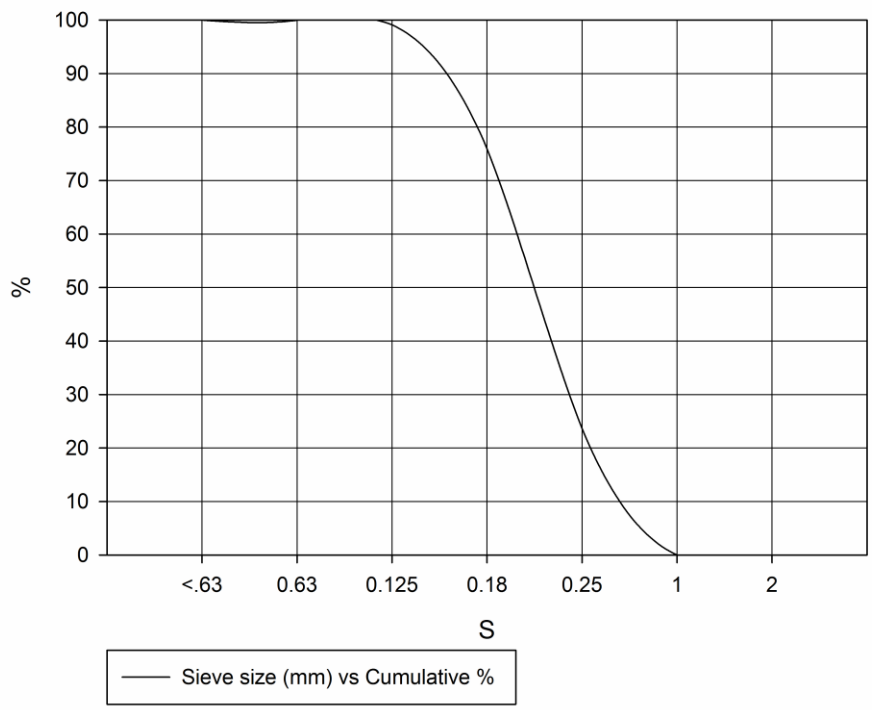
100
90
80
70
60
50
40
30
20
10
0
%
<.63
0.63
0.125
0.18
0.25
1
2
S
Sieve size (mm) vs Cumulative %

7-2

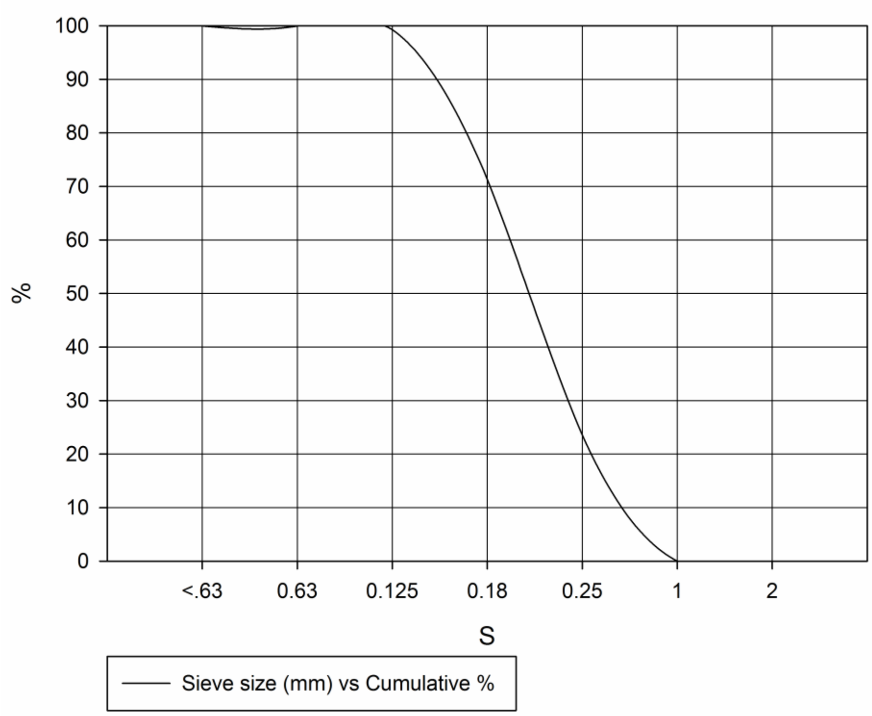
100
90
80
70
60
50
40
30
20
10
0
%
<.63
0.63
0.125
0.18
0.25
1
2
S
Sieve size (mm) vs Cumulative %

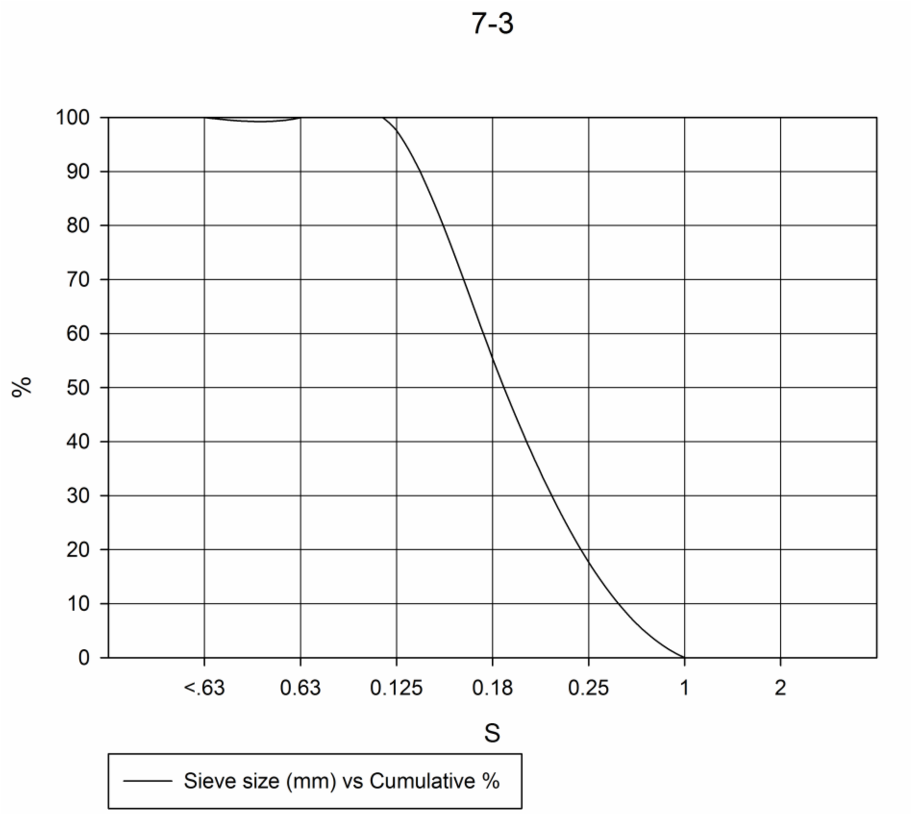
7-3
100
90
80
70
60
50
40
30
20
10
0
%
<.63
0.63
0.125
0.18
0.25
1
2
S
Sieve size (mm) vs Cumulative %

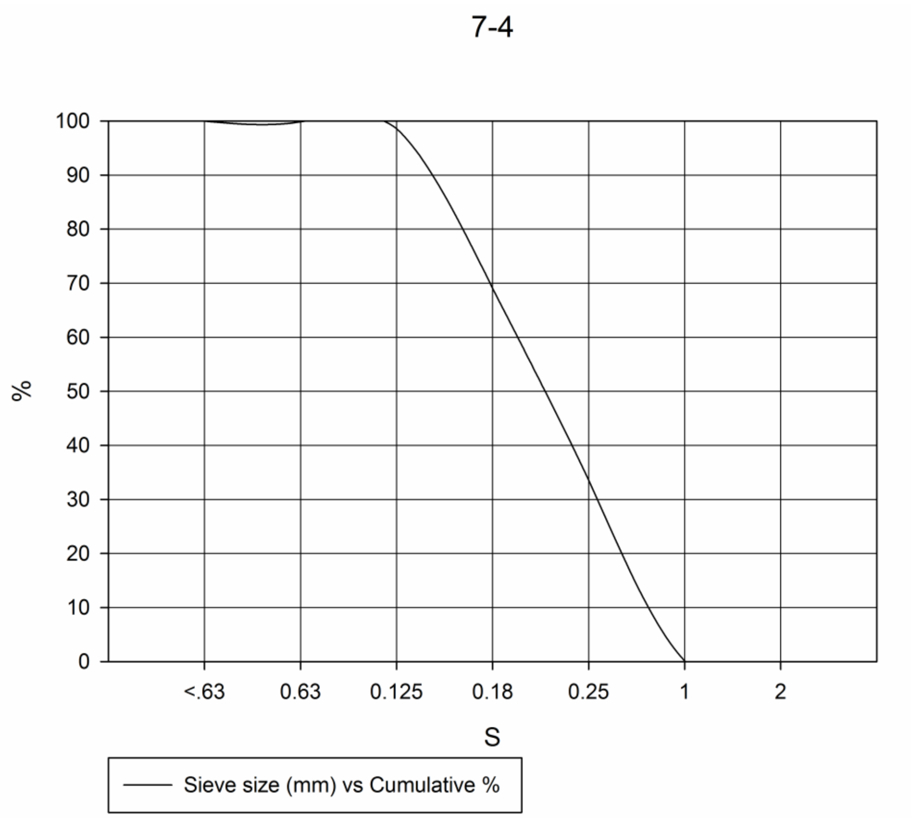
7-4
100
90
80
70
60
50
40
30
20
10
0
%
<.63
0.63
0.125
0.18
0.25
1
2
S
Sieve size (mm) vs Cumulative %

7-5

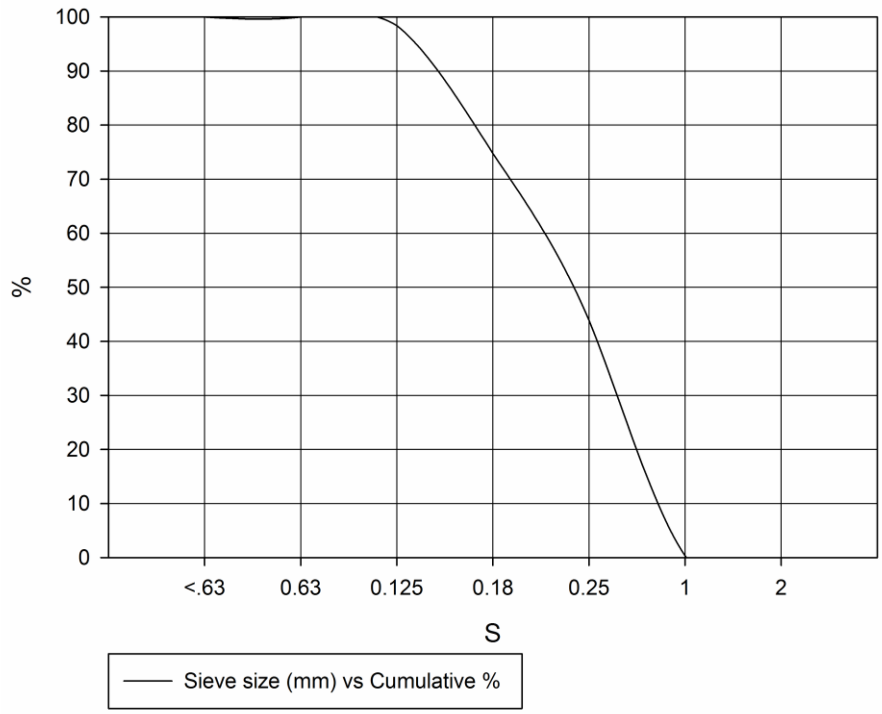
100
90
80
70
60
50
40
30
20
10
0
%
<.63
0.63
0.125
0.18
0.25
1
2
S
Sieve size (mm) vs Cumulative %

8S

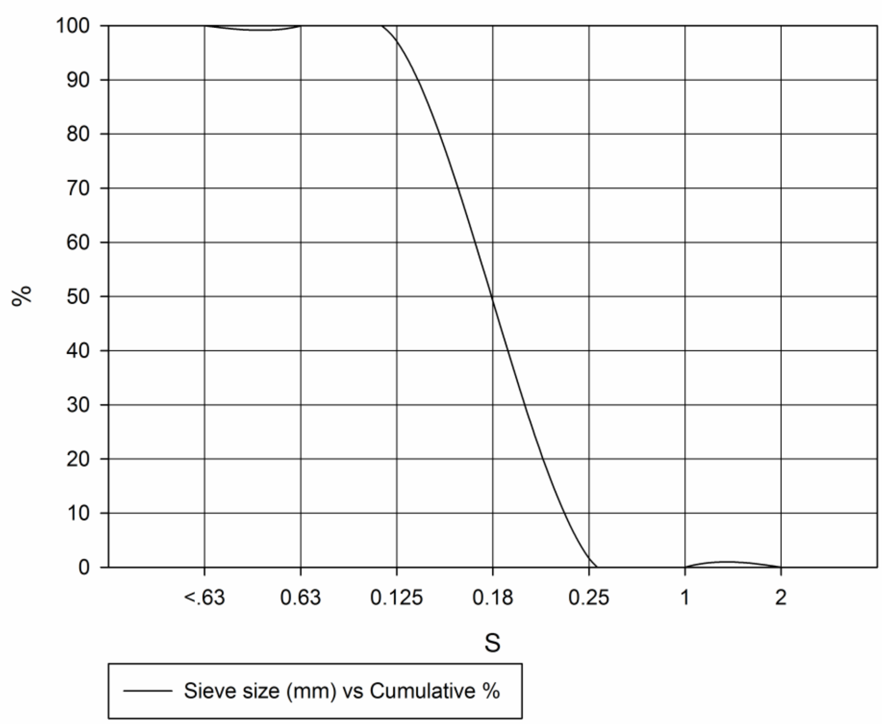
100
90
80
70
60
50
40
30
20
10
0
%
<.63
0.63
0.125
0.18
0.25
1
2
S
Sieve size (mm) vs Cumulative %

8I

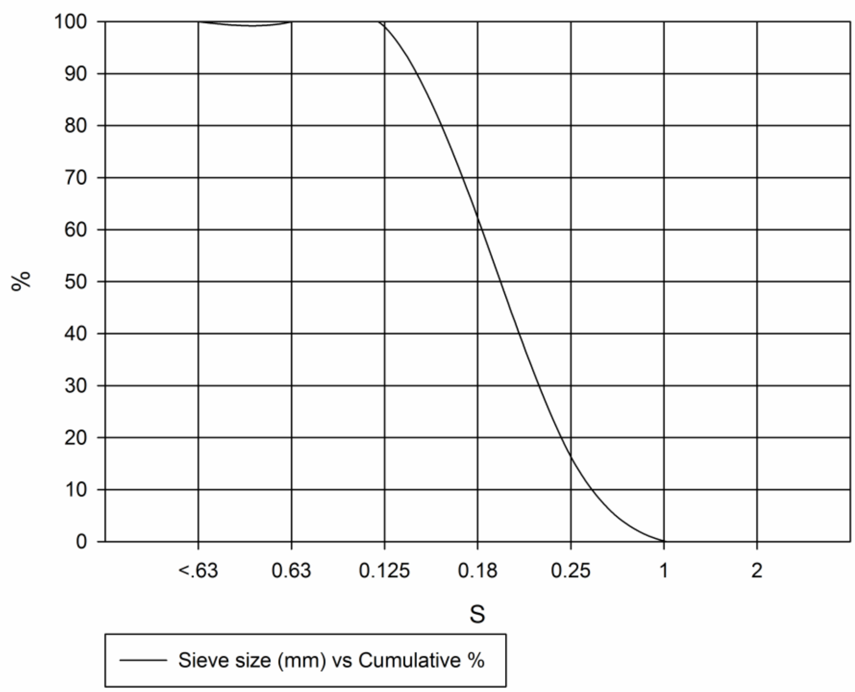
100
90
80
70
60
50
40
30
20
10
0
%
<.63
0.63
0.125
0.18
0.25
1
2
S
Sieve size (mm) vs Cumulative %

8D

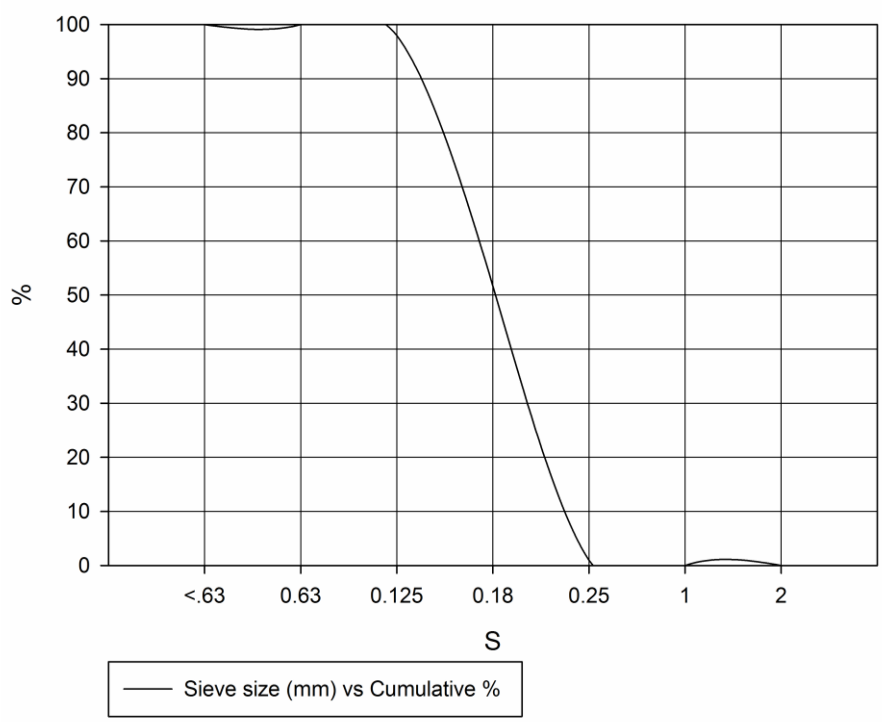
100
90
80
70
60
50
40
30
20
10
0
%
<.63
0.63
0.125
0.18
0.25
1
2
S
Sieve size (mm) vs Cumulative %

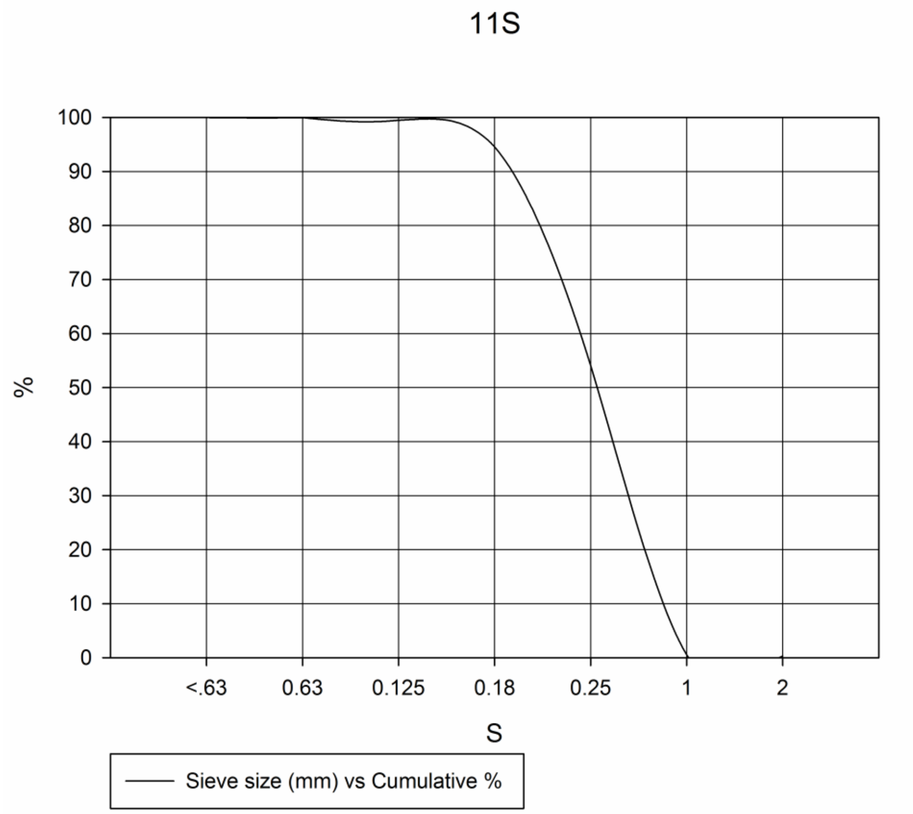
11S
100
90
80
70
60
50
40
30
20
10
0
%
<.63
0.63
0.125
0.18
0.25
1
2
S
Sieve size (mm) vs Cumulative %

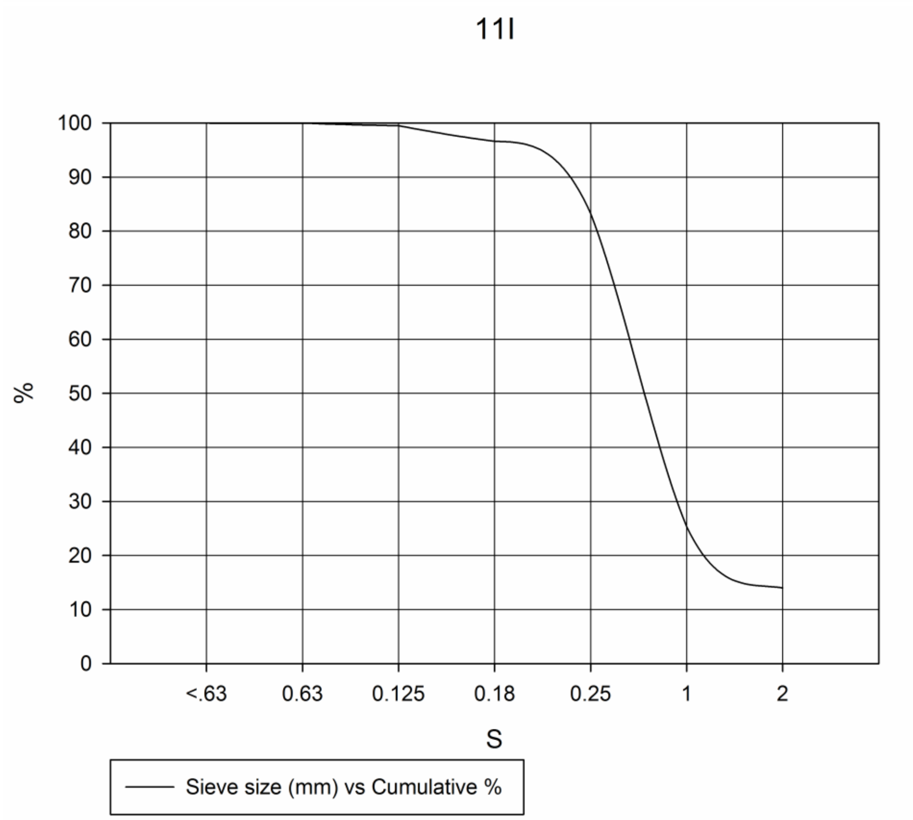
11I
100
90
80
70
60
50
40
30
20
10
0
%
<.63
0.63
0.125
0.18
0.25
1
2
S
Sieve size (mm) vs Cumulative %

12-1

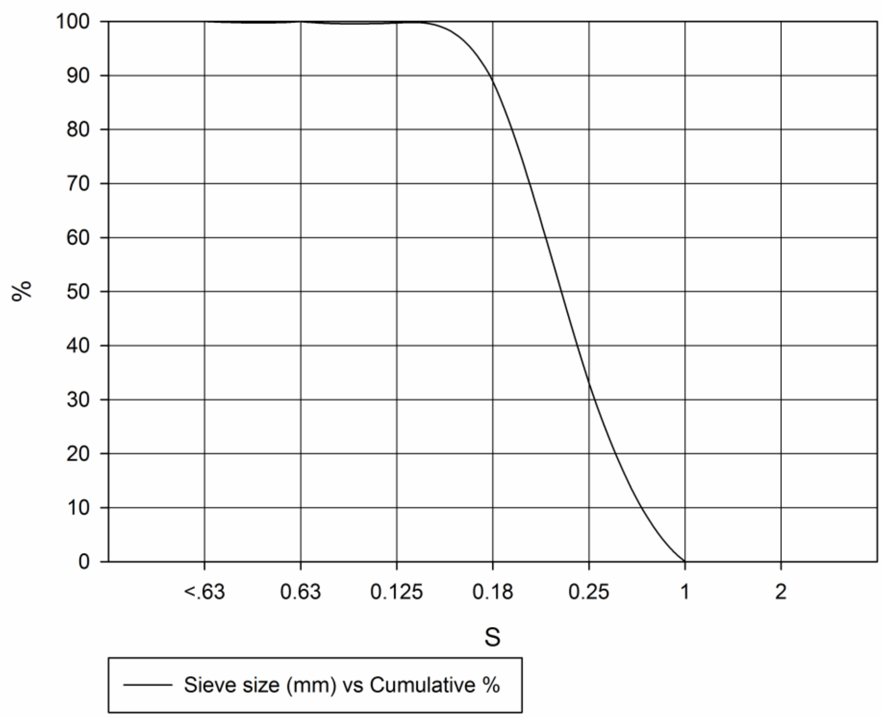
100
90
80
70
60
50
40
30
20
10
0
%
<.63
0.63
0.125
0.18
0.25
1
2
S
Sieve size (mm) vs Cumulative %

12-2

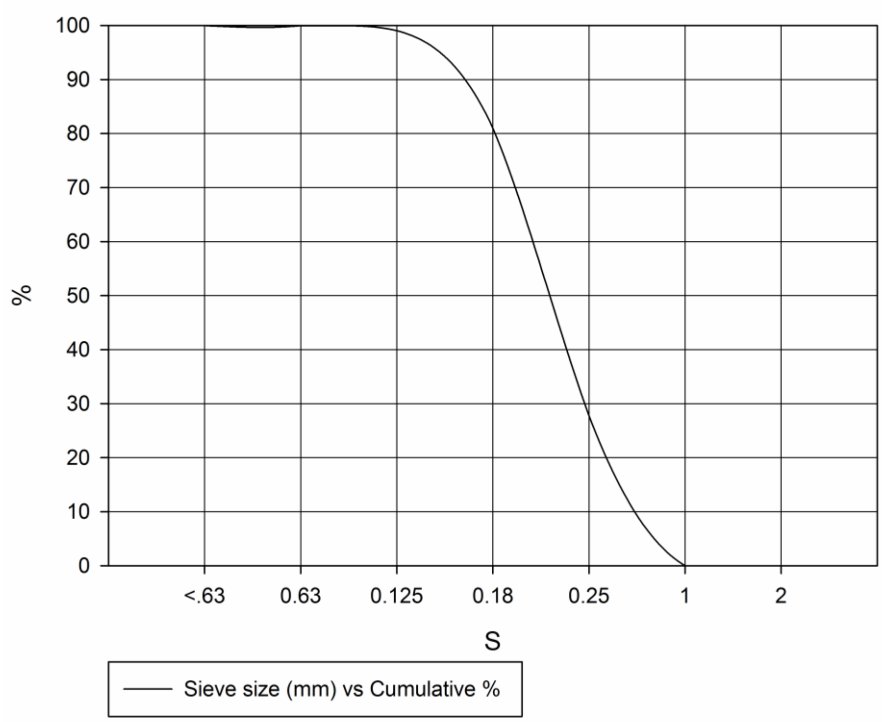
100
90
80
70
60
50
40
30
20
10
0
%
<.63
0.63
0.125
0.18
0.25
1
2
S
Sieve size (mm) vs Cumulative %

12-3

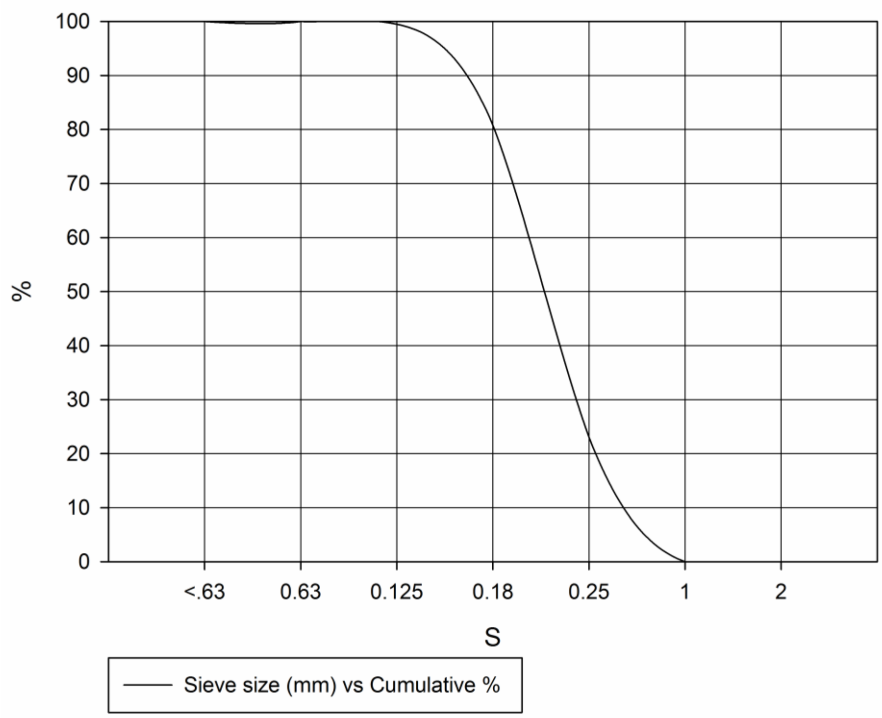

%
100
90
80
70
60
50
40
30
20
10
0
<.63
0.63
0.125
0.18
0.25
1
2
S
Sieve size (mm) vs Cumulative %

12-4

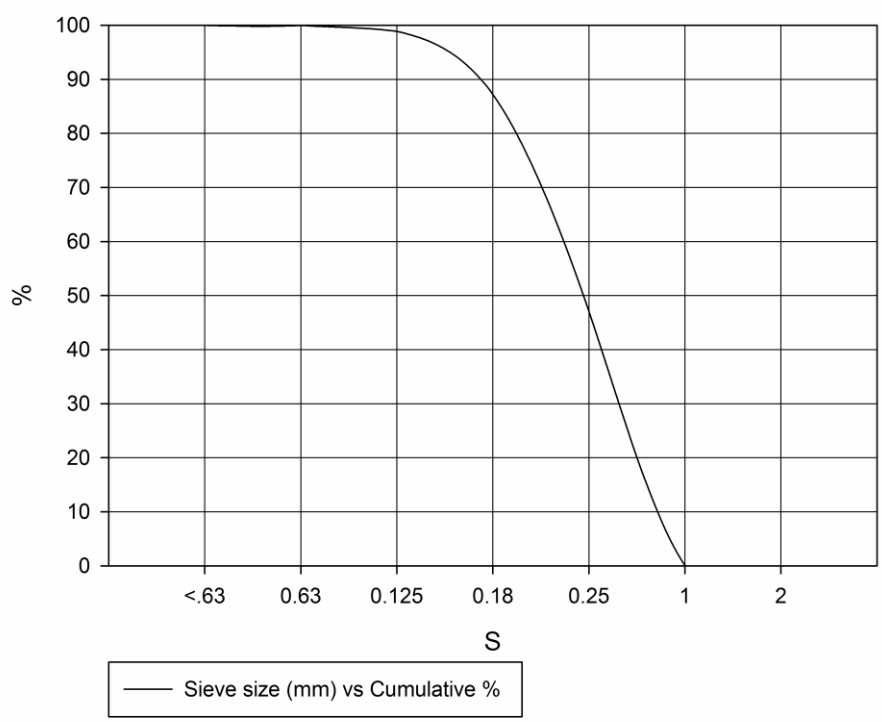

%
100
90
80
70
60
50
40
30
20
10
0
<.63
0.63
0.125
0.18
0.25
1
2
S
Sieve size (mm) vs Cumulative %

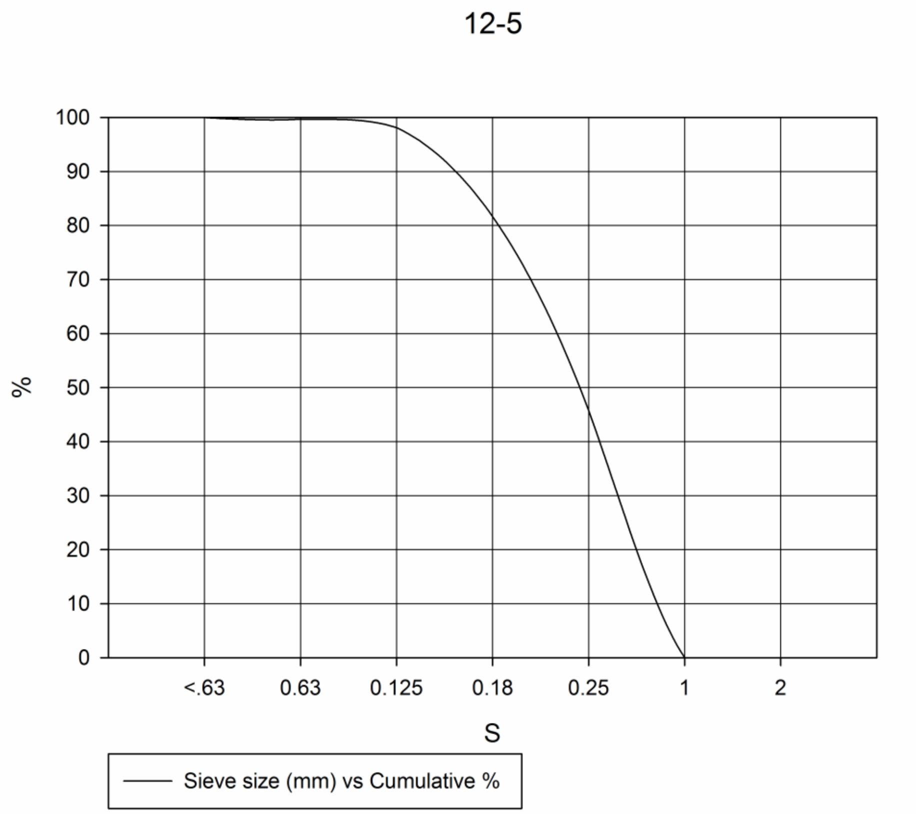
12-5
100
90
80
70
60
50
40
30
20
10
0
%
<.63
0.63
0.125
0.18
0.25
1
2
S
Sieve size (mm) vs Cumulative %

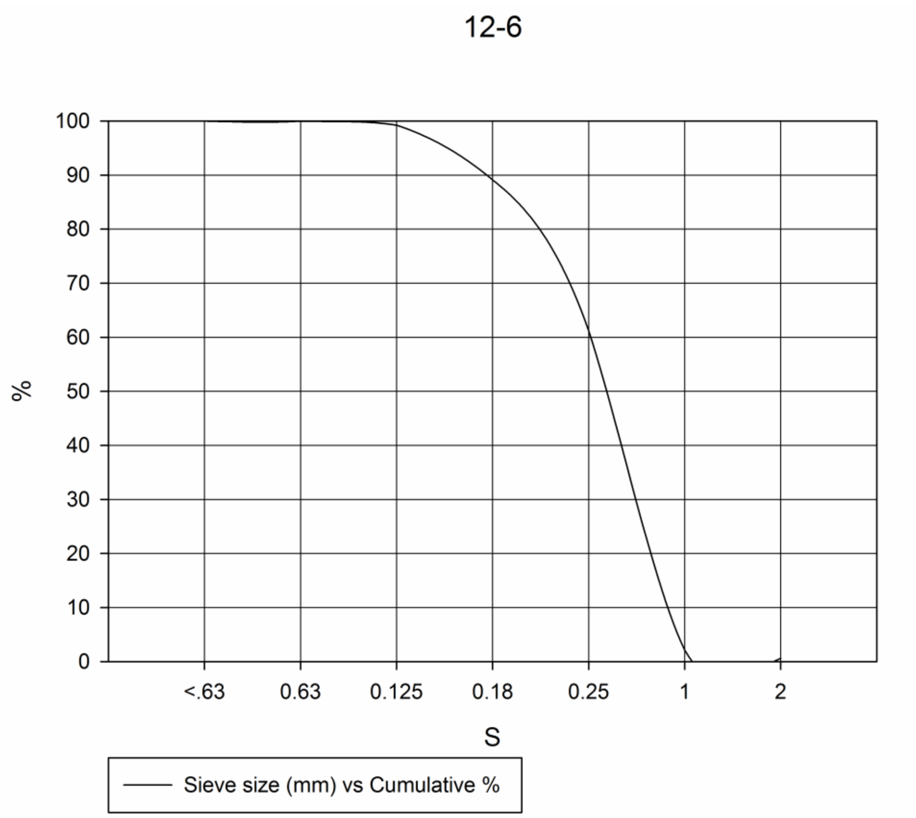
12-6
100
90
80
70
60
50
40
30
20
10
0
%
<.63
0.63
0.125
0.18
0.25
1
2
S
Sieve size (mm) vs Cumulative %

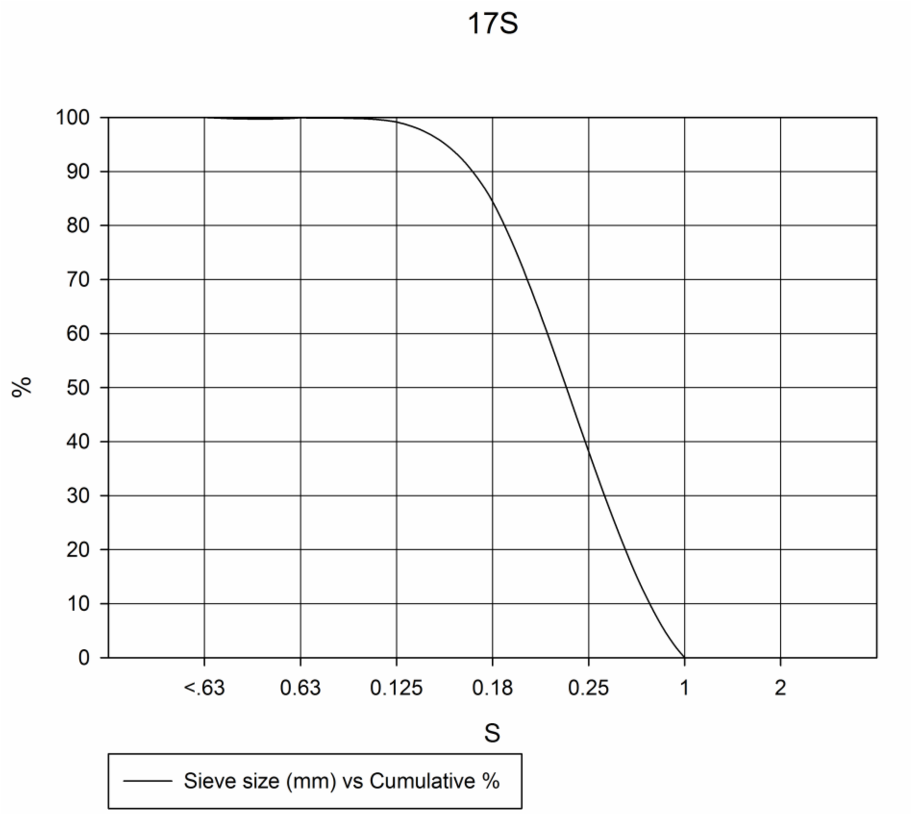
17S
100
90
80
70
60
50
40
30
20
10
0
%
<.63
0.63
0.125
0.18
0.25
1
2
S
Sieve size (mm) vs Cumulative %

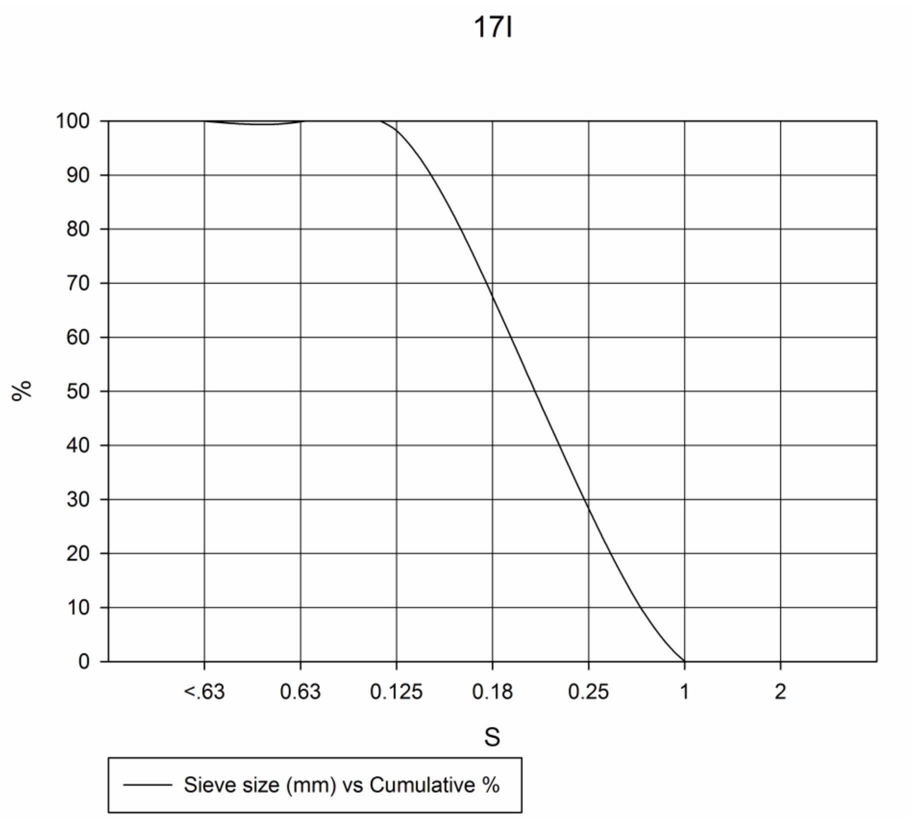
17I
100
90
80
70
60
50
40
30
20
10
0
%
<.63
0.63
0.125
0.18
0.25
1
2
S
Sieve size (mm) vs Cumulative %

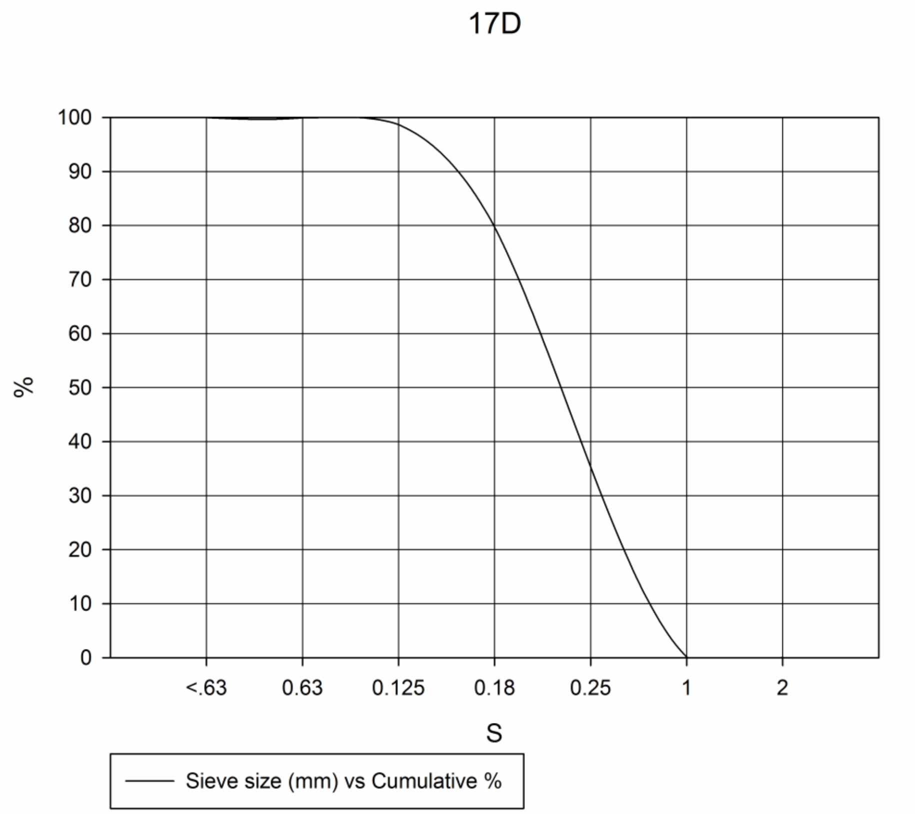
17D
100
90
80
70
60
50
40
30
20
10
0
%
<.63
0.63
0.125
0.18
0.25
1
2
S
Sieve size (mm) vs Cumulative %

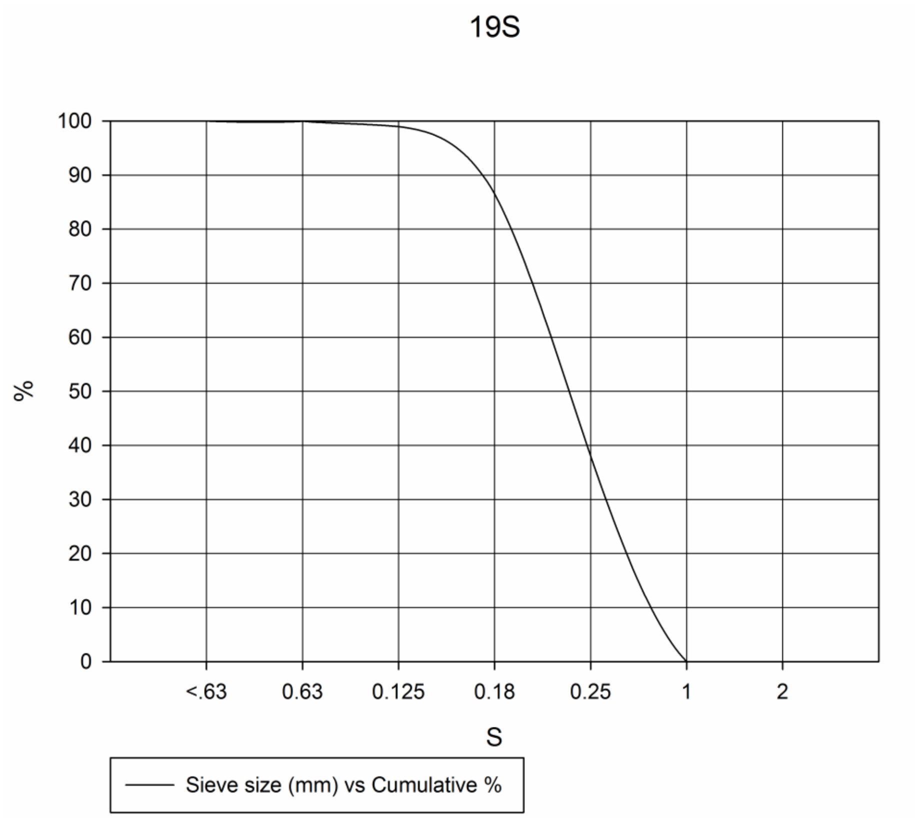
19S
100
90
80
70
60
50
40
30
20
10
0
%
<.63
0.63
0.125
0.18
0.25
1
2
S
Sieve size (mm) vs Cumulative %

19I

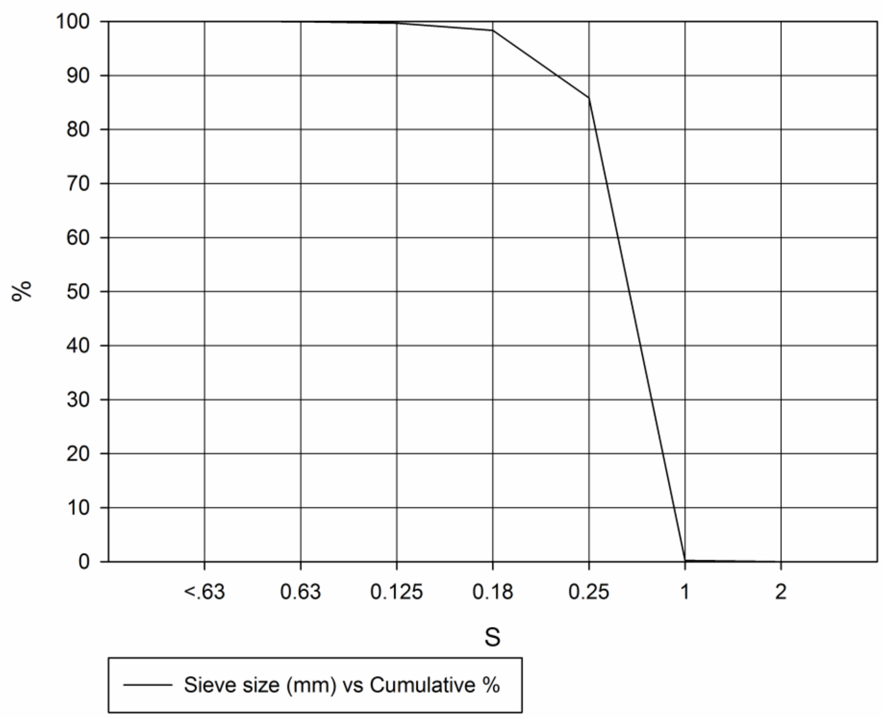
100
90
80
70
60
50
40
30
20
10
0
%
<.63
0.63
0.125
0.18
0.25
1
2
S
Sieve size (mm) vs Cumulative %

19D

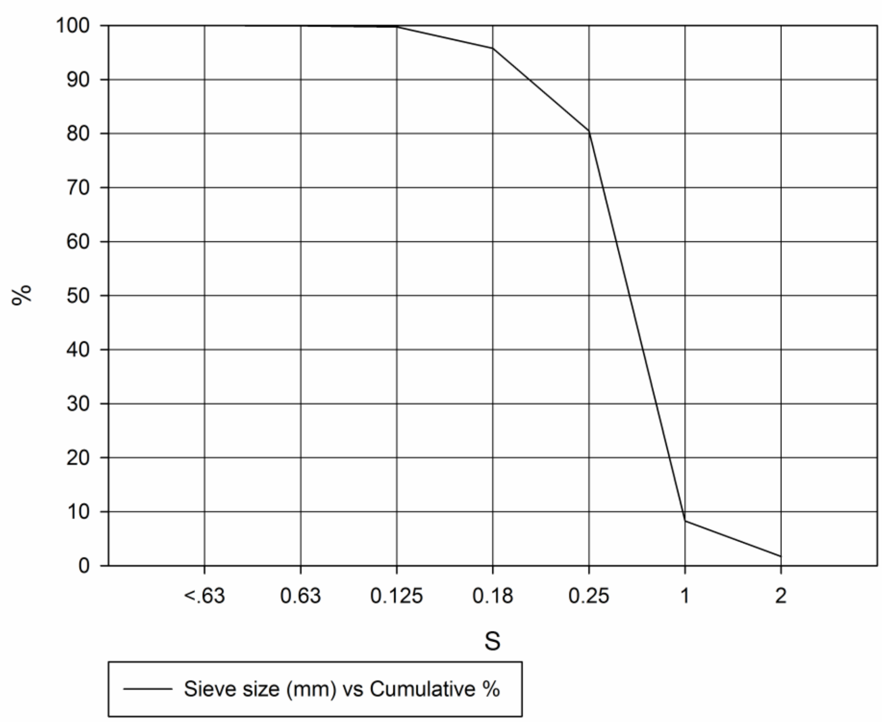
100
90
80
70
60
50
40
30
20
10
0
%
<.63
0.63
0.125
0.18
0.25
1
2
S
Sieve size (mm) vs Cumulative %

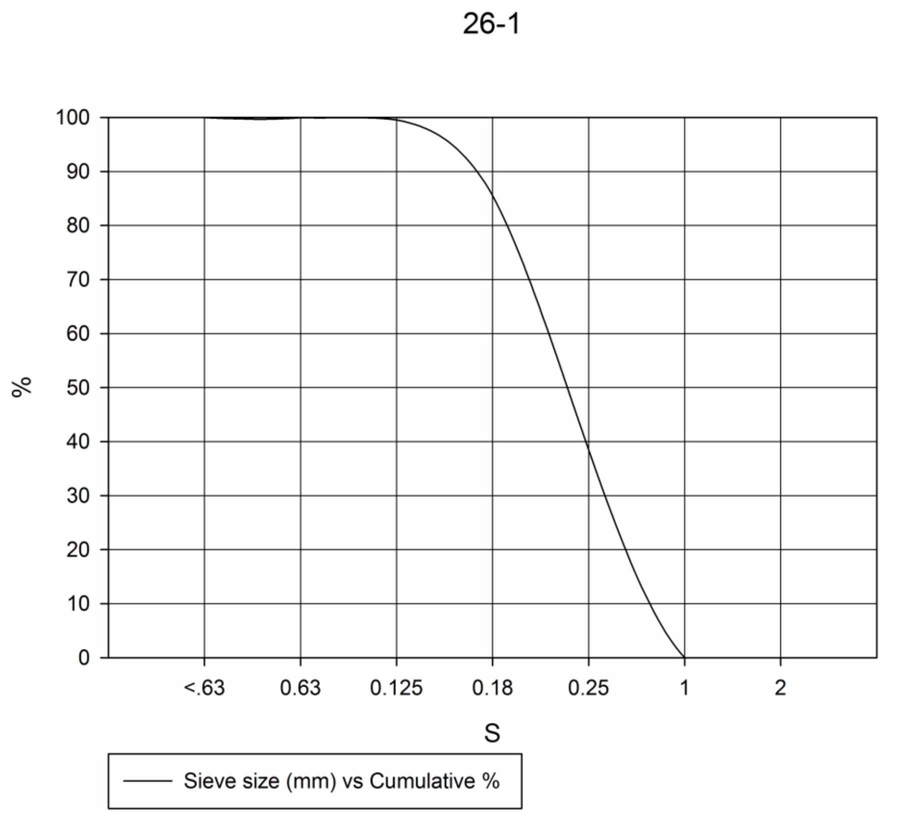
26-1
100
90
80
70
60
50
40
30
20
10
0
%
<.63
0.63
0.125
0.18
0.25
1
2
S
Sieve size (mm) vs Cumulative %

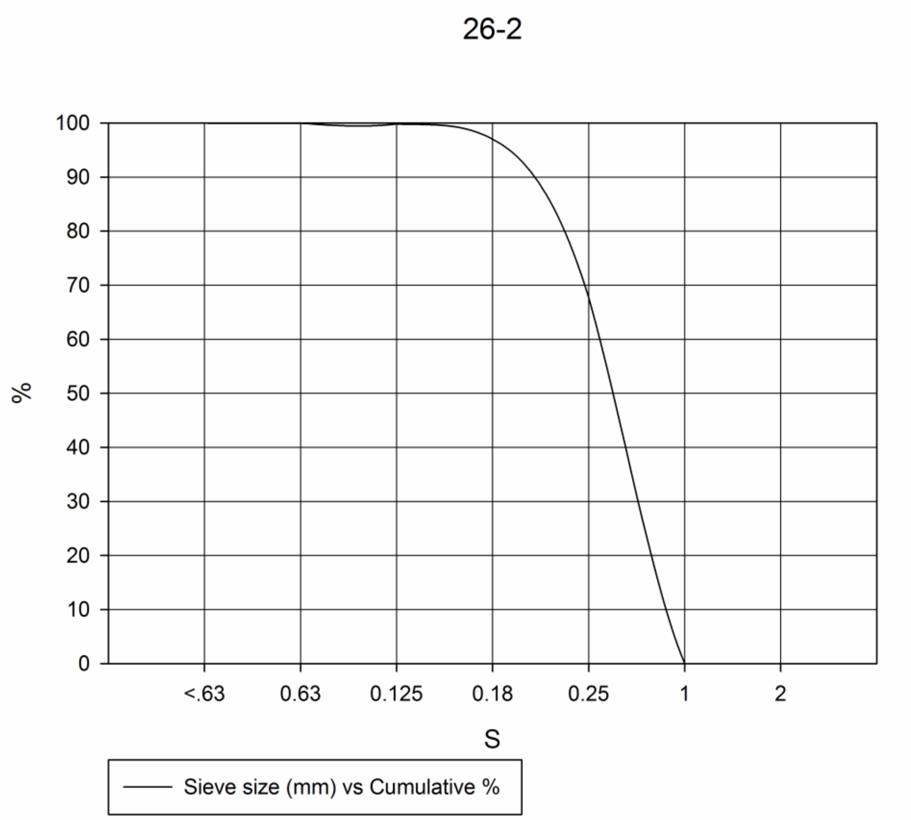
26-2
100
90
80
70
60
50
40
30
20
10
0
%
<.63
0.63
0.125
0.18
0.25
1
2
S
Sieve size (mm) vs Cumulative %

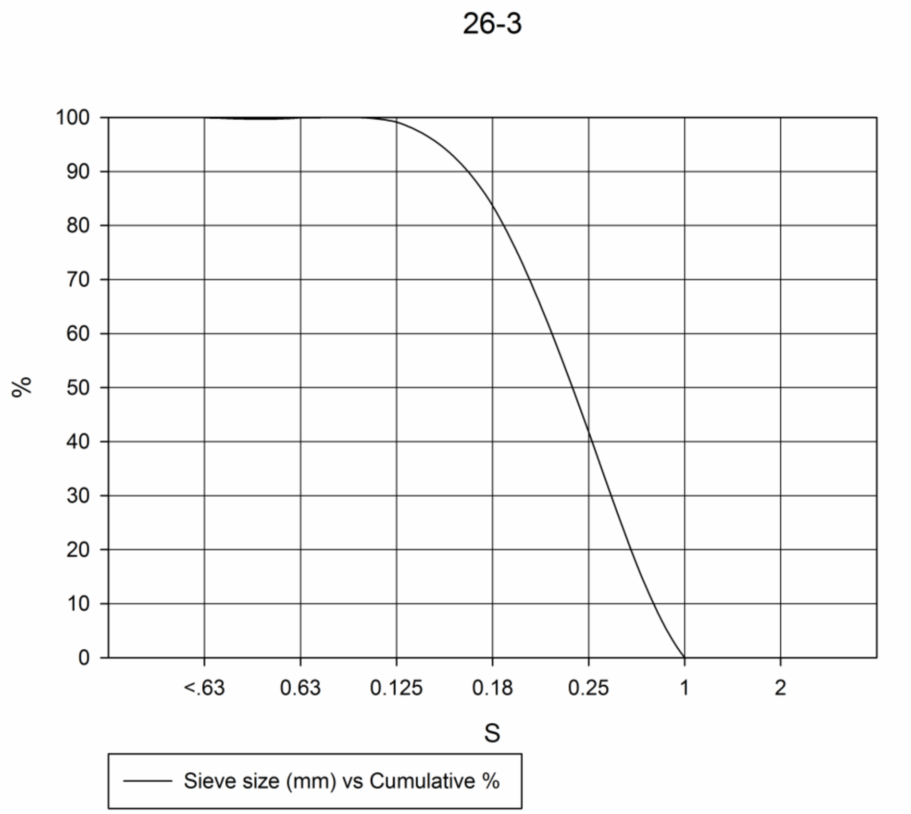
26-3
100
90
80
70
60
50
40
30
20
10
0
%
<.63
0.63
0.125
0.18
0.25
1
2
S
Sieve size (mm) vs Cumulative %

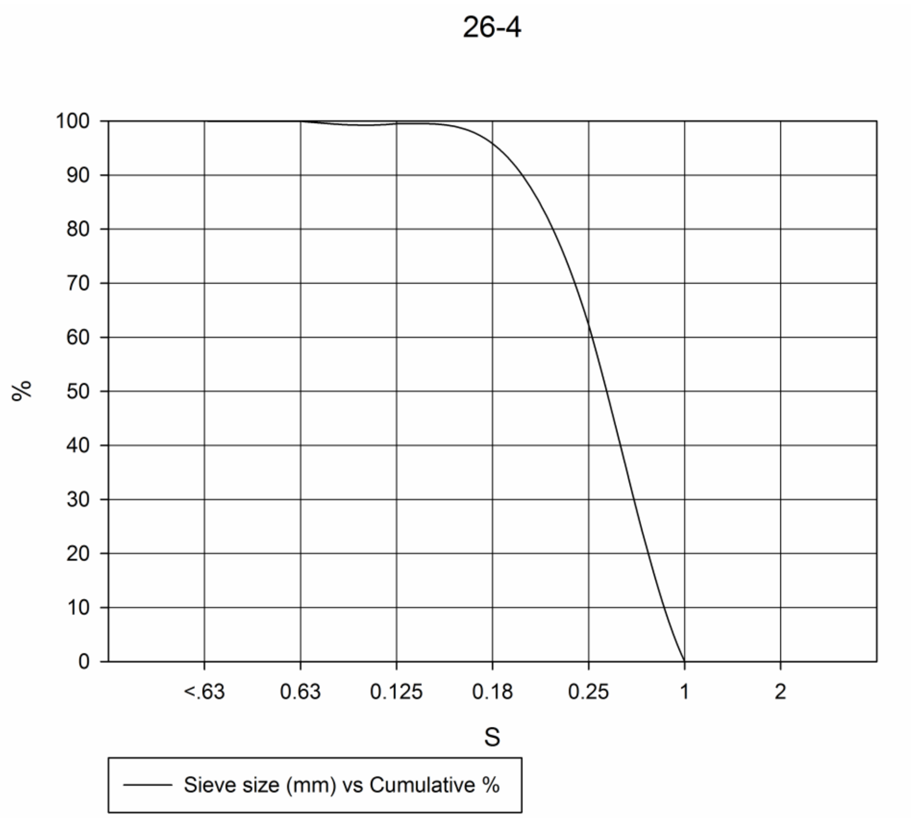
26-4
100
90
80
70
60
50
40
30
20
10
0
%
<.63
0.63
0.125
0.18
0.25
1
2
S
Sieve size (mm) vs Cumulative %

26-5

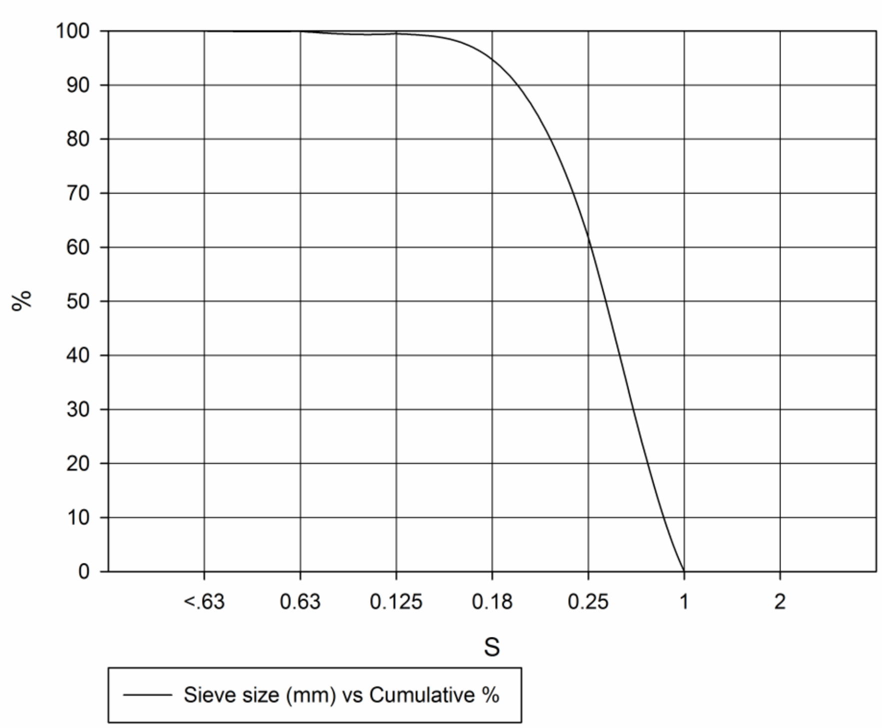
100
90
80
70
60
50
40
30
20
10
0
%
<.63
0.63
0.125
0.18
0.25
1
2
S
Sieve size (mm) vs Cumulative %

26-6

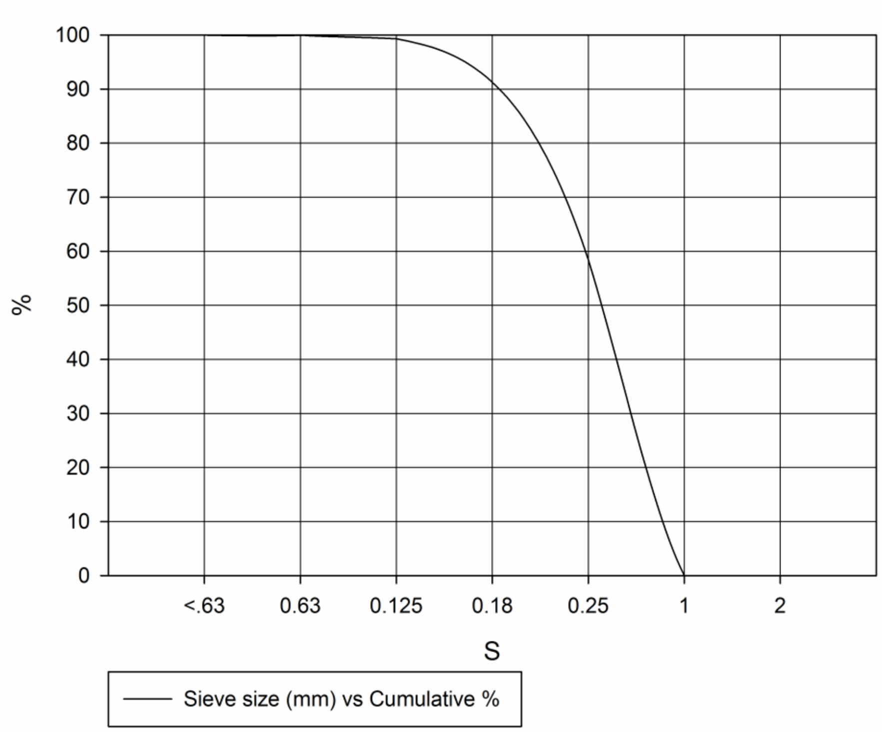
100
90
80
70
60
50
40
30
20
10
0
%
<.63
0.63
0.125
0.18
0.25
1
2
S
Sieve size (mm) vs Cumulative %

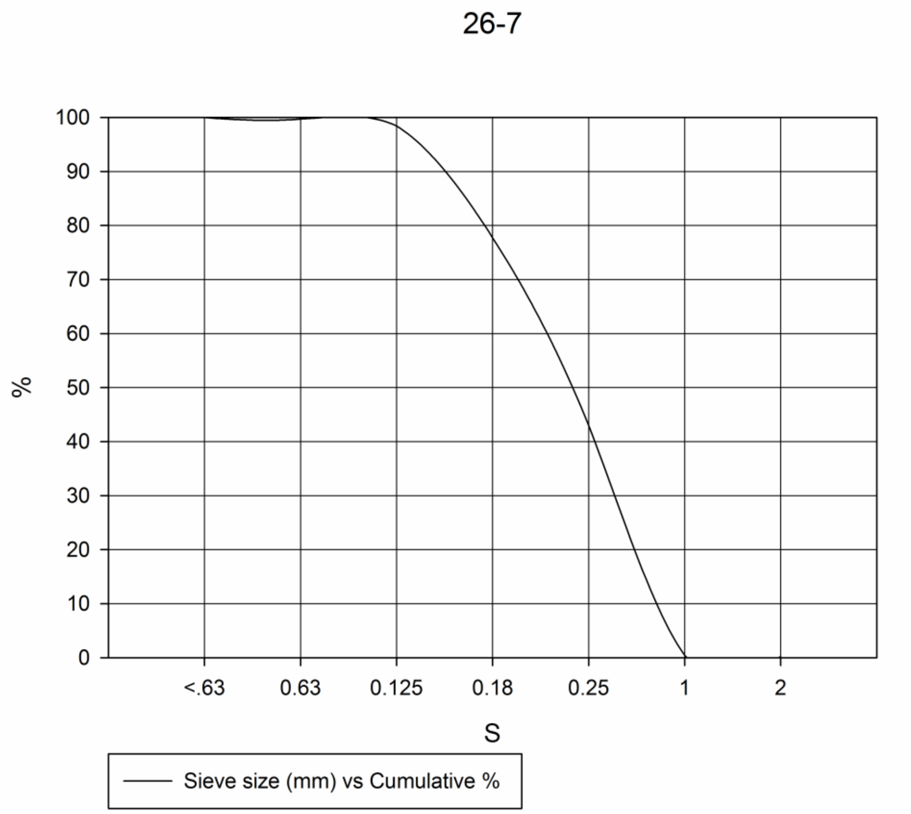
26-7
100
90
80
70
60
50
40
30
20
10
0
%
<.63
0.63
0.125
0.18
0.25
1
2
S
Sieve size (mm) vs Cumulative %

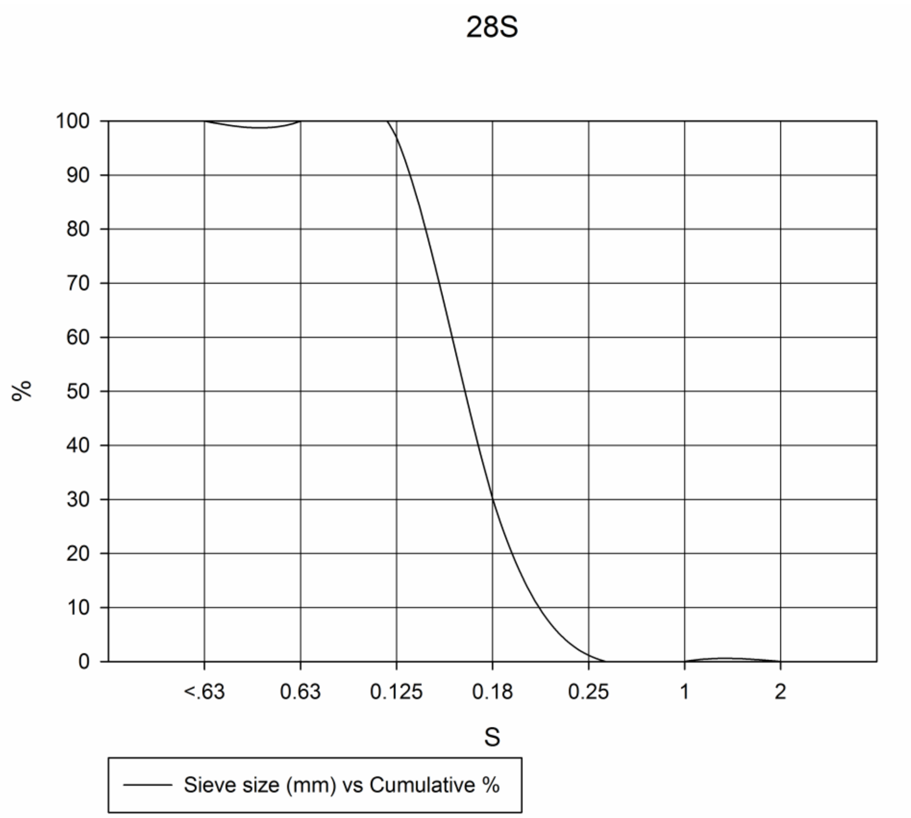
28S
100
90
80
70
60
50
40
30
20
10
0
%
<.63
0.63
0.125
0.18
0.25
1
2
S
Sieve size (mm) vs Cumulative %

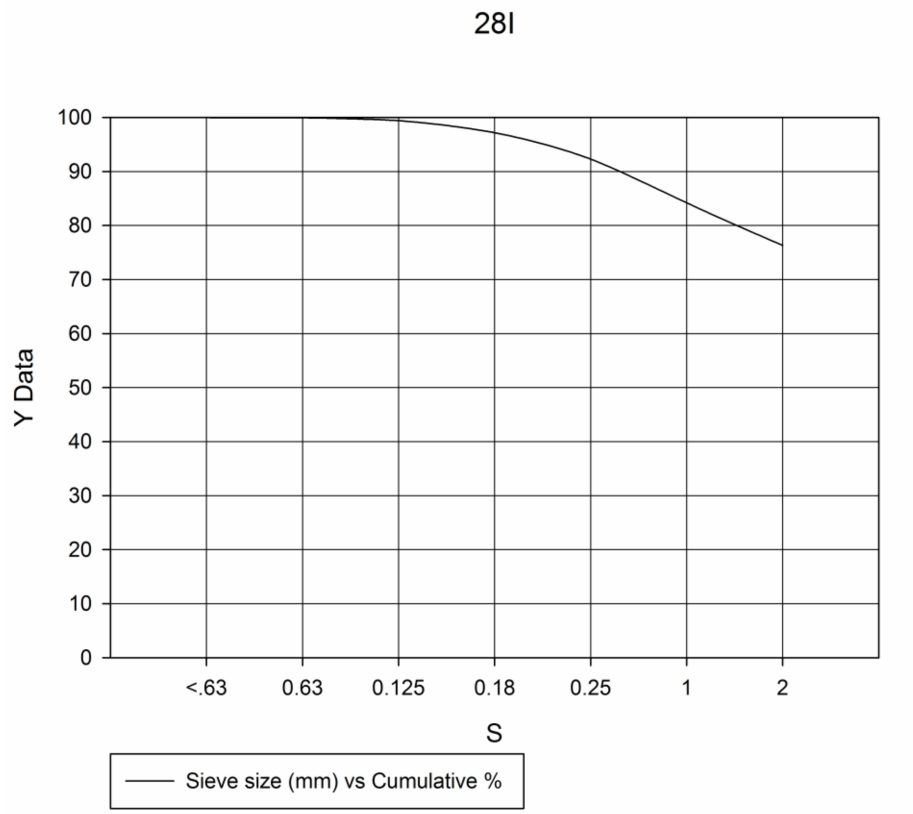
28I
100
90
80
70
60
50
40
30
20
10
0
Y Data
<.63
0.63
0.125
0.18
0.25
1
2
S
Sieve size (mm) vs Cumulative %

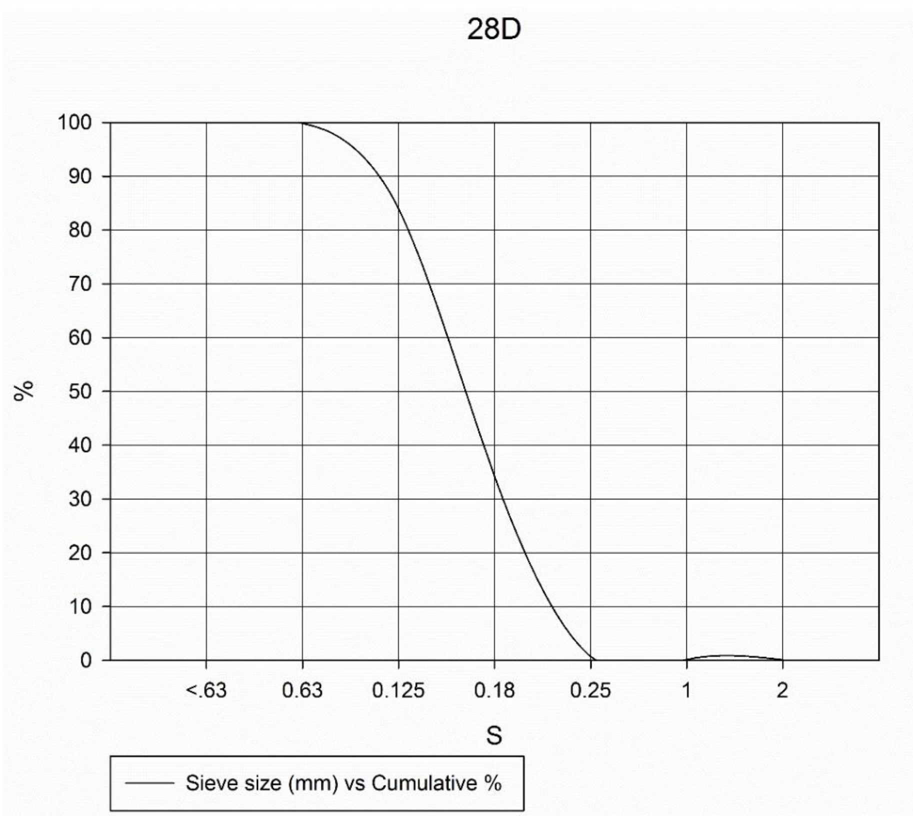
28D
100
90
80
70
60
50
40
30
20
10
0
%
<.63
0.63
0.125
0.18
0.25
1
2
S
Sieve size (mm) vs Cumulative %

Porosity

Pycnometer readings show porosity ranging from 0.29 to 0.40 with an average of 0.34 (Table 13). These values are consistent with accepted values for sediments ranging from sand to clay sized (Heath, 1983) and are consistent with the predominant sediment observed in the surficial aquifer. Two samples, from 11I and 28I, were removed due to anomalous readings caused by an abundance of materials which do not accurately represent the aquifer.

Table 13- Pycnometer Readings

Well	V1 (cm^3)	D1	V2 (cm^3)	D2	V3 (cm^3)	D3	V4 (cm^3)	D4	V5 (cm^3)	D5	V_{avg} (cm^3)	D_{avg}	Porosity
3-1	5.7645	-0.0015	5.7648	-0.0012	5.7657	-0.0003	5.7668	0.0008	5.7683	0.0023	5.7660	0.0000	0.34
3-2	5.5920	-0.0005	5.5920	-0.0004	5.5930	0.0006	5.5925	0.0001	5.5926	0.0002	5.5924	0.0000	0.36
3-3	5.9631	0.0001	5.9630	-0.0001	5.9630	-0.0001	5.9631	0.0000	5.9631	0.0001	5.9631	0.0000	0.32
3-4	5.6903	-0.0001	5.6893	-0.0011	5.6907	0.0002	5.6911	0.0007	5.6909	0.0004	5.6905	0.0000	0.35
3-5	5.7546	-0.0022	5.7555	-0.0013	5.7566	-0.0002	5.7577	0.0009	5.7596	0.0028	5.7568	0.0000	0.34
4S	5.2082	0.0001	5.2079	-0.0003	5.2085	0.0003	5.2077	-0.0005	5.2086	0.0004	5.2082	0.0000	0.40
4I	5.6807	-0.0007	5.6813	-0.0001	5.6835	0.0021	5.6804	-0.0010	5.6811	-0.0003	5.6814	0.0000	0.35
4D	5.4979	0.0001	5.4980	0.0002	5.4975	-0.0003	5.4981	0.0002	5.4977	-0.0001	5.4978	0.0000	0.37
7-1	5.6527	0.0004	5.6521	-0.0003	5.6525	0.0001	5.6524	0.0001	5.6519	-0.0004	5.6523	0.0000	0.35
7-2	5.7838	-0.0002	5.7838	-0.0006	5.7845	0.0001	5.7847	0.0003	5.7847	0.0004	5.7843	0.0000	0.34
7-3	5.7057	-0.0002	5.7066	0.0007	5.7052	-0.0007	5.7053	-0.0006	5.7066	0.0007	5.7059	0.0000	0.35
7-4	6.0014	0.0003	6.0011	0.0000	6.0010	-0.0002	6.0011	0.0000	6.0010	-0.0001	6.0011	0.0000	0.31
7-5	5.8664	-0.0001	5.8660	-0.0005	5.8666	0.0002	5.8671	0.0007	5.8662	-0.0003	5.8665	0.0000	0.33
8S	5.5789	-0.0024	5.5809	-0.0004	5.5814	0.0001	5.5822	0.0009	5.5831	0.0018	5.5813	0.0000	0.36
8I	5.4859	-0.0007	5.4864	-0.0002	5.4862	-0.0004	5.4868	0.0002	5.4878	0.0002	5.4866	-0.0002	0.37
8D	5.2585	-0.0008	5.2587	-0.0006	5.2592	0.0000	5.2590	-0.0003	5.2609	-0.0016	5.2593	-0.0007	0.40
11S	5.9610	-0.0001	5.9612	0.0001	5.9606	-0.0005	5.9613	0.0003	5.9612	0.0002	5.9611	0.0000	0.32
11I	6.6240	0.0006	6.6228	-0.0006	6.6234	-0.0001	6.6234	-0.0001	6.6327	0.0002	6.6253	0.0000	0.24
11D	6.1475	-0.0003	6.1476	-0.0002	6.1478	0.0000	6.1478	-0.0001	6.1486	0.0007	6.1479	0.0000	0.29
12-1	5.7030	0.0000	5.7029	-0.0002	5.7026	-0.0004	5.7034	0.0003	5.7033	-0.0003	5.7030	-0.0001	0.35
12-2	5.8603	-0.0005	5.8610	0.0002	5.8606	-0.0002	5.8607	0.0001	5.8614	0.0006	5.8608	0.0000	0.33
12-3	5.7968	-0.0001	5.7956	-0.0013	5.7975	0.0006	5.7972	0.0003	5.7975	0.0006	5.7969	0.0000	0.34
12-4	6.0783	0.0003	6.0784	0.0004	6.0786	0.0006	6.0788	0.0008	6.0760	-0.0020	6.0780	0.0000	0.30
12-5	6.0252	-0.0001	6.0253	0.0000	6.0253	0.0000	6.0252	-0.0001	6.0255	0.0002	6.0253	0.0000	0.31
12-6	5.9565	0.0000	5.9568	0.0003	5.5965	0.0000	5.9567	0.0002	5.9561	-0.0005	5.8845	0.0000	0.33
17S	5.8441	-0.0001	5.8436	-0.0006	5.8439	-0.0002	5.8446	0.0005	5.8446	0.0004	5.8442	0.0000	0.33
17I	5.9069	-0.0002	5.9063	-0.0008	5.9073	0.0001	5.9077	0.0006	5.9074	0.0003	5.9071	0.0000	0.32

Table 13 continued.

Well	V1 (cm^3)	D1	V2 (cm^3)	D2	V3 (cm^3)	D3	V4 (cm^3)	D4	V5 (cm^3)	D5	V_{avg} (cm^3)	D_{avg}	Porosity
17D	5.7262	0.0003	5.7258	-0.0001	5.7262	0.0003	5.7255	-0.0004	5.7257	-0.0002	5.7259	0.0000	0.34
19S	5.8918	-0.0014	5.8920	-0.0012	5.8927	-0.0004	5.8942	0.0010	5.8951	0.0019	5.8932	0.0000	0.32
19I	5.9880	-0.0004	5.9887	0.0002	5.9886	0.0001	5.9884	-0.0001	5.9887	0.0003	5.9885	0.0000	0.31
19D	5.9896	0.0004	5.9891	-0.0001	5.9888	-0.0004	5.9885	-0.0008	5.9902	0.0010	5.9892	0.0000	0.31
28S	5.5684	0.0000	5.5683	-0.0001	5.5678	-0.0006	5.5689	0.0005	5.5687	0.0003	5.5684	0.0000	0.36
28I	1.3678	-0.0010	1.3685	-0.0002	1.3787	0.0000	1.3696	0.0009	1.3691	0.0003	1.3707	0.0000	0.84
28D	5.5433	-0.0005	5.5435	-0.0004	5.5439	0.0000	5.5443	0.0004	5.5442	0.0004	5.5438	0.0000	0.36
26-1	5.7946	0.0000	5.7948	0.0002	5.7940	-0.0007	5.7949	0.0003	5.7948	0.0002	5.7946	0.0000	0.34
26-2	5.9102	-0.0003	5.9098	-0.0007	5.9103	-0.0003	5.9112	0.0007	5.9112	0.0006	5.9105	0.0000	0.32
26-3	5.8359	-0.0009	5.8372	0.0005	5.8370	0.0002	5.8368	0.0000	5.8370	0.0002	5.8368	0.0000	0.33
26-4	5.9669	-0.0004	5.9671	-0.0002	5.9672	-0.0001	5.9672	-0.0001	5.9680	0.0007	5.9673	0.0000	0.32
26-5	5.8740	-0.0006	5.8756	0.0010	5.8744	-0.0002	5.8747	0.0001	5.8744	-0.0002	5.8746	0.0000	0.33
26-6	5.8422	-0.0009	5.8429	-0.0002	5.8424	-0.0006	5.8439	0.0009	5.8438	0.0008	5.8430	0.0000	0.33
26-7	5.8293	-0.0008	5.8293	-0.0008	5.8295	-0.0006	5.8318	0.0017	5.8305	0.0004	5.8301	0.0000	0.33

* Indicates Anomalous Value

Appendix C: GIS Procedures for Determining Marine and Groundwater Inundation

Exporting the Water Table from Visual MODFLOW

1. In Visual MODFLOW, go to output- head. Export Layer- Active Only, save as a .txt.
2. In Excel, open the .txt file, add headings ‘X,Y,Elev’ and save as .csv.

Importing MODFLOW Water Level Data into ArcGIS

1. In ArcGIS, import the .csv file, display XY Data with Z as ELEV, click OK. Map should have a series of dots.
2. Right click the layer in Table of Contents- Data- export data to shapefile
3. In Arc Toolbox, go to 3D Analyst Tools- Raster Interpolation- Natural Neighbor and follow the wizard.

Determining the Area Impaired by Marine Inundation in ArcGIS

1. Import the DEM for the area of interest.
2. Go to the reclassify tool and reclassify the DEM based on the sea-level rise scenario. Set below sea-level to gridcode ‘zero’ and above sea-level to gridcode ‘999’
3. Convert the raster to a polygon.
4. Select features in polygon layer that are above sea-level. Right click the polygon, select by attribute, Gridcode= 999.
5. Create new layer from selected features. Right click the polygon, selection, create layer from selected features.
6. Fill donut holes within the polygon. Use the ‘eliminate polygon part’ tool and set the maximum area for which all polygons will be extracted. For this study, the area was set to 70,000 m^2 so the tool does not eliminate the area of Bogue Banks near the canal.
7. Compute total area of the polygon layer with shoreline for specific sea-level rise scenario.
8. Compute marine inundation. Calculate the difference in total area between the polygon representing one scenario and the total area of the polygon representing the next scenario.

Determining the Area Impaired by Groundwater Inundation in ArcGIS

1. Determine areas where the water table is above or below land surface. In Arc Toolbox, go to 3D Analyst Tools- Raster Math- Minus. For input raster 1, put the DEM. For input raster 2, put the interpolated raster from number 3 above.
2. Create a groundwater inundation raster by reclassifying the output raster to binary classification. Make all areas under the desired sea-level rise scenario ‘1’ and all areas above ‘0’.
3. Import the polygon layer with shoreline for specific sea-level rise scenario.
4. Clip the groundwater inundation raster with the aforementioned polygon layer with shoreline for specific sea-level rise scenario.
5. Convert the resulting layer from a raster to a polygon.

6. Compute area of the features in the polygon layer. Right click the layer, open attribute table, and create a new field titled 'Area'. Right click the area column and calculate geometry.
7. Compute the sum of areas represented by the different features. Right click the gridcode column and select Summarize. In 1, put gridcode. In 2, select area- sum. Save as .TXT. In the resulting text file, gridcode 1 gives the sum of the area impaired by groundwater inundation.

Appendix D- Impairment % by Sea-Level Rise Scenario

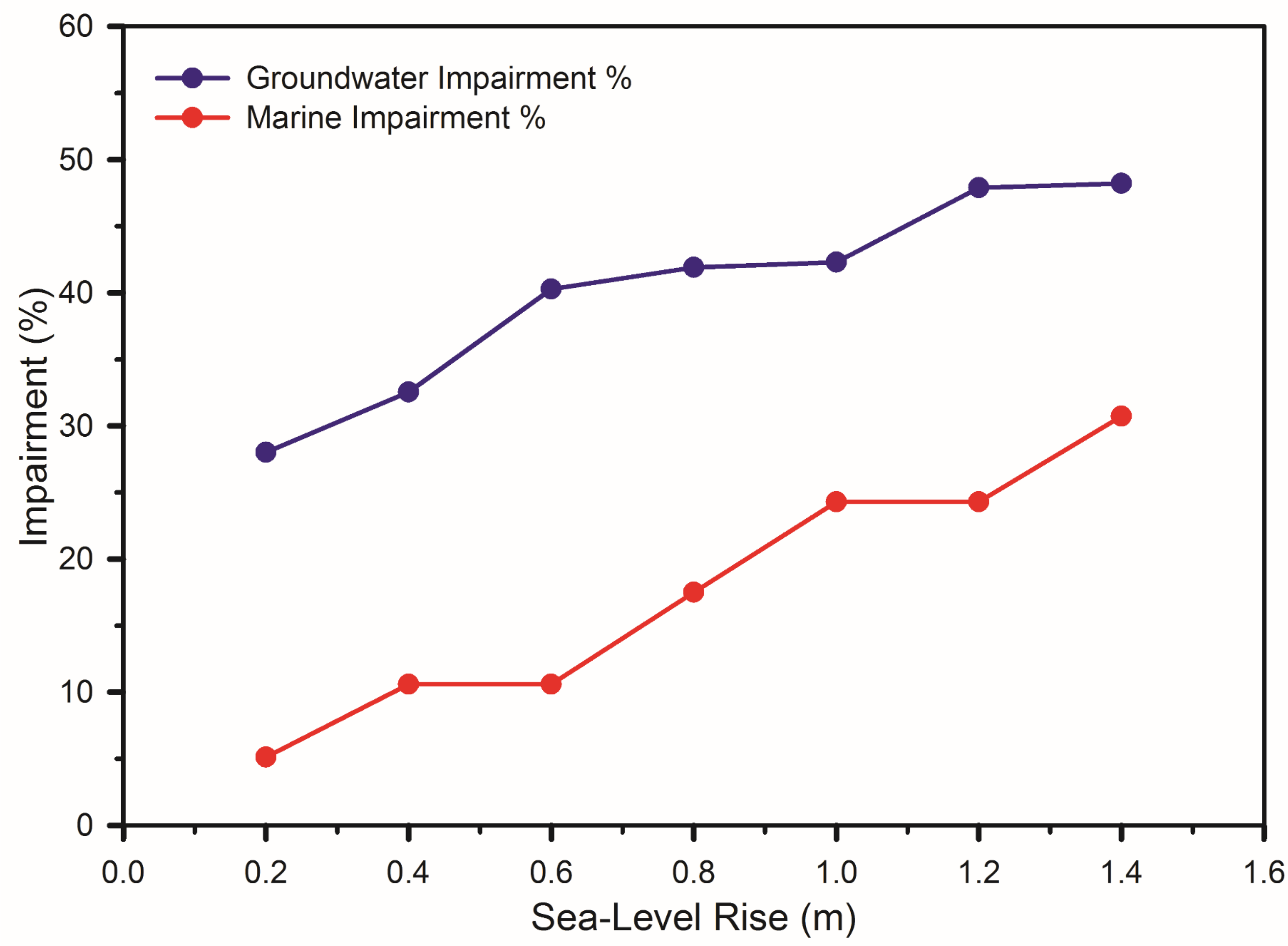

Appendix E- Inundation Maps

0.2 m

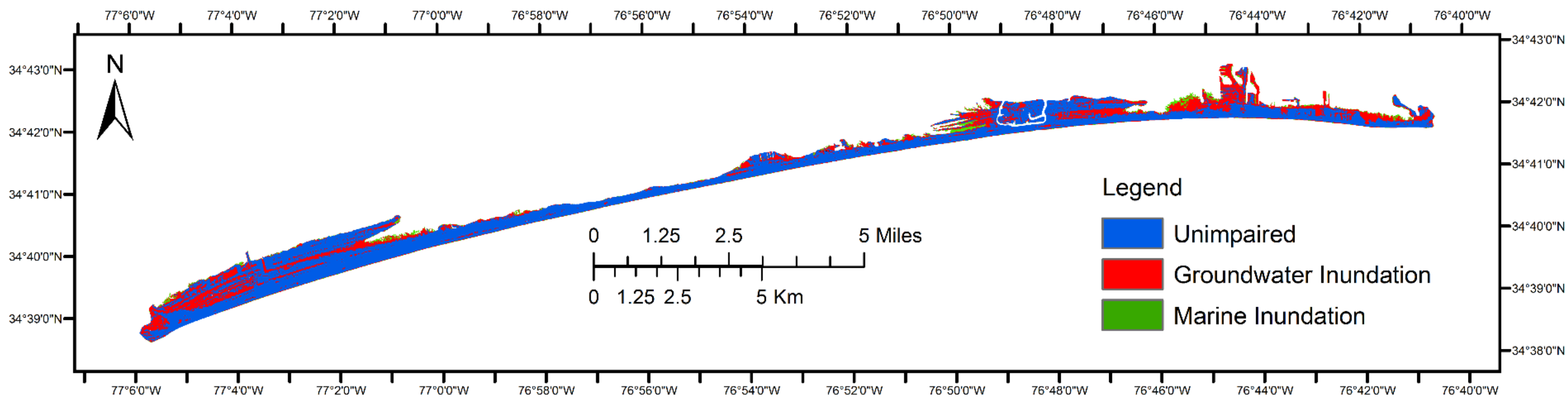

0.4 m

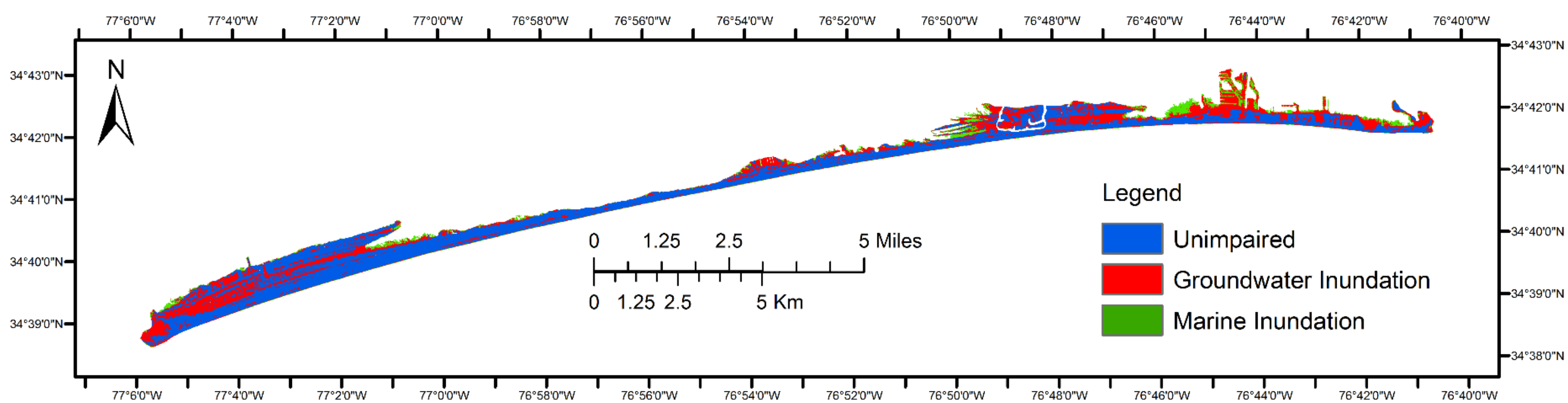

0.6 m

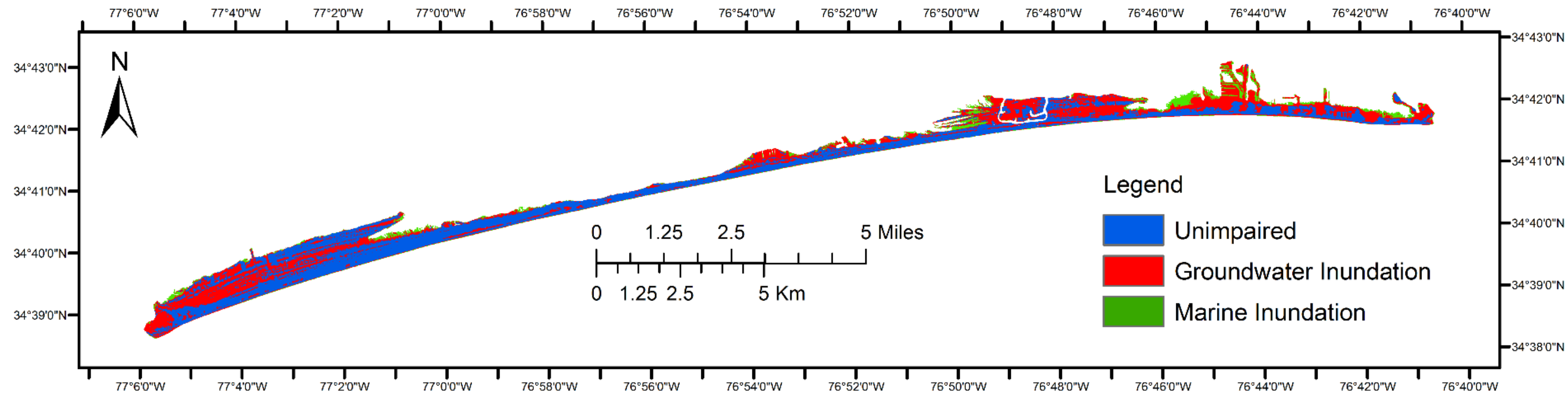
N
Legend
Unimpaired
Groundwater Inundation
Marine Inundation
0
1.25
2.5
5 Miles
0
1.25
2.5
5 Km
77°6'0"W
77°4'0"W
77°2'0"W
77°0'0"W
76°58'0"W
76°56'0"W
76°54'0"W
76°52'0"W
76°50'0"W
76°48'0"W
76°46'0"W
76°44'0"W
76°42'0"W
76°40'0"W
34°43'0"N
34°42'0"N
34°41'0"N
34°40'0"N
34°39'0"N
34°38'0"N

0.8 m

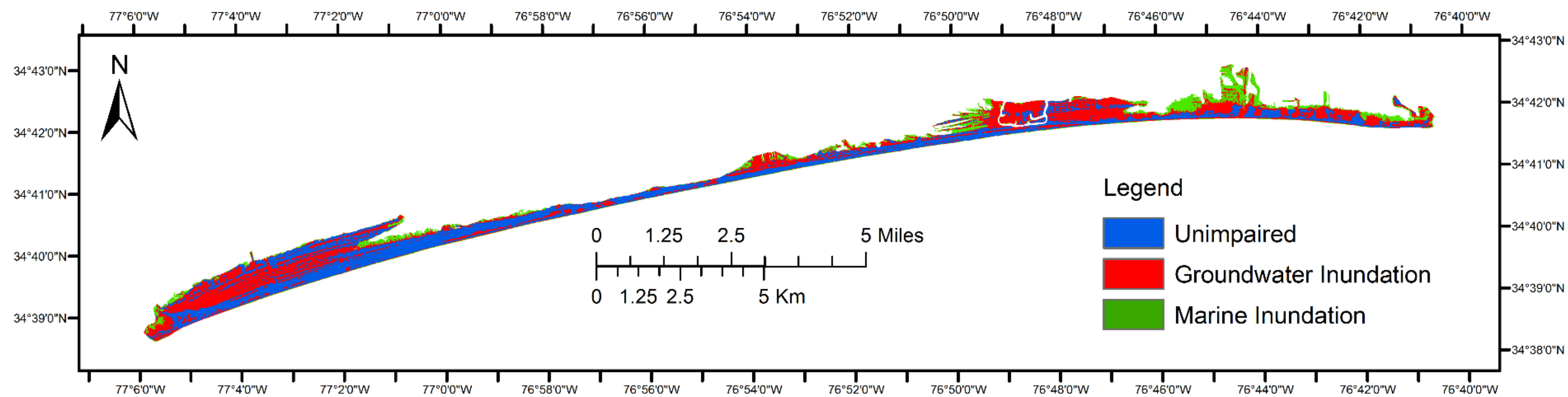
N
Legend
Unimpaired
Groundwater Inundation
Marine Inundation
0
1.25
2.5
5 Miles
0
1.25
2.5
5 Km
77°6'0"W
77°4'0"W
77°2'0"W
77°0'0"W
76°58'0"W
76°56'0"W
76°54'0"W
76°52'0"W
76°50'0"W
76°48'0"W
76°46'0"W
76°44'0"W
76°42'0"W
76°40'0"W
34°43'0"N
34°42'0"N
34°41'0"N
34°40'0"N
34°39'0"N
34°38'0"N

1.0 m

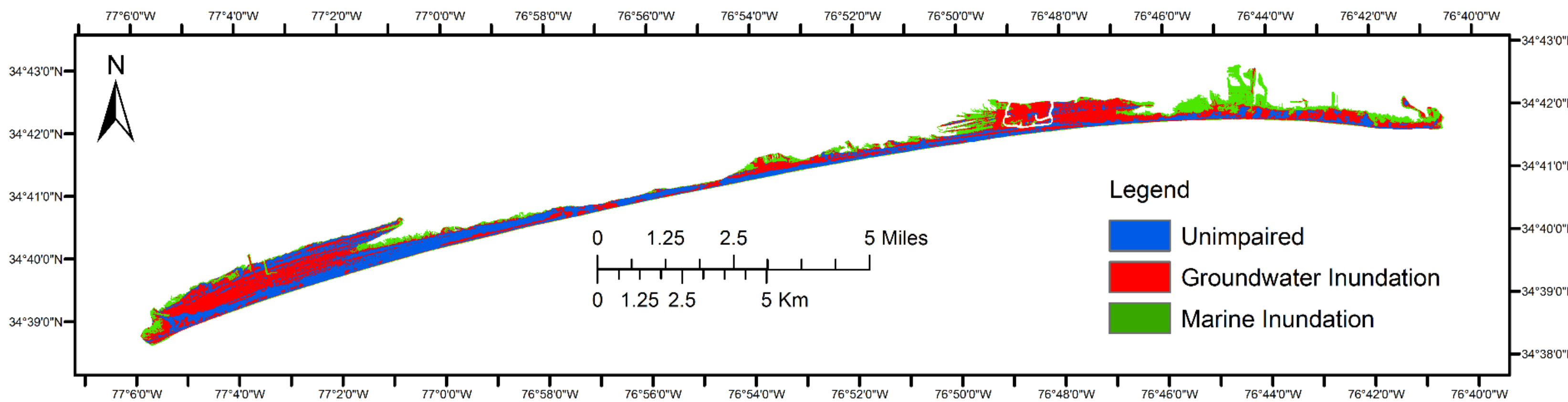
N
0
1.25
2.5
5 Miles
0
1.25
2.5
5 Km
Legend
Unimpaired
Groundwater Inundation
Marine Inundation

1.2 m

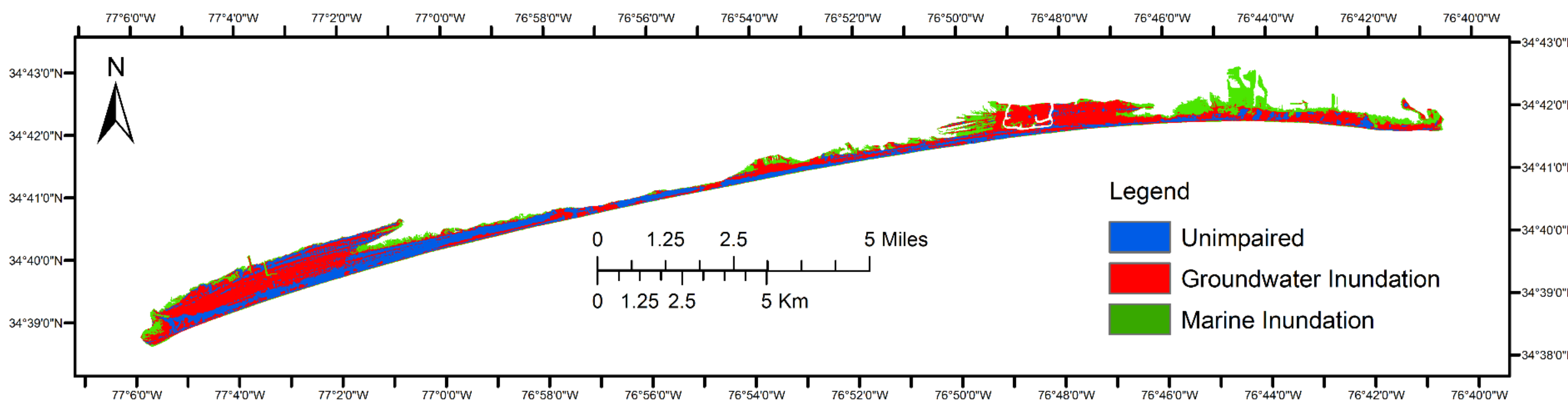
N
0
1.25
2.5
5 Miles
0
1.25
2.5
5 Km
Legend
Unimpaired
Groundwater Inundation
Marine Inundation

1.4 m

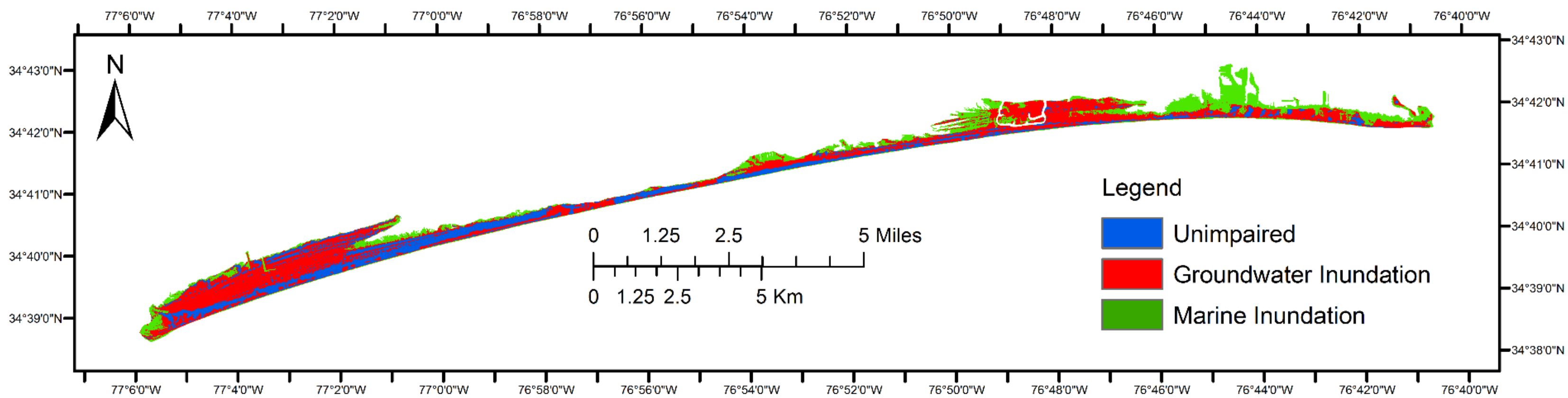
N
77°6'0"W
77°4'0"W
77°2'0"W
77°0'0"W
76°58'0"W
76°56'0"W
76°54'0"W
76°52'0"W
76°50'0"W
76°48'0"W
76°46'0"W
76°44'0"W
76°42'0"W
76°40'0"W
34°43'0"N
34°42'0"N
34°41'0"N
34°40'0"N
34°39'0"N
34°38'0"N
0 1.25 2.5 5 Miles
0 1.25 2.5 5 Km
Legend
Unimpaired
Groundwater Inundation
Marine Inundation